

**COLORADO STATE IMPLEMENTATION  
PLAN FOR REGIONAL HAZE  
*TECHNICAL SUPPORT DOCUMENT***

**Mandatory Class I Federal Area:**

***GREAT SAND DUNES  
NATIONAL PARK & PRESERVE***



---

**Colorado Department  
of Public Health  
and Environment**

Prepared by  
The Colorado Department of Public Health and Environment  
Air Pollution Control Division  
4300 Cherry Creek Drive South  
Denver, Colorado 80246-1530  
(303) 692-3100

*October 2007*

# **Table of Contents**

SECTION 1: OVERVIEW .....	1
A. Description .....	1
B. Location.....	2
SECTION 2: VISIBILITY MONITORING.....	3
A. Monitoring Approaches .....	3
(1) <i>Scene Monitoring:</i> .....	3
(2) <i>Aerosol Monitoring:</i> .....	3
(3) <i>Optical Monitoring:</i> .....	3
B. IMPROVE Program.....	3
C. Monitor Location.....	4
D. Monitoring Strategy .....	4
SECTION 3: VISIBILITY CONDITIONS .....	5
A. Visibility Metrics.....	5
B. Baseline Visibility.....	6
(1) <i>Baseline Period - Best Days Visibility</i> .....	6
(2) <i>Baseline Period – Worst Days Visibility</i> .....	6
C. Natural Visibility.....	7
(1) <i>Natural Conditions - Best Days Visibility</i> .....	7
(2) <i>Natural Conditions – Worst Days Visibility</i> .....	7
D. Split-Image of Best and Worst Days .....	8
E. Uniform Rate of Progress Glide Path.....	9
F. Determination of Uniform Rate of Progress .....	10
SECTION 4: HAZE IMPACTING PARTICLES .....	11
A. Aerosol Components.....	11
B. Aerosol Composition on Best and Worst Days .....	11
C. Comparison of Baseline Extinction for Best & Worst Days.....	13
D. Visibility Improvement Needed – 20% Worst Days.....	14
E. Aerosol Pollutant Trends – 20% Worst Days.....	15
F. Monthly Distribution - 20% Worst Days .....	16
G. Monthly Distribution - 20% Best Days.....	16
SECTION 5: EMISSION SOURCE CHARACTERIZATION .....	17
A. State Emission Inventory and Regional Emission Maps .....	17
(1) <i>Colorado SO<sub>2</sub> Emission Inventory for 2002 &amp; 2018</i> .....	18
(2) <i>Regional Map of SO<sub>x</sub> Emissions for 2002 &amp; 2018</i> .....	19
(3) <i>Colorado NO<sub>x</sub> Emission Inventory for 2002 &amp; 2018</i> .....	20

(4)	<i>Regional Map of NOx Emissions for 2002 &amp; 2018</i> .....	21
(5)	<i>Colorado NH<sub>3</sub> Emission Inventory for 2002 &amp; 2018</i> .....	22
(6)	<i>Colorado POA Emission Inventory for 2002 &amp; 2018</i> .....	24
(7)	<i>Regional Map of POA Emissions for 2002 &amp; 2018</i> .....	25
(8)	<i>Colorado VOC Emission Inventory for 2002 &amp; 2018</i> .....	26
(9)	<i>Colorado EC Emission Inventory for 2002 &amp; 2018</i> .....	27
(10)	<i>Regional Map of EC Emissions for 2002 &amp; 2018</i> .....	28
(11)	<i>Colorado Soil Emission Inventory for 2002 &amp; 2018</i> .....	29
(12)	<i>Regional Map of PM<sub>2.5</sub> Emissions for 2002 and 2018</i> .....	30
(13)	<i>Colorado Coarse Mass Emission Inventory for 2002 &amp; 2018</i> .....	31
(14)	<i>Regional Map of PMC Emissions for 2002 &amp; 2018</i> .....	32
B.	<b>Weighted Emissions Potential (WEP)</b> .....	33
(1)	<i>Overview</i> .....	33
(2)	<i>Sulfur Oxides - Regional WEP Map for 2018 Worst Days</i> .....	34
(3)	<i>Sulfur Oxides - Regional WEP Map for 2018 Best Days</i> .....	35
(4)	<i>Nitrogen Oxides - Regional WEP Map for 2018 Worst Days</i> .....	36
(5)	<i>Nitrogen Oxides - Regional WEP Map for 2018 Best Days</i> .....	37
(6)	<i>Primary Organic Aerosol - Regional WEP Map for 2018 Worst Days</i> .....	38
(7)	<i>Primary Organic Aerosol - Regional WEP Map for 2018 Best Days</i> .....	39
(8)	<i>Primary Elemental Carbon - Regional WEP Map for 2018 Worst Days</i> .....	40
(9)	<i>Primary Elemental Carbon - Regional WEP Map for 2018 Best Days</i> .....	41
(10)	<i>Particulate Matter Fine - Regional WEP Map for 2018 Worst Days</i> .....	42
(11)	<i>Particulate Matter Fine - Regional WEP Map for 2018 Best Days</i> .....	43
(12)	<i>Particulate Matter Coarse - Regional WEP Map for 2018 Worst Days</i> .....	44
(13)	<i>Particulate Matter Coarse - Regional WEP Map for 2018 Best Days</i> .....	45
	<b>SECTION 6: REGIONAL VISIBILITY MODELING</b> .....	46
A.	<b>Overview</b> .....	46
B.	<b>Air Quality Models</b> .....	46
(1)	<i>Community Multi-Scale Air Quality Model</i> .....	46
(2)	<i>Comprehensive Air Quality Model with Extensions</i> .....	47
C.	<b>Modeling Performance</b> .....	47
(1)	<i>Model Performance for 2002 Worst Days</i> .....	48
(2)	<i>Model Performance for 2002 Best Days</i> .....	49
D.	<b>Modeling Projections</b> .....	50
(1)	<i>2018 Worst Days Model Projection using Haze Index Metric</i> .....	50
(2)	<i>2018 Worst Days Model Projection using Extinction Metric</i> .....	50
(3)	<i>2018 Best Days Model Projection using Haze Index Metric</i> .....	51

SECTION 7: PM SOURCE APPORTIONMENT TECHNOLOGY (PSAT) MODELING.....	52
A. PSAT Overview .....	52
B. Particulate Sulfate PSAT for Worst Days in 2002 and 2018.....	52
C. Particulate Sulfate PSAT for Best Days in 2002 and 2018.....	53
D. Particulate Nitrate PSAT for Worst Days in 2002 and 2018 .....	54
E. Particulate Nitrate PSAT for Best Days in 2002 and 2018 .....	55
F. Organic Aerosol PSAT for Worst Days in 2002 and 2018 .....	56
G. Organic Aerosol PSAT for Best Days in 2002 and 2018 .....	56
H. Organic Aerosol PSAT for All Days in 2002 and 2018 .....	57
SECTION 8: EMISSIONS TRACE .....	58
A. ET Overview.....	58
B. Sulfate Emissions Trace for 2018 Worst Days .....	59
C. Nitrate Emissions Trace for 2018 Worst Days .....	60
D. Organic Carbon Emissions Trace for 2018 Worst Days .....	61
E. Elemental Carbon Emissions Trace for 2018 Worst Days.....	62
F. Fine Soil Emissions Trace for 2018 Worst Days.....	63
G. Coarse Mass Emissions Trace for 2018 Worst Days .....	64
Appendix A: IMPROVE Monitoring Program.....	66
Appendix B: Photographic Images of Visibility .....	67
Appendix C: Seasonal Wind Patterns .....	69
Appendix D: Weighted Emissions Potential .....	70
Appendix E: Standard Aerosol-Type Equations.....	73
Appendix F: Procedure for Reconstructing Light Extinction.....	76
Appendix G: Pollutant Statistical Trends .....	83
Appendix H: PM Source Apportionment Technology (PSAT) Modeling.....	87

**List of Tables**

Table 1- 1: Great Sand Dunes National Park & Preserve – Determination of Uniform ROP .....	10
Table 2- 1 IMPROVE Monitor Aerosol Composition.....	11

**Table of Figures**

Figure 1-1: The Sangre de Cristo Mountains loft over the great dunes (Photo courtesy of NPS).....	1
Figure 1-2: Great Sand Dunes, Medano Creek and Cleveland Peak (Photo courtesy of NPS).....	1
Figure 1-3: Location of Great Sand Dunes National Park & Preserve .....	2
Figure 1-4: Map of Great Sand Dunes National Park & Preserve .....	2

Figure 2-1: IMPROVE Monitor Location Map .....	4
Figure 3-1: Baseline Best Days .....	6
Figure 3-2: Baseline Worst Days .....	6
Figure 3-3: Natural Best Days.....	7
Figure 3-4: Natural Worst Days .....	7
Figure 3-5: WinHaze Simulation of the Best & Worst Baseline Conditions .....	8
Figure 3-6: URP Glide Path .....	9
Figure 4-1: Reconstructed Extinction for 20% Worst Days over Baseline Period .....	11
Figure 4-2: Reconstructed Extinction for 20% Worst Days over Baseline Period .....	12
Figure 4-3: Reconstructed Extinction for 20% Best Days over Baseline Period .....	12
Figure 4-4: Reconstructed Extinction for 20% Best Days over Baseline Period .....	13
Figure 4-5: Comparison of Baseline Extinction for 20% Best & Worst Days.....	13
Figure 4-6: Average Contributions to Reconstructed Extinction for 20% Worst Days.....	14
Figure 4-7: Monthly Distribution of 20% Worst Days .....	16
Figure 4-8: Monthly Distribution of 20% Best Days .....	16
Figure 5-1: Colorado SO <sub>2</sub> Emissions – 2002 & 2018 Inventory.....	18
Figure 5-2: Regional SO <sub>x</sub> Emissions – 2002 & 2018 Inventory.....	19
Figure 5-3: Colorado NO <sub>x</sub> Emissions – 2002 & 2018 Inventory .....	20
Figure 5-4: Regional NO <sub>x</sub> Emissions – 2002 & 2018 Inventory .....	21
Figure 5-5: Colorado NH <sub>3</sub> Emissions – 2002 & 2018 Inventory .....	22
Figure 5-6: Colorado POA Emissions – 2002 & 2018 Inventory .....	24
Figure 5-7: Regional POA Emissions – 2002 & 2018 Inventory .....	25
Figure 5-8: Colorado VOC Emissions – 2002 & 2018 Inventory .....	26
Figure 5-9: Colorado EC Emissions – 2002 & 2018 Inventory .....	27
Figure 5-10: Regional EC Emissions – 2002& 2018 Inventory.....	28
Figure 5-11: Colorado Soil Emissions – 2002 & 2018 Inventory .....	29
Figure 5-12: Regional PM <sub>2.5</sub> Emissions – 2002 & 2018 Inventory .....	30
Figure 5-13: Colorado Coarse Mass Emissions – 2002 & 2018 Inventory .....	31
Figure 5-14: Regional PMC Emissions – 2002 & 2018 Inventory.....	32
Figure 5-15: Regional SO <sub>x</sub> WEP for 2018 Worst Days .....	34
Figure 5-16: Regional SO <sub>x</sub> WEP for 2018 Best Days .....	35
Figure 5-17: Regional NO <sub>x</sub> WEP for 2018 Worst Days .....	36
Figure 5-18: Regional NO <sub>x</sub> WEP for 2018 Best Days .....	37
Figure 5-19: Regional POA WEP for 2018 Worst Days.....	38
Figure 5-20: Regional POA WEP for 2018 Best Days.....	39
Figure 5-21: Regional PEC WEP for 2018 Worst Days.....	40
Figure 5-22: Regional PEC WEP for 2018 Best Days.....	41

Figure 5-23: Regional PM Fine WEP for 2018 Worst Days.....	42
Figure 5-24: Regional PM Fine WEP for 2018 Best Days .....	43
Figure 5-25: Regional PMC WEP for 2018 Worst Days .....	44
Figure 5-26: Regional PMC WEP for 2018 Best Days .....	45
Figure 6-1: CMAQ Model Performance for GRSA 2002 Worst Days .....	48
Figure 6-2: Relative Error: CMAQ Model vs IMPROVE data for ROMO 2002 Worst Days .....	48
Figure 6-3: CMAQ Model Performance for GRSA 2002 Best Days .....	49
Figure 6-4: Relative Error: CMAQ Model vs IMPROVE data for ROMO 2002 Best Days .....	49
Figure 6-5: CMAQ Model Projections in Haze Index for GRSA 2018 Worst Days.....	50
Figure 6-6: CMAQ Model Projections in Extinction for GRSA 2018 Worst Days .....	50
Figure 6-7: Percent Towards Species-Specific UPG for GRSA 2018 Worst Days.....	51
Figure 6-8: CMAQ Model Projections in Haze Index for GRSA 2018 Worst Days.....	51
Figure 7-1: Sulfate PSAT - Source Region Bar Chart for Worst Days in 2002 and 2018 .....	52
Figure 7-2: Sulfate PSAT - Regional Pie Chart for Worst Days in 2002 and 2018.....	53
Figure 7-3: Sulfate PSAT - Source Region Bar Chart for Best Days in 2002 and 2018.....	53
Figure 7-4: Sulfate PSAT - Regional Pie Chart for Best Days in 2002 and 2018.....	54
Figure 7-5: Nitrate PSAT – Source Region Bar Chart for Worst Days in 2002 and 2018 .....	54
Figure 7-6: Nitrate PSAT - Regional Pie Chart for Worst Days in 2002 and 2018 .....	55
Figure 7-7: Nitrate PSAT – Source Region Bar Chart for Best Days in 2002 and 2018 .....	55
Figure 7-8: Nitrate PSAT - Regional Pie Chart for Best Days in 2002 and 2018 .....	56
Figure 7-9: Organic Carbon PSAT - Bar Chart for Worst Days in 2002 and 2018 .....	56
Figure 7-10: Organic Carbon PSAT - Bar Chart for Best Days in 2002 and 2018 .....	57
Figure 7-11: Organic Carbon PSAT - Bar Chart for All Days in 2002 and 2018.....	57
Figure 8-1: Sulfate Emissions Trace for 2018 Worst Days.....	59
Figure 8-2: Nitrate Emissions Trace for 2018 Worst Days .....	60
Figure 8-3: Organic Carbon Emissions Trace for 2018 Worst Days.....	61
Figure 8-4: Elemental Carbon Emissions Trace for 2018 Worst Days .....	62
Figure 8-5: Fine Soil Emissions Trace for 2018 Worst Days .....	63
Figure 8-6: Coarse Mass Emissions Trace for 2018 Worst Days.....	64

## SECTION 1: OVERVIEW

### A. Description

The Great Sand Dunes National Park & Preserve encompasses North America's tallest dunes that rise over 750 feet high against the rugged Sangre de Cristo Mountains. The wind-shaped dunes seem to glow beneath the rugged backdrop of the mountains. This geologic wonderland, containing over 30 square miles of massive dunes, became a national monument in 1932.

*Figure 1-1: The Sangre de Cristo Mountains loft over the great dunes (Photo courtesy of NPS)*



With the passage of the Great Sand Dunes National Park and Preserve Act in late 2000, the area expanded to over 84,600 acres and gained new resources including alpine lakes and tundra, six peaks over 13,000' in elevation, ancient spruce and pine forests, large stands of aspen and cottonwood, grasslands, and wetlands.

*Figure 1-2: Great Sand Dunes, Medano Creek and Cleveland Peak (Photo courtesy of NPS)*



## B. Location

Great Sand Dunes National Park and Preserve is located in south central Colorado, northeast of Alamosa in portions of Saguache and Alamosa County.

Figure 1-3: Location of Great Sand Dunes National Park & Preserve

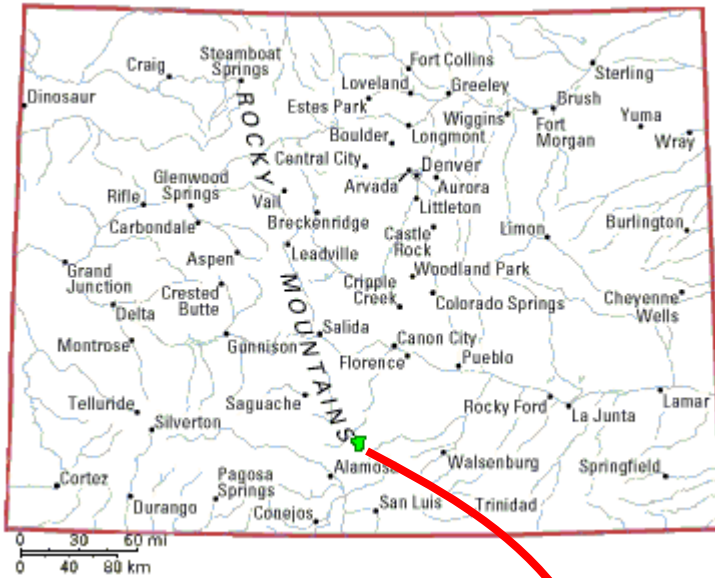


Figure 1-4: Map of Great Sand Dunes National Park & Preserve



## **SECTION 2: VISIBILITY MONITORING**

### **A. Monitoring Approaches**

A variety of monitoring techniques exist to document visibility conditions and to make quantitative measurements of the atmospheric properties that effect visibility. The IMPROVE Program has partitioned visibility-related characteristics and measurements into three groups:

#### **(1) Scene Monitoring:**

Scene monitoring is defined as the appearance of a scene viewed through the atmosphere. Scene characteristics include observer visual range, scene contrast, color, texture, clarity, and other descriptive terms. Scene characteristics change with illumination and atmospheric composition. Photographs, video images, and digital images are effective ways to document scene characteristics. Detailed information on the types of slides, and the selection process can be found in Appendix B – Photographic Images of Visibility.

#### **(2) Aerosol Monitoring:**

Aerosol monitoring is defined as the physical properties of the ambient atmospheric aerosols (chemical composition, size, shape, concentration, temporal and spatial distribution, and other physical properties) through which a scene is viewed. Fine particle measurements are commonly made to quantify aerosol characteristics. Detailed information on the chemical species and the assumptions utilized in the determining components of the aerosol sample are in Appendix E - Standard Aerosol-Type Equations. The procedures used to calculate the light extinction for each aerosol sample are in Appendix F - Procedure for Reconstructing Light Extinction from Aerosol Measurements. Reconstructed extinction from aerosol monitoring is the primary method identified by EPA for tracking reasonable progress under its Regional Haze Rule.

#### **(3) Optical Monitoring:**

Optical monitoring is defined as the ability of the atmosphere to scatter or absorb light passing through it. Extinction, scattering, and absorption coefficients, plus an angular dependence of the scattering, known as the scattering phase function, describe the physical properties of the atmosphere. Optical characteristics integrate the effects of atmospheric aerosols and gases. Commonly applied optical monitoring instruments include transmissometers and nephelometers.

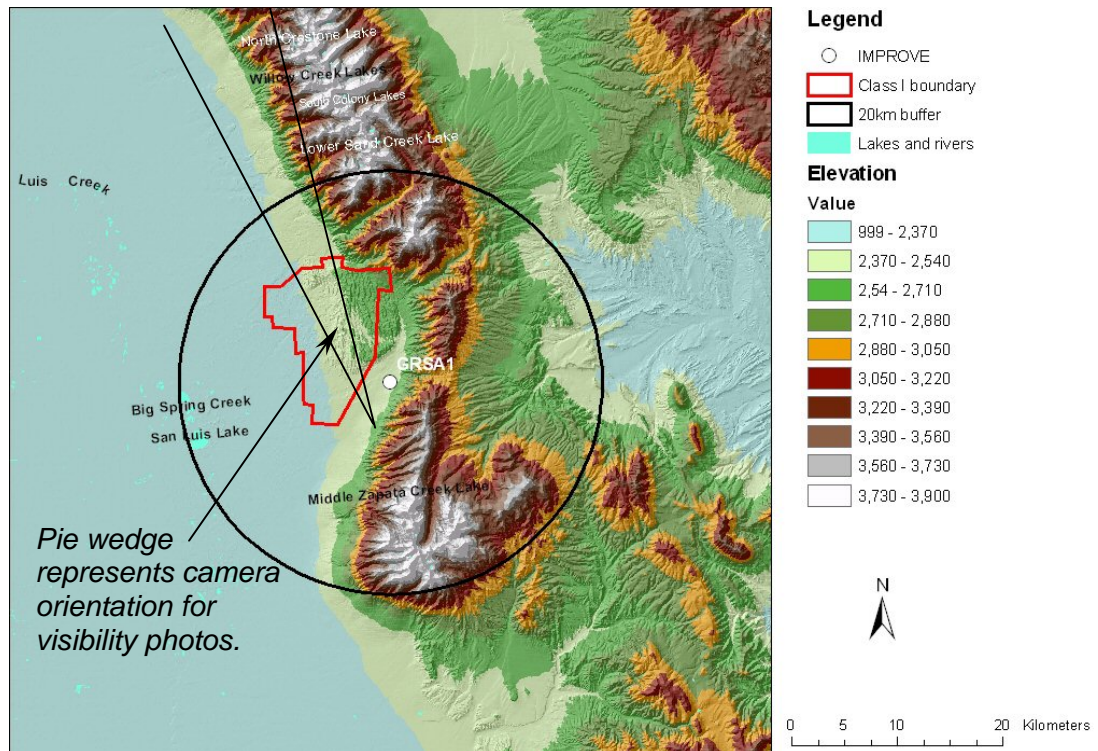
### **B. IMPROVE Program**

Visibility conditions are measured by the IMPROVE (Interagency Monitoring of Protected Visual Environments) monitoring network. More information on the IMPROVE monitoring program can be found in Appendix A.

### C. Monitor Location

The Great Sand Dunes National Park and Preserve has an IMPROVE monitor (known as GRSA1) that is operated and maintained by the National Park Service. GRSA1 was started in the spring of 1988 and is sited near the headquarters office area (off SH 150) at an elevation of 8,196 feet.

Figure 2-1: IMPROVE Monitor Location Map



### D. Monitoring Strategy

The APCD considers the GRSA1 site as adequate for assessing reasonable progress goals of the Great Sand Dunes and no additional monitoring sites or equipment are necessary at this time.

The APCD routinely participates in the IMPROVE monitoring program by attending IMPROVE Steering Committee meetings and indirectly via its membership the Western States Air Resources Council (WESTAR).

## SECTION 3: VISIBILITY CONDITIONS

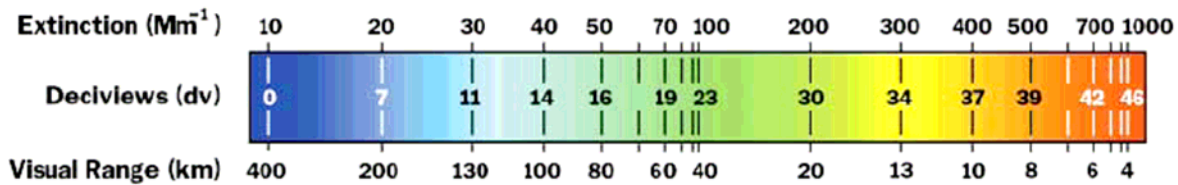
### A. Visibility Metrics

Each IMPROVE monitor collects particulate concentration data which are converted into reconstructed light extinction through a complex calculation using the IMPROVE equation (see Appendix F). Reconstructed light extinction (denoted as  $b_{ext}$ ) is expressed in units of inverse megameters ( $1/\text{Mm}$  or  $\text{Mm}^{-1}$ ). The Regional Haze Rule requires the tracking of visibility conditions in terms of the Haze Index (HI) metric expressed in the deciview (dv) unit. Generally, a one deciview change in the haze index is likely humanly perceptible under ideal conditions regardless of background conditions. There is a logarithmic relationship between the haze index and reconstructed light extinction expressed by the following conversion equation:

$$HI = 10 \ln(b_{ext}/10)$$

Where:  $HI$  is the Haze Index  
 $\ln$  is the natural log  
 $B_{ext}$  is the reconstructed light extinction

The relationship between extinction ( $\text{Mm}^{-1}$ ), haze index (dv) and visual range (km) are indicated by the following scale:



Under ideal visibility conditions, where only Rayleigh light scatter from air molecules would contribute to visibility impairment, the maximum visual range would be about 400 kilometers.

## B. Baseline Visibility

Baseline visibility is determined from on-site IMPROVE monitoring data for the 20% best and the 20% worst days for the years 2000 through 2004 as specified in the Regional Haze regulations under 40 CFR §51.308(d)(2)(i). The baseline visibility for Great Sand Dunes National Park and Preserve is calculated at 4.5 deciviews for the 20% best days and 12.8 deciviews for the 20% worst days. The photos in Figures 3-1 and 3-2 are representative of best and worst baseline visibility conditions.

### (1) Baseline Period - Best Days Visibility

Figure 3-1: Baseline Best Days



Reference Vista of Gibson Peak

Photo taken at 9:00 am

Haze Index (HI) = 5 deciviews

$B_{\text{ext}} = 17 \text{ Mm}^{-1}$

Visual Range = 230 km/143 mi

### (2) Baseline Period – Worst Days Visibility

Figure 3-2: Baseline Worst Days



Reference Vista of Gibson Peak

Photo taken at 9:00 am

Haze Index (HI) = 12 deciviews

$B_{\text{ext}} = 33 \text{ Mm}^{-1}$

Visual Range = 120 km/75 mi

## C. Natural Visibility

Natural visibility represents the visibility condition that would be experienced in the absence of human-caused impairment. Based on EPA guidance, the natural visibility for the Great Sand Dunes National Park and Preserve is 1.24 deciviews for the 20% best days and 6.7 deciviews for the 20% worst days. Figure 3-3 is representative of the best natural visibility condition. The natural worst days in Figure 3-4 represents the long-term natural visibility goal for year 2064.

### (1) Natural Conditions - Best Days Visibility

Figure 3-3: Natural Best Days



Reference Vista of Gibson Peak

Photo taken at 9:00 am

Haze Index (HI) = 3 deciviews

$B_{\text{ext}} = 13 \text{ Mm}^{-1}$

Visual Range = 300 km/186 mi

### (2) Natural Conditions – Worst Days Visibility

Figure 3-4: Natural Worst Days



Reference Vista of Gibson Peak

Photo taken at 9:00 am

Haze Index (HI) = 7 deciviews

$B_{\text{ext}} = 21 \text{ Mm}^{-1}$

Visual Range = 190 km/118 mi

## D. Split-Image of Best and Worst Days

Figure 3-5 shows a split-image created in WinHaze software to simulate the average 20% best (left – 4.5 deciviews) and 20% worst (right – 12.8 deciviews) visibility based on an average of monitored data for years 2000-2004. WinHaze has a limited number of base photos that does not include Great Sand Dunes, so a photo of the Great Basin National Park area was selected for the background.

*Figure 3-5: WinHaze Simulation of the Best & Worst Baseline Conditions*



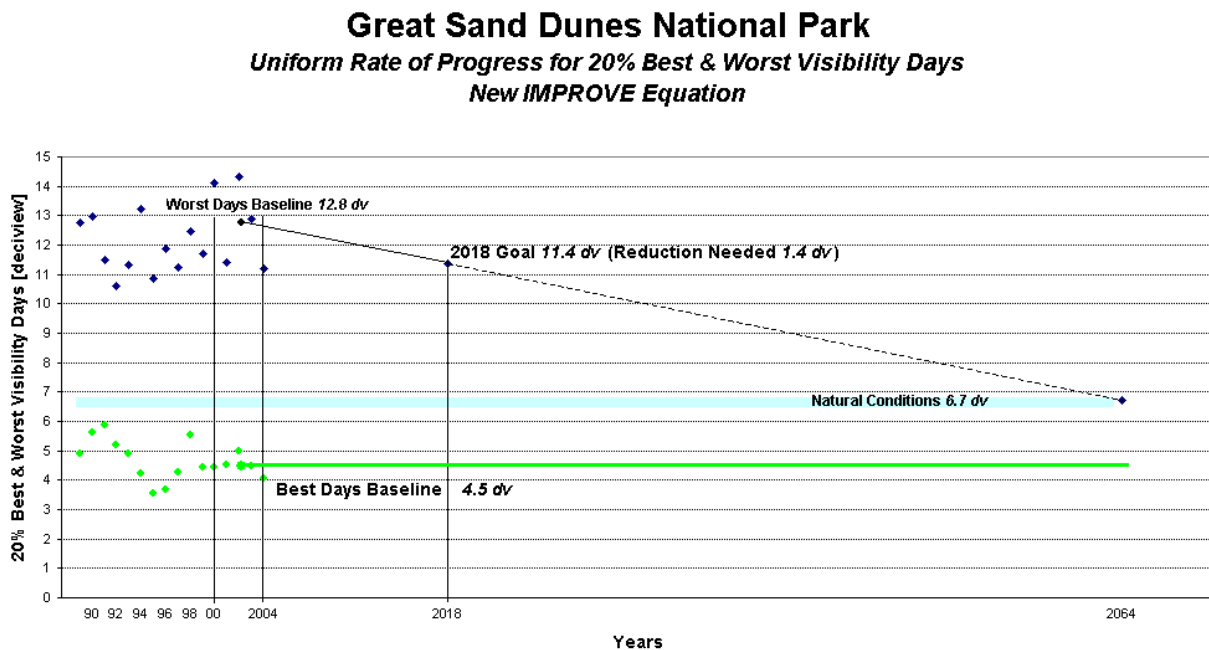
## E. Uniform Rate of Progress Glide Path

Figure 3-6 depicts the “glide path” for a uniform rate of progress (URP) toward reaching the goal of natural conditions. The Regional Haze Regulations (under 40 CFR §51.308) establish that the Class I area progress goals must provide for an improvement in visibility for the most impaired (i.e., 20% worst) days over the period of the implementation plan, and ensure no degradation in visibility for the least impaired (i.e., 20% best) days over the same period.

The baseline condition (12.8 deciviews) is an average of the haze index (from IMPROVE data using the new IMPROVE equation) over the 5-year baseline period of 2000-2004. The 1<sup>st</sup> planning period visibility improvement of 1.4 deciviews is determined by multiplying the uniform rate of progress (the amount of visibility improvement needed per year over the 60-year period) by the number of years in the initial planning period.

The best days baseline (4.5 deciviews) is an average of the haze index (from IMPROVE data using the new IMPROVE equation) over the 5-year baseline period of 2000-2004.

Figure 3-6: URP Glide Path



## F. Determination of Uniform Rate of Progress

Table 3-1 provides the calculations for determining the Uniform Rate of Progress Glide Path and Best Days Baseline.

Table 3- 1: Great Sand Dunes National Park & Preserve – Determination of URP

Great Sand Dunes National Park										
Determination of Uniform Rate of Progress										
<i>New IMPROVE Algorithm used to calculate light extinction values</i>										
Site Code	Year		Parameter	20% Worst Day Average Value	Baseline Condition*	20% Best Day Average Value	BD Baseline Condition			
GRSA1	1989		Deciview (dv)	12.8		4.9				
GRSA1	1990		Deciview (dv)	13.0		5.6				
GRSA1	1991		Deciview (dv)	11.5		5.9				
GRSA1	1992		Deciview (dv)	10.6		5.2				
GRSA1	1993		Deciview (dv)	11.3		4.9				
GRSA1	1994		Deciview (dv)	13.2		4.2				
GRSA1	1995		Deciview (dv)	10.8		3.6				
GRSA1	1996		Deciview (dv)	11.9		3.7				
GRSA1	1997		Deciview (dv)	11.2		4.2				
GRSA1	1998		Deciview (dv)	12.5		5.5				
GRSA1	1999		Deciview (dv)	11.7		4.4				
GRSA1	2000		Baseline 2000-2004	Deciview (dv)		14.1		12.78	4.4	4.50
GRSA1	2001			Deciview (dv)		11.4			4.5	
GRSA1	2002	Deciview (dv)		14.3	5.0					
GRSA1	2003	Deciview (dv)		12.9	4.5					
GRSA1	2004	Deciview (dv)		11.2	4.1					
		2018			11.35	2018 Goal**				
		2064			6.66	Natural Conditions***				
Baseline Condition:				12.78	dv					
Natural Conditions:				6.66	dv					
Improvement needed by 2064:				6.12	dv					
Reduction/yr (60yrs)				0.102	dv					
						Range	Running Total			
Baseline-SIP Submittal (4 yrs):				0.41	dv	2005-08	0.41			
1st Planning Period (10 yrs):				1.02	dv	2008-18	1.43			
2nd Planning Period (10 yrs):				1.02	dv	2018-28	2.45			
3rd Planning Period (10 yrs):				1.02	dv	2028-38	3.47			
4th Planning Period (10 yrs):				1.02	dv	2038-48	4.49			
5th Planning Period (10 yrs):				1.02	dv	2048-58	5.51			
6th Planning Period (6 yrs):				0.61	dv	2058-64	6.12			
				6.12						
*Baseline Condition is defined as the 5 yr avg of the annual values for 20% Worst Days [2000-04] based on EPA's "Guidance for Tracking Progress Under the Regional Haze Program"										
**2018 Goal = [Baseline Condition - (14*Uniform Rate of Progress)]										
***Natural Conditions is based on Natural Haze Levels II Committee proposal Final Report: "Natural Haze Levels II: Application of the New IMPROVE Algorithm to Natural Species Concentrations"										

## SECTION 4: HAZE IMPACTING PARTICLES

### A. Aerosol Components

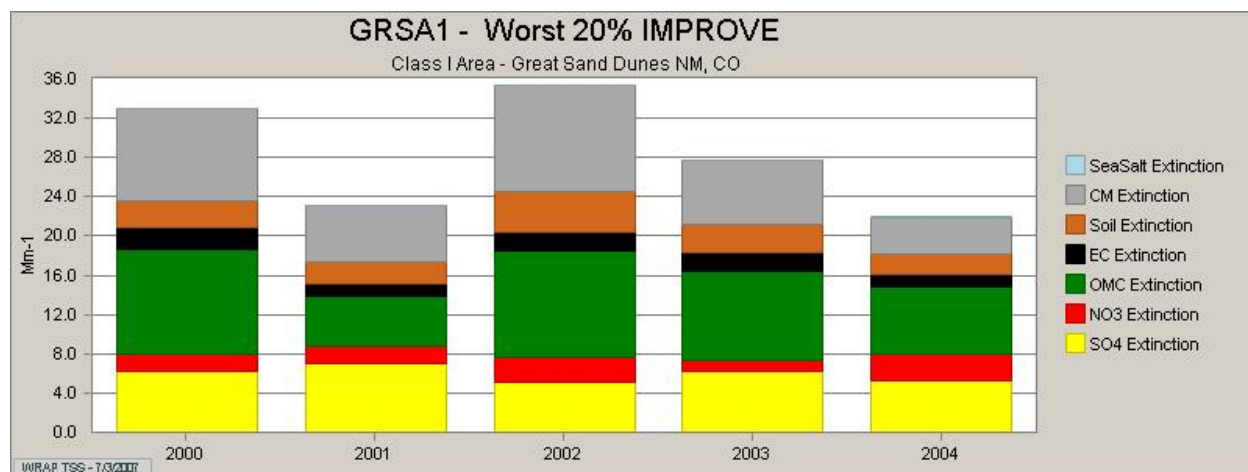
An aerosol is a gaseous suspension of fine solid or liquid particles. Some of these particles absorb light and others reflect or scatter light resulting in light extinction between the viewer and the light source. The IMPROVE monitor collects a 24-hour sample these particles onto a filter and they are analyzed at a laboratory to determine the components of the aerosol. In order to simplify the data analysis, some elemental particles and compounds are grouped together (based on scientific principals) into seven standard components. The components' differing effects on visibility are addressed through a complex calculation using the IMPROVE equation. The resultant output from the IMPROVE equation is known as reconstructed light extinction. Appendix G provides more detailed information on the IMPROVE equation. Table 4-1 lists the seven standard aerosol components of light extinction with the abbreviation and the default color used in the below listed graphics.

Aerosol Component	Abbreviation (Color)
1. Ammonium Sulfate	SO4 (yellow)
2. Ammonium Nitrate	NO3 (red)
3. Organic Mass Carbon	OMC (green)
4. Elemental Carbon	EC (black)
5. Fine Soil	Soil (orange)
6. Coarse Mass	CM (gray)
7. Sea Salt	Sea Salt (light blue)

### B. Aerosol Composition on Best and Worst Days

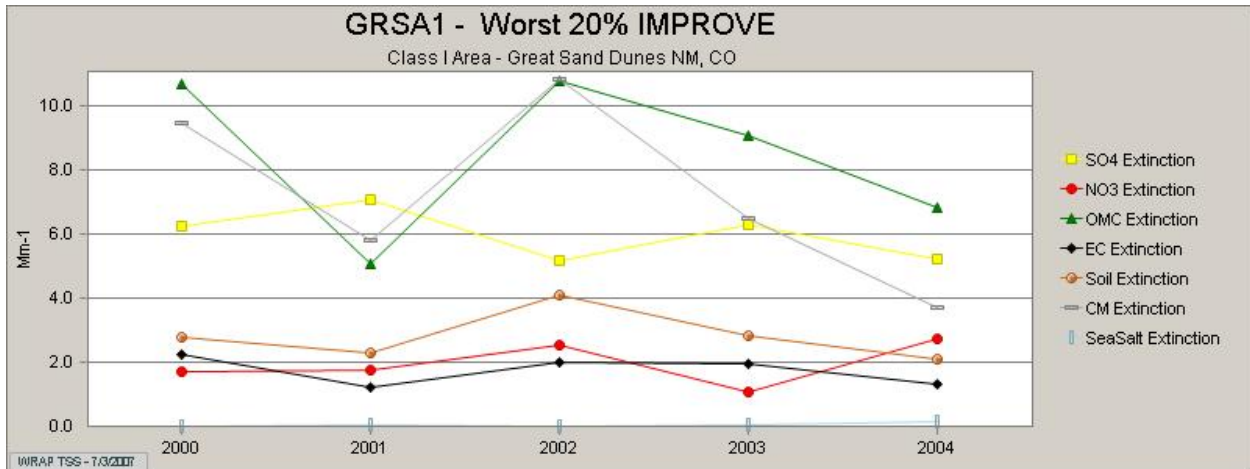
In Figure 4-1, the bar chart denotes the variability in the reconstructed light extinction over the baseline period based on IMPROVE data from the GRSA1 monitoring site for the 20% worst days.

Figure 4-1: Reconstructed Extinction for 20% Worst Days over Baseline Period



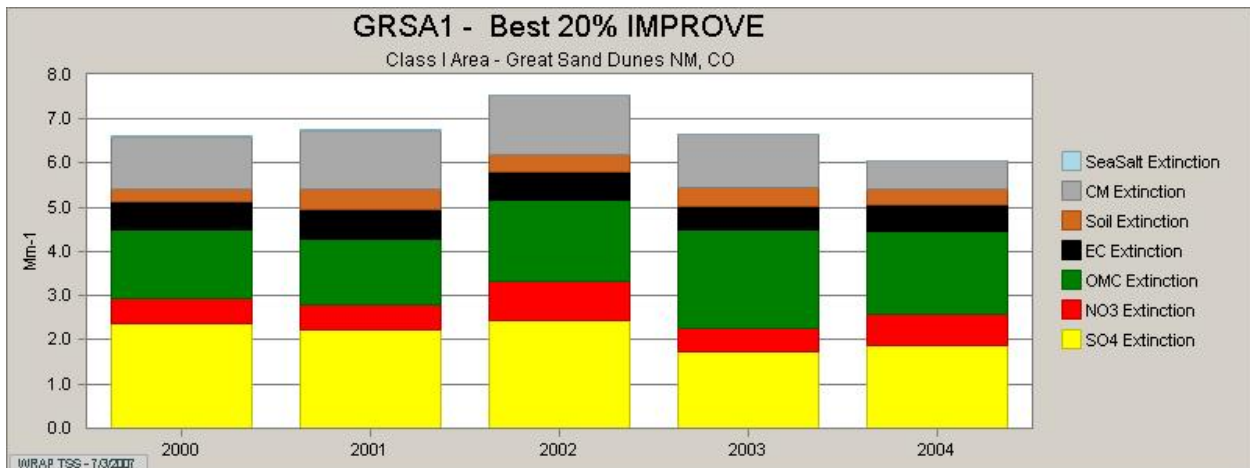
In Figure 4-2, the line graph denotes the variability in the individual components of reconstructed light extinction over the baseline period based on IMPROVE data from the GRSA1 monitoring site for the 20% worst days. The baseline period variation in OMC is over  $5 \text{ Mm}^{-1}$ , which indicates the range of effects produced by wildfire smoke. Not surprising for an area comprised of sand dunes, the baseline variation in CM is over  $7 \text{ Mm}^{-1}$  which is probably due to variations in meteorology.

Figure 4-2: Reconstructed Extinction for 20% Worst Days over Baseline Period



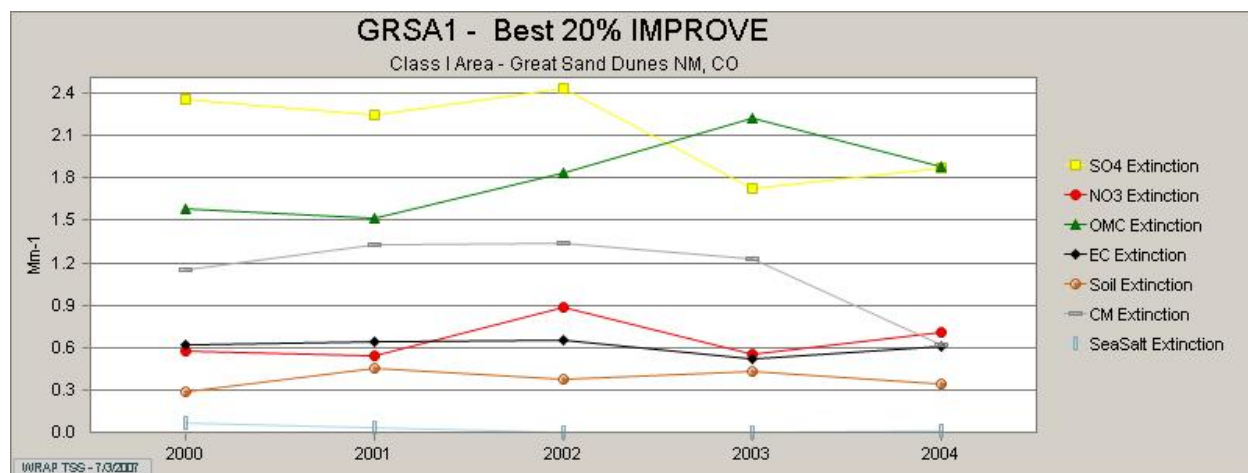
In Figure 4-3, the bar chart denotes the variability in the reconstructed light extinction over the baseline period based on IMPROVE data from the GRSA1 monitoring site for the 20% best days. Note the range for the best days is about 1/4 of the worst days.

Figure 4-3: Reconstructed Extinction for 20% Best Days over Baseline Period



In Figure 4-4, the line graph denotes the variability in the individual components of reconstructed light extinction over the baseline period based on IMPROVE data from the GRSA1 monitoring site for the 20% best days.

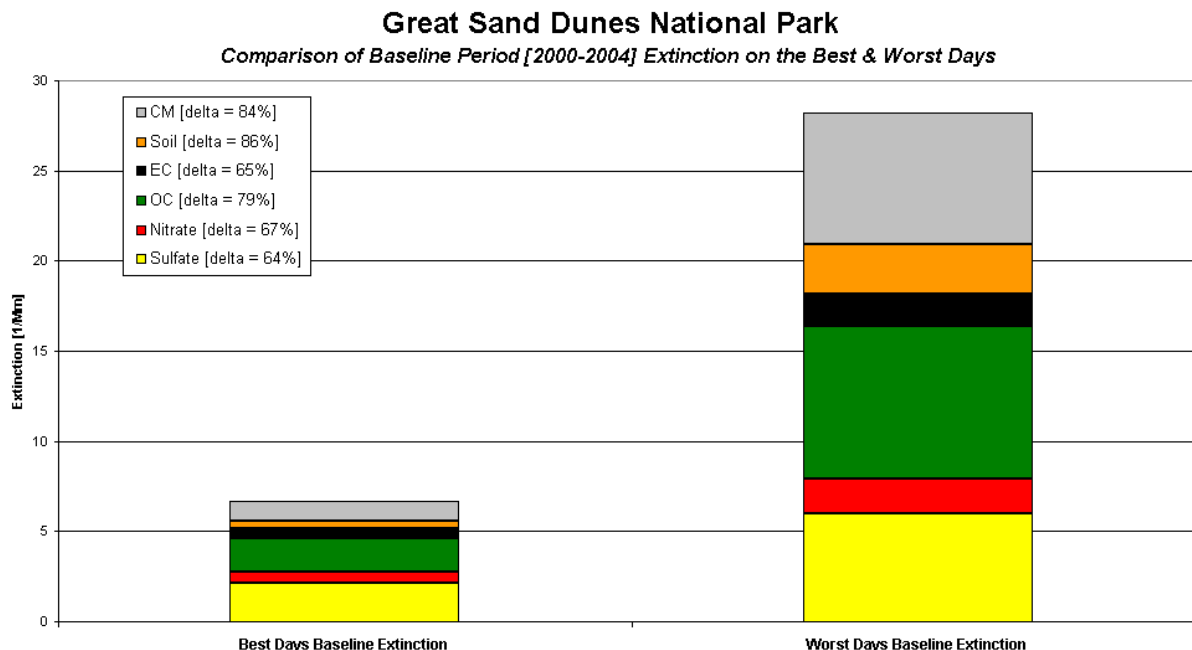
Figure 4-4: Reconstructed Extinction for 20% Best Days over Baseline Period



### C. Comparison of Baseline Extinction for Best & Worst Days

In Figure 4-5, the bar graphs compare the baseline average for the 20% best days with the 20% worst days based on GRSA1 IMPROVE monitoring data. Although all components of extinction are considerably less on the best days, it seems that significant changes (>80%) in CM and soil result in visibility improvements on the best days.

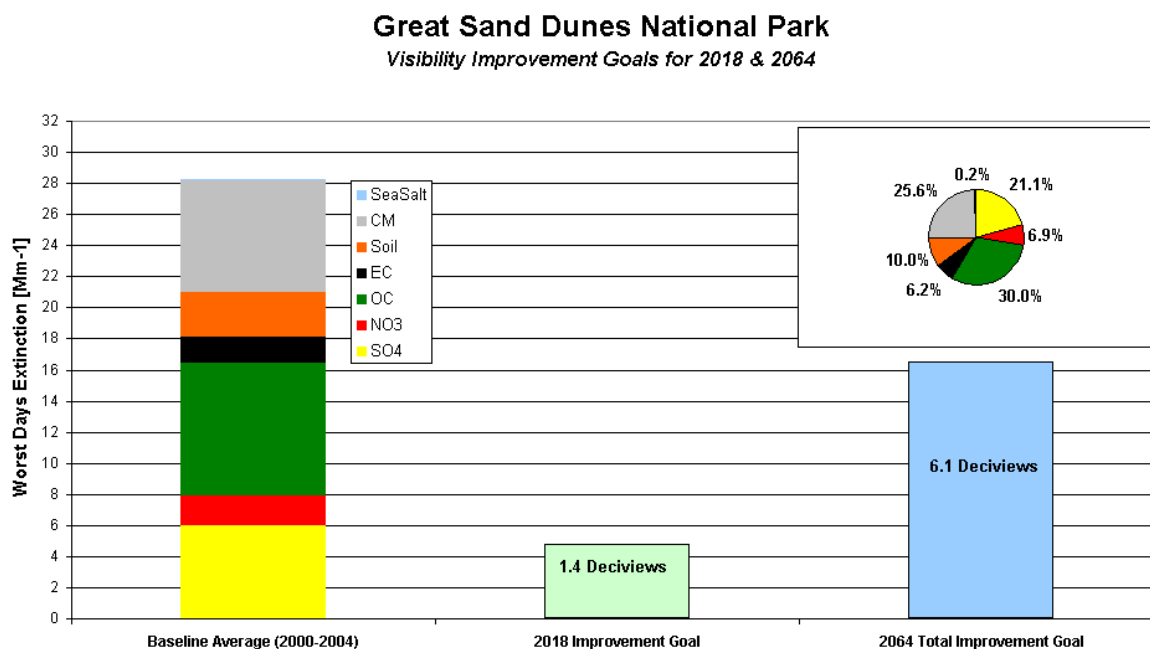
Figure 4-5: Comparison of Baseline Extinction for 20% Best & Worst Days



## D. Visibility Improvement Needed – 20% Worst Days

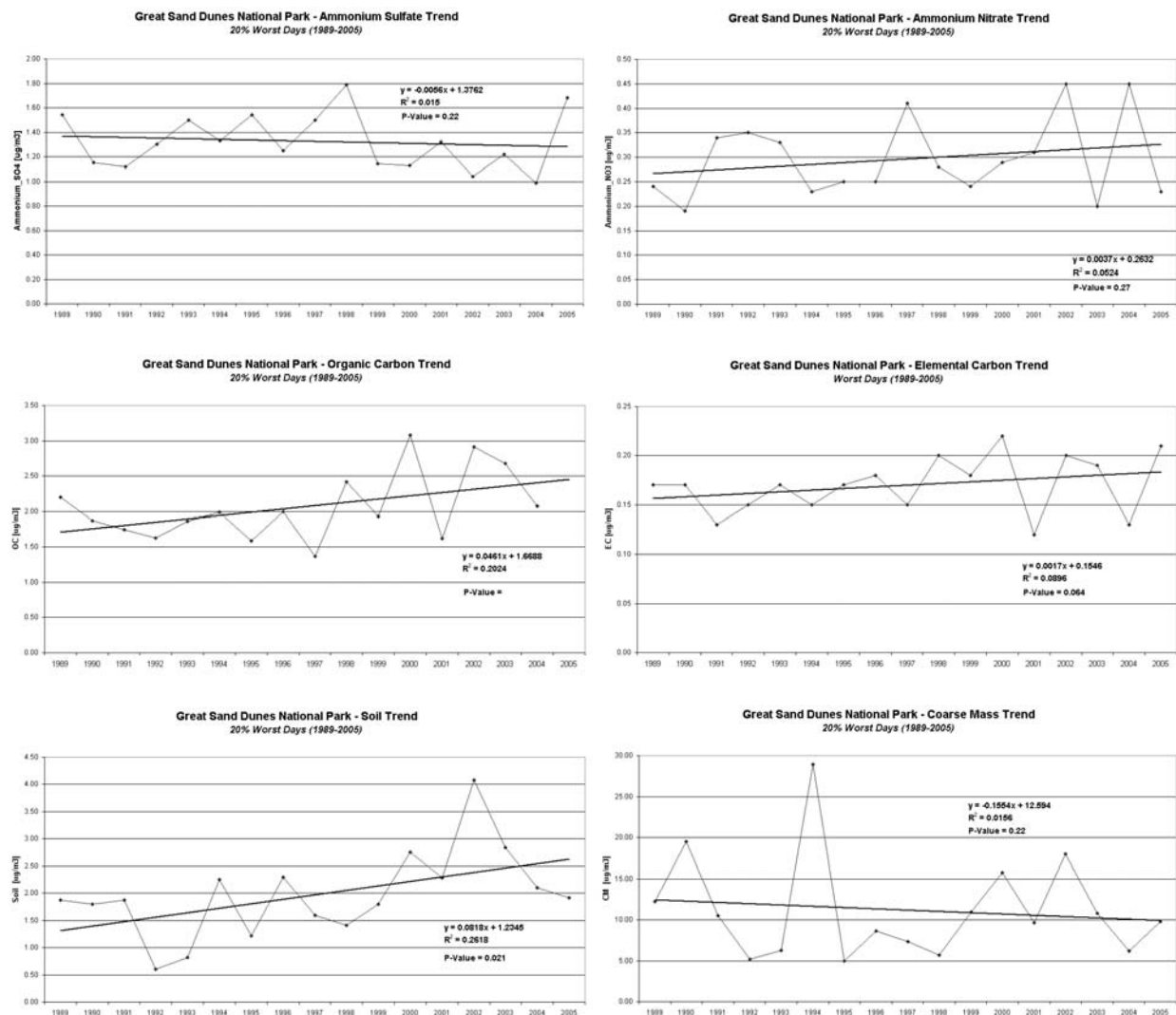
Figure 4-6 displays the relative contributions to visibility extinction averaged over the baseline conditions period for the 20% worst days. The significant contributors to visibility degradation, as depicted in the stacked bar graph and pie chart, appear to be ammonium sulfate, organic carbon and coarse material. In the middle, the light green bar indicates the magnitude of improvement (bext = 4.78 Mm<sup>-1</sup> or 1.43 deciviews) necessary to achieve the 2018 uniform progress (UP) goal. To the far right, the light blue bar indicates the magnitude of improvement (bext = 16.43 Mm<sup>-1</sup> or 6.1 deciviews) necessary to achieve the 2064 natural conditions goal.

Figure 4-6: Average Contributions to Reconstructed Extinction for 20% Worst Days



## E. Aerosol Pollutant Trends – 20% Worst Days

The following graphs are a linear regression of the annual data points for the six haze causing pollutants from the GRSA1 IMPROVE monitor site for years 1989-2005:



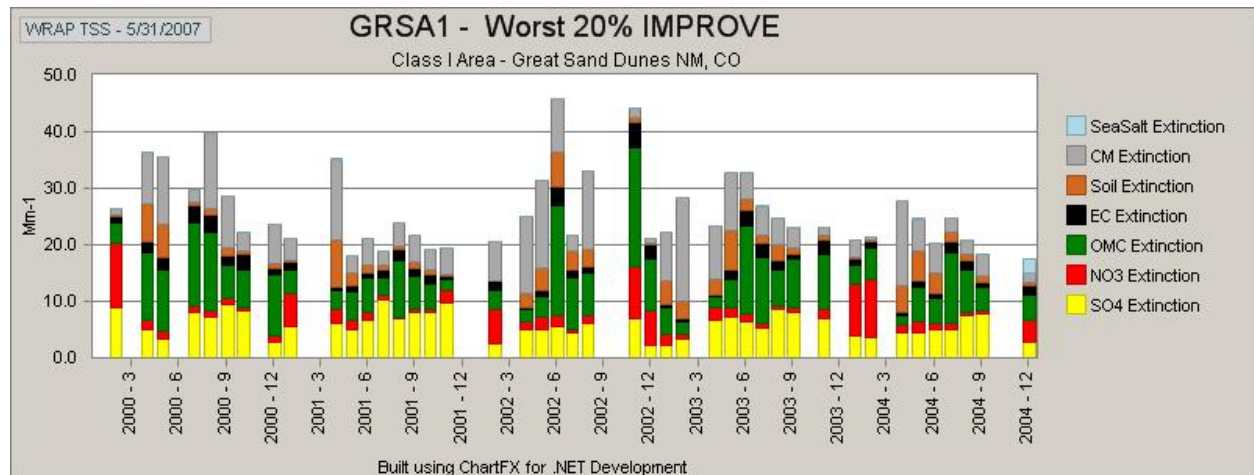
The graphs utilize valid data from years prior to and after the baseline conditions period. The trends for Elemental Carbon and Soil are statistically significant. Appendix G contains detailed statistical information on each trend.

Continued improvements in sulfate levels are expected in the West as further controls are realized on major sulfur dioxide sources. Since sulfates have a disproportionately high impact on visibility in contrast to coarse mass particulates, we expect the downward trend in sulfates will provide continued visibility improvement. However, trends in organic carbon and fine soil are not as encouraging. The protracted drought throughout the West could be contributing to the recent upswing in organic carbon, due to wildfires, and the increasing trend in fine soil (PM<sub>2.5</sub>), due to dusty and dry conditions.

## F. Monthly Distribution - 20% Worst Days

Figure 4-7 displays in reconstructed extinction the monthly distribution of 20% worst days on 5-year basis over the baseline period for GRSA1. The worst days appear scattered throughout the year although more occur in the second and third quarters when fires, dust events, and photochemical processes maximize organic and elemental readings as well as elevating secondary particulate formation.

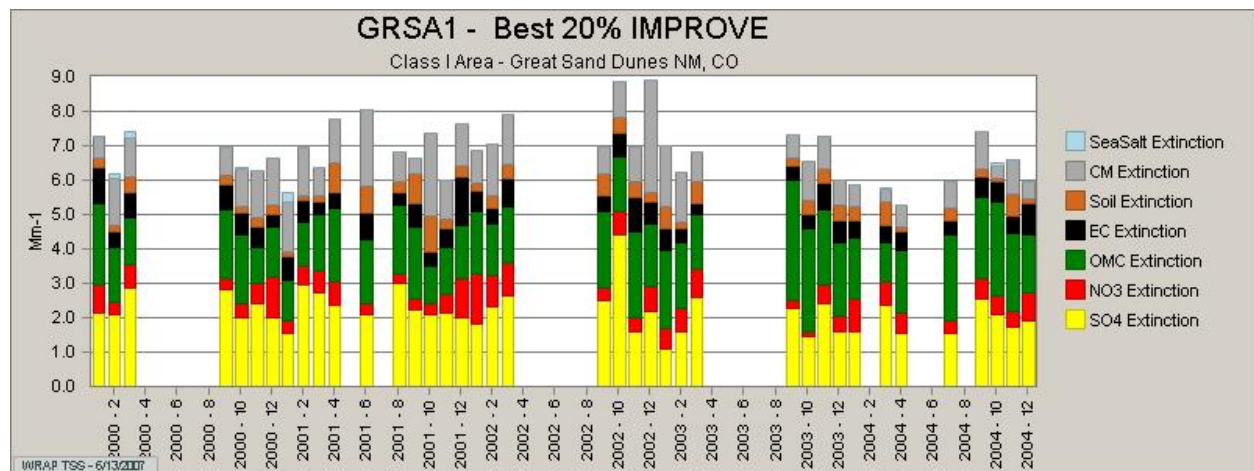
Figure 4-7: Monthly Distribution of 20% Worst Days



## G. Monthly Distribution - 20% Best Days

Figure 4-8 displays in reconstructed extinction the monthly distribution of 20% best days on 5-year basis over the baseline period for GRSA1. The best days appear scattered throughout the year although more occur in the late fall, winter and spring when there is an absence of fires, dust events, and photochemical processes that maximize organic and elemental readings as well as elevating secondary particulate formation.

Figure 4-8: Monthly Distribution of 20% Best Days



## **SECTION 5: EMISSION SOURCE CHARACTERIZATION**

### **A. State Emission Inventory and Regional Emission Maps**

The following tables provide summary information for the planning 2002c (Plan 02c) emission inventory and the baseline 2018b (Base 18b) emission inventory along with the net change in emissions that were used in the regional modeling analysis.

The Plan 02c emission inventory represents an annual (calendar year) snapshot of emissions for ten source categories (point, area, on-road/off-road mobile, oil & gas, road dust, fugitive dust, anthropogenic fire, natural fire and biogenic) that were derived from a number of sources including Division permits, MOBILE 6 modeling, or other modeled estimates based on activity level.

The State has several existing regulatory programs that mitigate the emissions from point sources (Regulations 1, 3, 6 and Common Provisions), mobile sources (Regulations 10, 11 and 12), area sources (Regulations 4, 7 and 16) and fire (Regulation 9). Future emission reductions anticipated from recent changes to Regulation 7 (adopted in Dec. 2006) and Best Available Retrofit Technology (BART) under Regulation 3 are partially included in the 2018b emission inventory. Further, a revised WRAP region oil and gas inventory (phase II) was completed in summer 2007 and is included in this 2018b emission inventory and modeling analyses. The phase II oil & gas update builds upon the phase I work and provides more basin specific emission data from local producers and a more comprehensive inventory of area sources.

The WRAP developed a revised preliminary reasonable progress emission inventory for 2018, known as the 2018PRP, that reflects not only recent changes to Reg 7 and all Colorado BART but projected BART emission reductions across the WRAP region. The WRAP released the 2018PRP emission inventory in the fall of 2007 along with updated regional modeling.

The WRAP anticipates that a final emission inventory update, known as 2018FRP, along with final regional modeling demonstration would be completed near the end of 2008 to early 2009 timeframe. The 2018FRP emission inventory would include the final BART determinations for the entire WRAP region along with other on-the-books (OTB) and on-the-way (OTW) controls. These future updates to the 2018 emission estimates and visibility forecasts will be included in future presentations of emissions and modeling and will be reflected in future editions of this TSD.

The emission inventories are based on statewide data that include tables for sulfur dioxide (SO<sub>2</sub>), oxides of nitrogen (NO<sub>x</sub>), ammonia (NH<sub>3</sub>), primary organic aerosol (POA), volatile organic compounds (VOCs), elemental carbon (EC), fine soil (PM<sub>2.5</sub>) and coarse mass (CM) that list as many as ten different source categories.

The following maps of the regional modeling domain depict 36x36 km grid cells that include color-coded emission rates for selected air pollutants. Emissions for each grid cell represent summations from point, area, mobile, dust, fire and biogenic sources in tons for year 2002 and 2018.

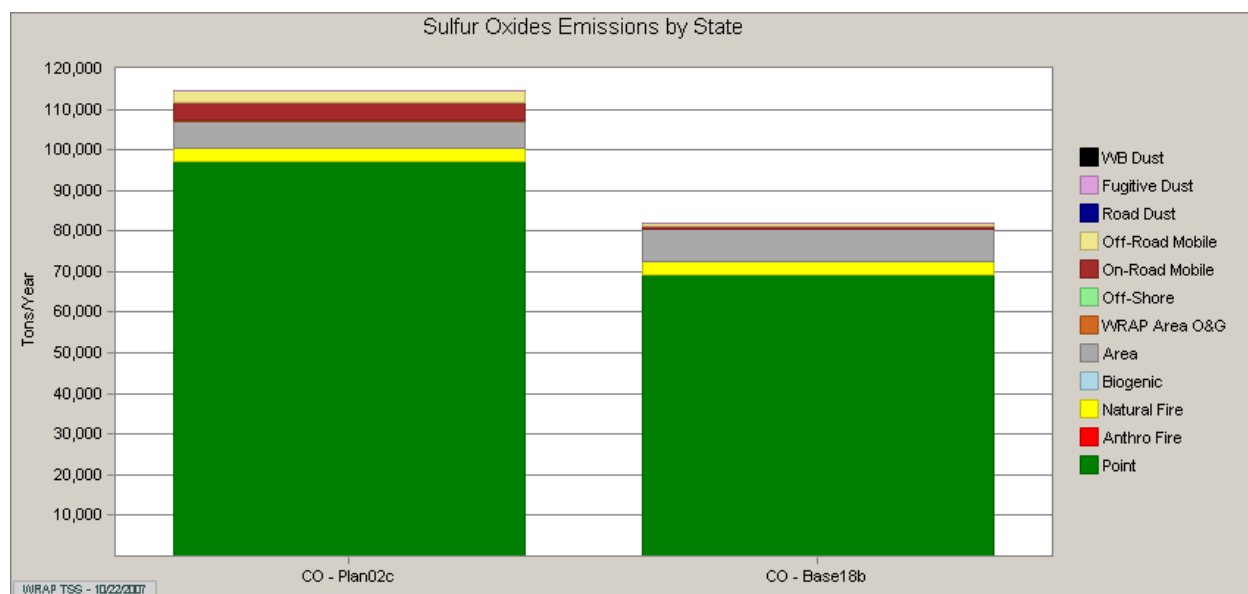
### (1) Colorado SO<sub>2</sub> Emission Inventory for 2002 & 2018

Sulfur dioxide gases (SO<sub>2</sub>) are formed when sulfur-containing fuels, such as diesel or coal, are burned, when gasoline is extracted from oil or when metals are extracted from ore. SO<sub>2</sub> dissolves in water vapor to form acid, and contributes to the formation of sulfate compounds [e.g. (NH<sub>4</sub>)<sub>2</sub>SO<sub>4</sub>] when ammonia is available. These compounds can scatter the transmission of light, contributing to visibility reduction on a regional scale at our Class I Areas.

In Figure 5-1, the projected statewide SO<sub>2</sub> emission reduction is about 29%. The anticipated 29% reduction in point source emissions statewide are largely due to the early implementation of BART level emission controls on several large power plants prior to the 2002 baseline period. The 18% increase in area sources is largely due to forecast increases in activity levels based on population growth. The substantial reduction in on-road and off-road mobile sources are primarily due to new federal fuel standards that require lower sulfur content.

Figure 5-1: Colorado SO<sub>2</sub> Emissions – 2002 & 2018 Inventory

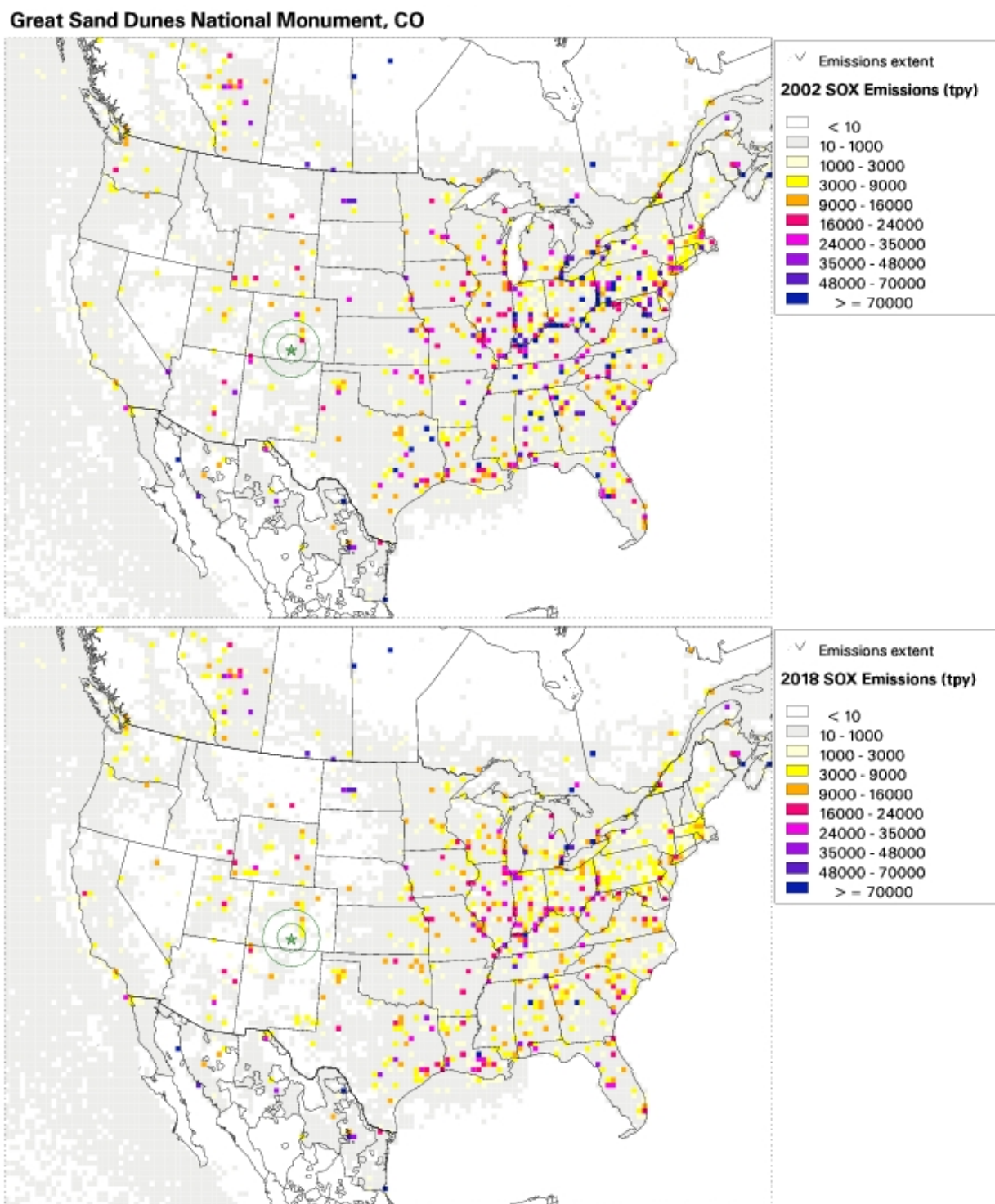
Colorado Planning and Baseline Emission Inventories			
Source Category	Statewide SO <sub>2</sub>		
	Plan 02c [tpy]	Base 18b [tpy]	Net Change
Point	97,016	69,262	-29%
Area	6,504	7,676	18%
On-Road Mobile	4,389	677	-85%
Off-Road Mobile	3,015	781	-74%
Oil & Gas	260	9	-97%
Road Dust	4	0	-100%
Fugitive Dust	5	6	29%
Anthro Fire	108	91	-15%
Natural Fire	3,335	3,335	0%
Biogenic	0	0	0%
<b>Total:</b>	<b>114,636</b>	<b>81,837</b>	<b>-29%</b>



## (2) Regional Map of SOx Emissions for 2002 & 2018

Figure 5-2, provides the plan02c and base18b regional SOx emission maps with the location of the GRSA1 IMPROVE monitor identified with a green star surrounded by 100 km and 200 km radius concentric circles.

Figure 5-2: Regional SOx Emissions – 2002 & 2018 Inventory



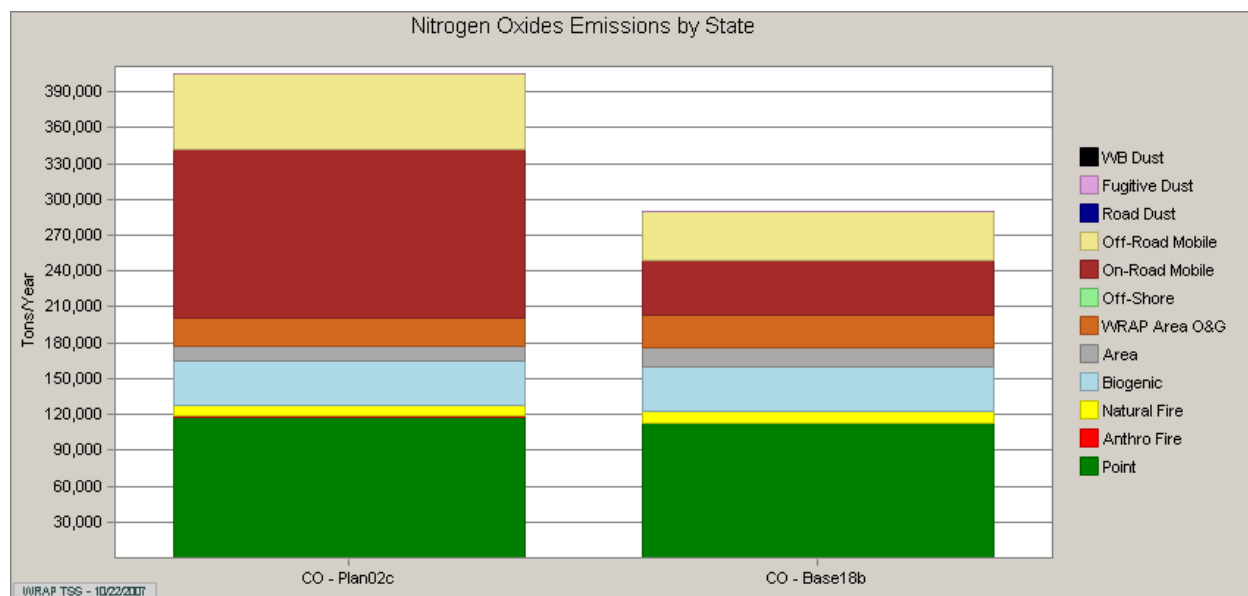
### (3) Colorado NOx Emission Inventory for 2002 & 2018

Nitrogen oxides (NOx) form when fuel is burned at high temperatures. NOx emissions are highly reactive and can form nitrate compounds [e.g. NH<sub>4</sub>NO<sub>3</sub>] when ammonia is available. These compounds can scatter the transmission of light, contributing to visibility reduction on a regional scale at our Class I Areas.

In Figure 5-3, the projected statewide NOx emission reduction is about 28%. The anticipated 5% point source reduction statewide is due to BART emission controls on large industrial boilers and cleaner engine standards. The 40% increase in area sources is largely due to forecast increases in activity levels based on population growth. The substantial reduction in on-road and off-road mobile sources are primarily due to new federal vehicle emission standards (Tier 2). The 20% increase in O&G is attributed to the recent growth surge in this sector.

Figure 5-3: Colorado NOx Emissions – 2002 & 2018 Inventory

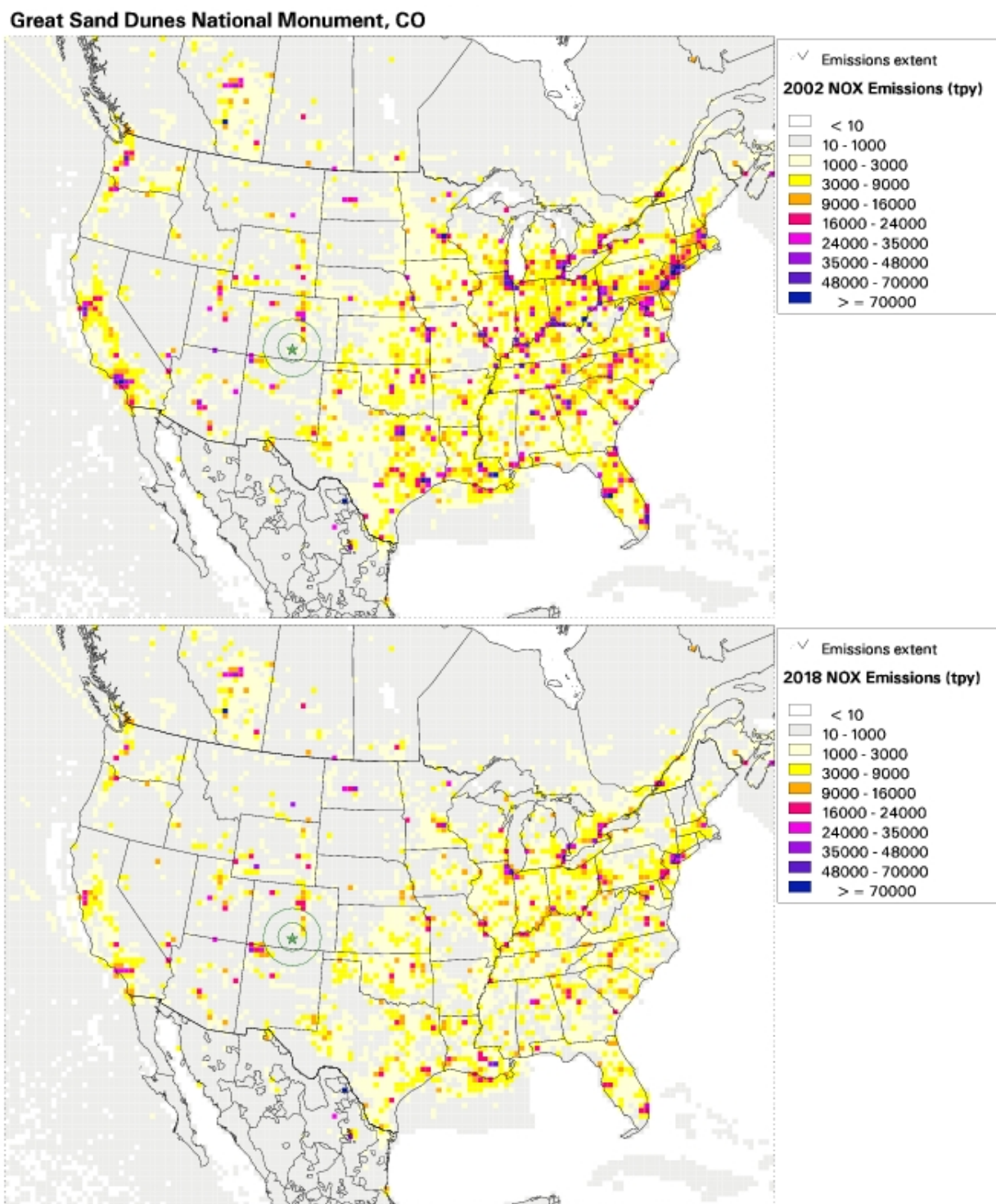
Colorado Planning and Baseline Emission Inventories			
Source Category	Statewide NOx		
	Plan 02c [tpy]	Base 18b [tpy]	Net Change
Point	117,869	112,241	-5%
Area	11,645	16,360	40%
On-Road Mobile	141,883	45,249	-68%
Off-Road Mobile	62,447	40,804	-35%
Oil & Gas	23,351	27,993	20%
Road Dust	1	0	-100%
Fugitive Dust	13	17	29%
Anthro Fire	520	408	-21%
Natural Fire	9,377	9,377	0%
Biogenic	37,349	37,349	0%
<b>Total:</b>	<b>404,455</b>	<b>289,799</b>	<b>-28%</b>



#### (4) Regional Map of NOx Emissions for 2002 & 2018

Figure 5-4, provides the plan02c and base18b regional NOx emission maps with the location of the GRSA1 IMPROVE monitor identified with a green star surrounded by 100 km and 200 km radius concentric circles.

Figure 5-4: Regional NOx Emissions – 2002 & 2018 Inventory



## (5) Colorado NH<sub>3</sub> Emission Inventory for 2002 & 2018

Ammonia (NH<sub>3</sub>) is a compound that is normally encountered as a gas with a characteristic pungent odor. Ammonia occurs both naturally and is produced by human activity that is an important source of nitrogen, which is needed by plants and animals.

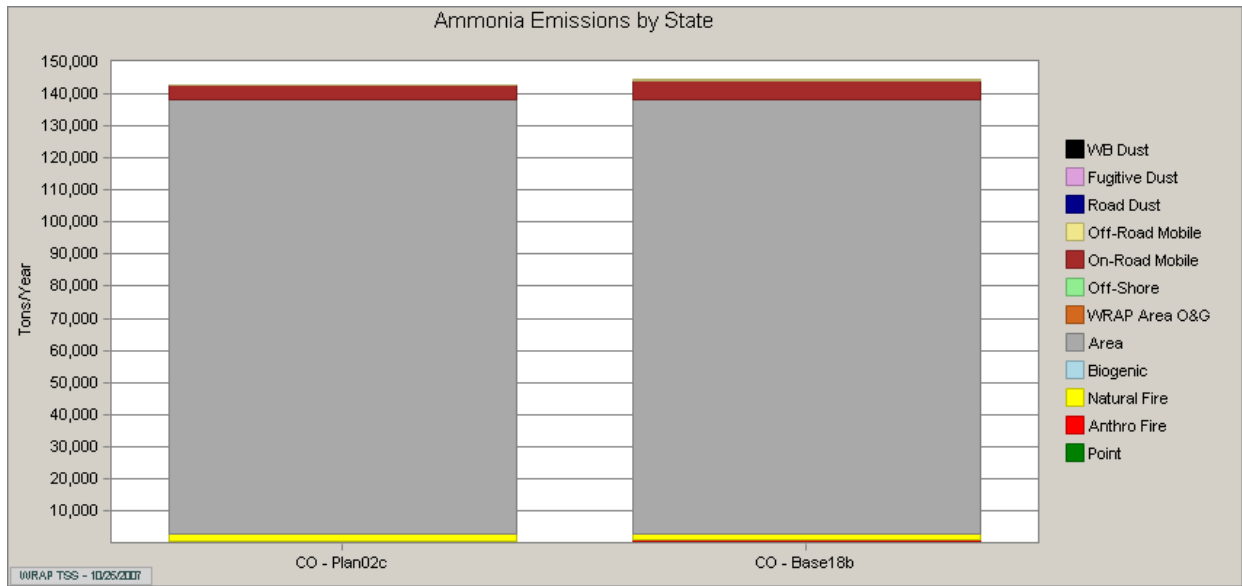
Recent advances in the understanding of the health impacts of particulate pollution and the important role ammonia (NH<sub>3</sub>) emissions play in the formation of secondary particulate matter (PM) has spawned a great deal of new research into ammonia emissions. Major sources of NH<sub>3</sub> emissions include livestock operations, fertilizer use, waste management, mobile sources, industrial point sources, and various biological sources including human respiration, wild animals, and soil microbial processes. For each of these source categories there remain large uncertainties in the magnitude of emissions, the diurnal and seasonal variation, and the spatial distribution. Uncertainty in NH<sub>3</sub> emissions is a key source of uncertainty in the formation of sulfate and nitrate aerosols. Thus, development of improved NH<sub>3</sub> emissions inventories is essential for modeling the formation of fine PM, regional haze, and for developing effective plans to mitigate visibility impairment at National Parks, Forests and Wilderness Areas.

Significant improvements have been made in the understanding of ammonia emissions since the development of the current 1996 National Emissions Inventory (NEI) that was used in the Western Regional Air Partnership (WRAP) visibility modeling to meet Clean Air Act Section 309 requirements. Particularly, the temporal dependence of ammonia emissions on environmental parameters has been the focus of several recent research efforts. The WRAP has provided funding to the Regional Modeling Center (RMC) to develop an improved NH<sub>3</sub> emissions inventory for the WRAP States and tribes to use in Clean Air Act Section 308 modeling.

In Figure 5-5, the projected statewide NH<sub>3</sub> emission increase is about 1%. The anticipated 16% increase in statewide point sources is attributed to population growth. The 37-38% increase in on-road mobile and off-road sources is largely due to forecast increases in vehicle traffic associated with population growth.

Figure 5-5: Colorado NH<sub>3</sub> Emissions – 2002 & 2018 Inventory

Colorado Planning and Baseline Emission Inventories			
Source Category	Statewide Ammonia		
	Plan 02c [tpy]	Base 18b [tpy]	Net Change
Point	539	623	16%
Area	135,736	135,757	0%
On-Road Mobile	4,317	5,894	37%
Off-Road Mobile	43	60	38%
Oil & Gas	0	0	0%
Road Dust	0	0	0%
Fugitive Dust	0	0	0%
Windblown Dust	0	0	0%
Anthro Fire	137	95	-31%
Natural Fire	1,965	1,965	0%
Biogenic	0	0	0%
<b>Total:</b>	<b>142,737</b>	<b>144,393</b>	<b>1%</b>



The WRAP has not produced regional maps comparing 2002 and 2018 ammonia emissions.

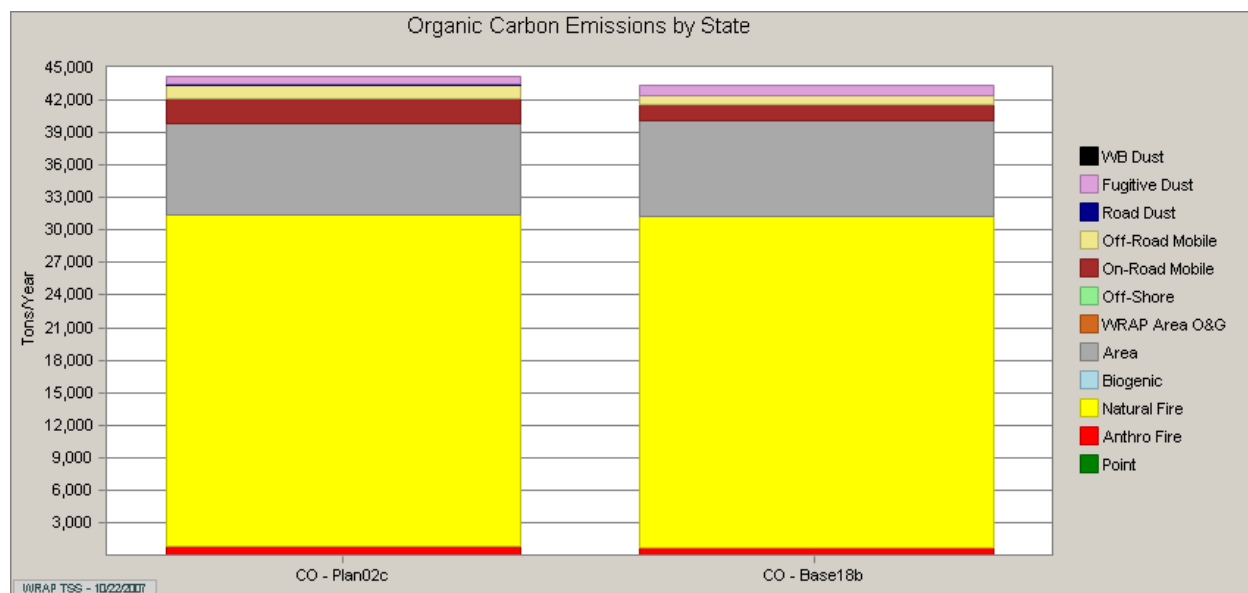
## (6) Colorado POA Emission Inventory for 2002 & 2018

Primary Organic Aerosol (POA) is the directly emitted particulate form of organic carbon that is created through the combustion of fossil fuels or organic matter and meat cooking. POA particulates scatter the transmission of light that contributes to visibility reduction on a regional scale at our Class I Areas.

In Figure 5-6, the projected statewide POA emission reduction is about 2%. Most of the anticipated reduction comes from new federal vehicle emission standards applicable to on-road and off-road mobile sources.

Figure 5-6: Colorado POA Emissions – 2002 & 2018 Inventory

Colorado Planning and Baseline Emission Inventories			
Source Category	Statewide POA		
	Plan 02c [tpy]	Base 18b [tpy]	Net Change
Point	17	62	255%
Area	8,444	8,786	4%
On-Road Mobile	2,189	1,568	-28%
Off-Road Mobile	1,286	865	-33%
Oil & Gas	0	0	0%
Road Dust	100	0	-100%
Fugitive Dust	660	853	29%
Anthro Fire	850	621	-27%
Natural Fire	30,581	30,581	0%
Biogenic	0	0	0%
<b>Total:</b>	<b>44,129</b>	<b>43,335</b>	<b>-2%</b>

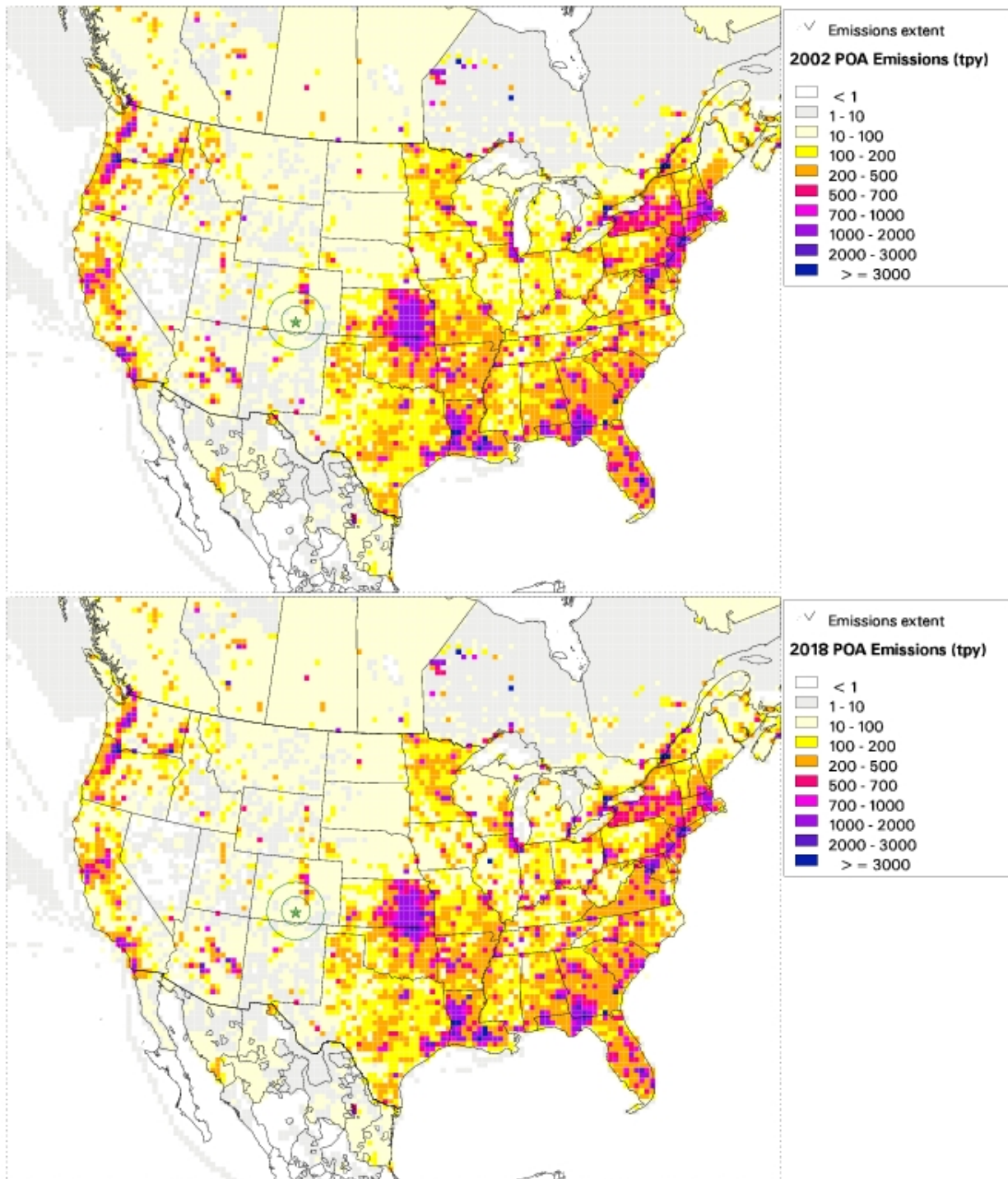


**(7) Regional Map of POA Emissions for 2002 & 2018**

Figure 5-7, provides the plan02c and base18b regional POA emissions with the location of the GRSA1 IMPROVE monitor identified with a green star surrounded by 100 km and 200 km radius concentric circles.

Figure 5-7: Regional POA Emissions – 2002 & 2018 Inventory

**Great Sand Dunes National Monument, CO**



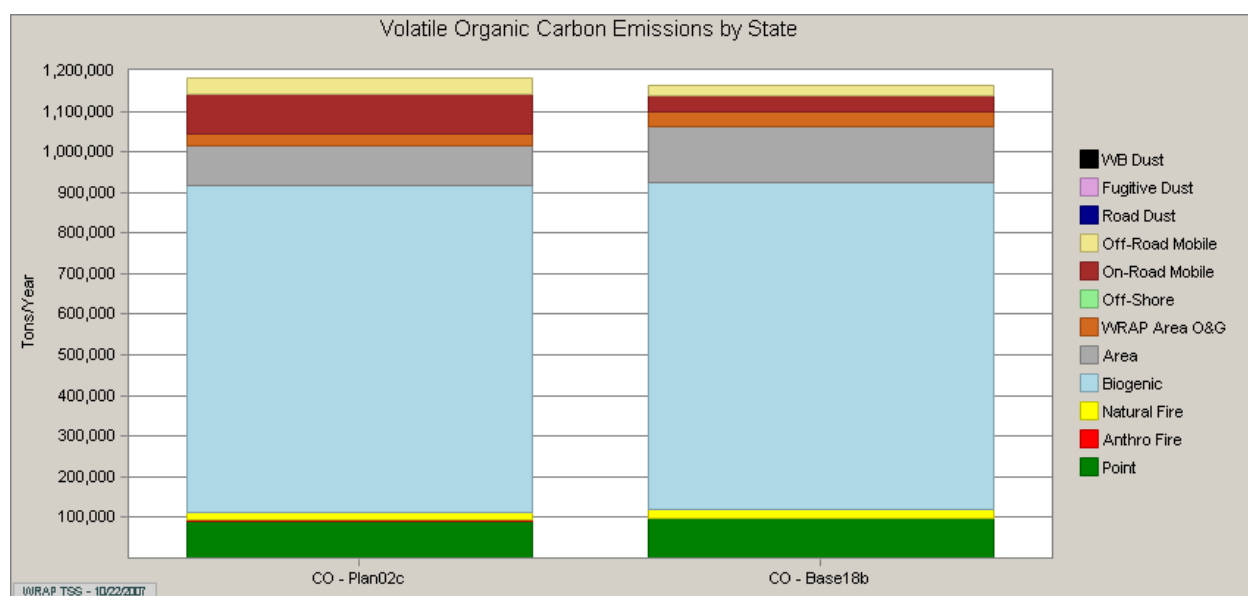
## (8) Colorado VOC Emission Inventory for 2002 & 2018

Organic carbon particulates can be emitted as a primary organic aerosol (POA) or they can be formed as a secondary organic aerosol (SOA). Secondary organics are formed when volatile organic carbon (VOC) emissions react with oxides of nitrogen and sunlight to form ozone, which acts as a catalyst for particulate formation. VOCs may also condense to form particulate organic carbon (OC). The WRAP did not create regional VOC emission maps denoting the origin of these emissions. Some example sources of volatile organic compounds include trees, fires, vehicle refueling, industrial processes and application of architectural coatings.

In Figure 5-8, the projected statewide VOC emission reduction is about 1%. Most of the anticipated reduction comes from new federal fuel standards applicable to on-road and off-road mobile sources.

Figure 5-8: Colorado VOC Emissions – 2002 & 2018 Inventory

Colorado Planning and Baseline Emission Inventories			
Source Category	Statewide VOC		
	Plan 02c [tpy]	Base 18b [tpy]	Net Change
Point	91,750	98,630	7%
Area	98,695	136,032	38%
On-Road Mobile	100,860	41,489	-59%
Off-Road Mobile	38,401	25,004	-35%
Oil & Gas	25,954	37,855	46%
Road Dust	0	0	0%
Fugitive Dust	0	0	0%
Anthro Fire	915	666	-27%
Natural Fire	20,404	20,404	0%
Biogenic	804,777	804,777	0%
<b>Total:</b>	<b>1,181,756</b>	<b>1,164,855</b>	<b>-1%</b>



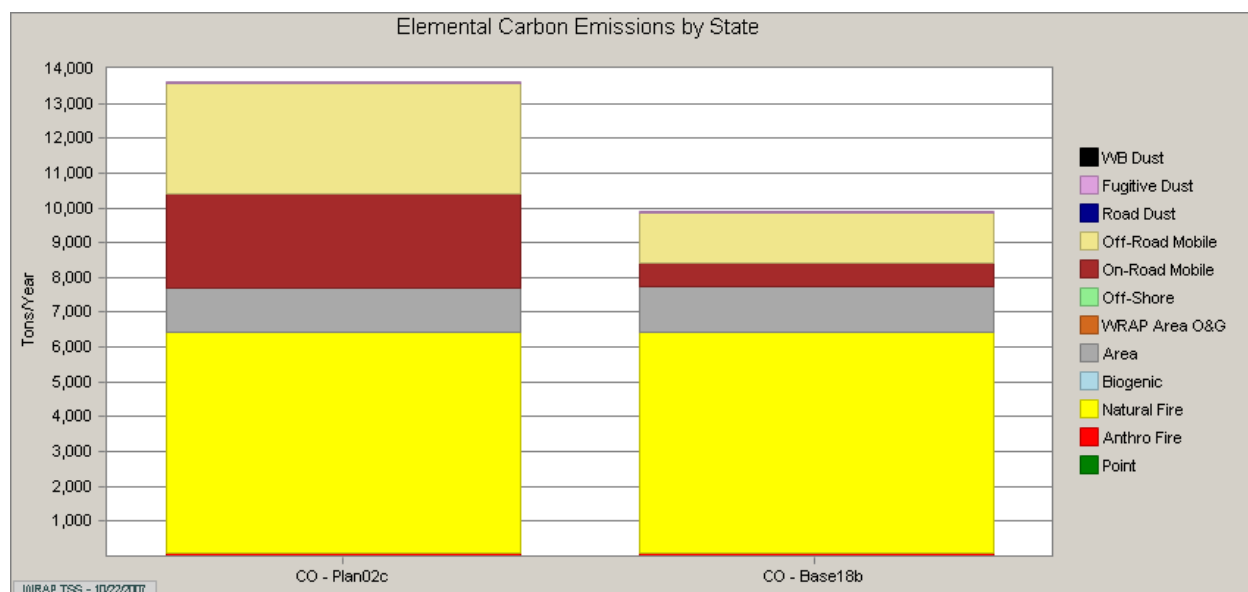
### (9) Colorado EC Emission Inventory for 2002 & 2018

Elemental carbon particulates are directly emitted as a primary aerosol. Some example sources of elemental carbon include fossil fuel combustion (vehicles, boilers & other industrial processes), wildfires and all other types of burning. EC particulates absorb the transmission of light that contributes to visibility reduction on a regional scale at our Class I Areas.

In Figure 5-9, the projected statewide EC emission reduction is about 27%. Most of the anticipated reduction comes from new federal standards on vehicle emissions and fuels that are applicable to on-road and off-road mobile sources.

Figure 5-9: Colorado EC Emissions – 2002 & 2018 Inventory

Colorado Planning and Baseline Emission Inventories			
Source Category	Statewide EC		
	Plan 02c [tpy]	Base 18b [tpy]	Net Change
Point	0	3	0%
Area	1,263	1,328	5%
On-Road Mobile	2,698	682	-75%
Off-Road Mobile	3,175	1,431	-55%
Oil & Gas	0	0	0%
Road Dust	8	0	-100%
Fugitive Dust	45	58	29%
Anthro Fire	92	74	-20%
Natural Fire	6,337	6,337	0%
Biogenic	0	0	0%
<b>Total:</b>	<b>13,619</b>	<b>9,913</b>	<b>-27%</b>

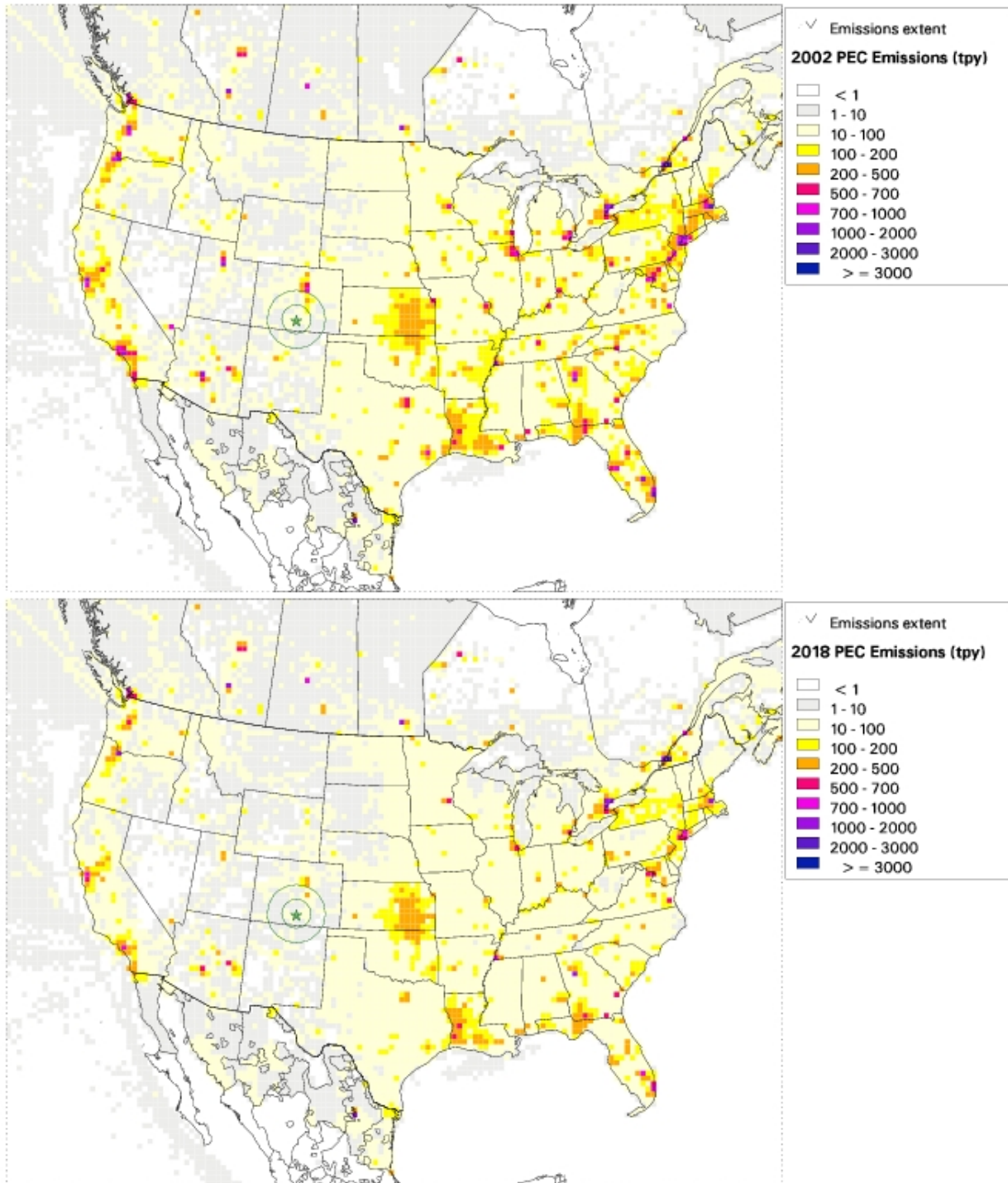


### (10) Regional Map of EC Emissions for 2002 & 2018

Figure 5-10, provides the plan02c and base18b regional elemental carbon emissions with the location of the GRSA1 IMPROVE monitor identified with a green star surrounded by 100 km and 200 km radius concentric circles.

Figure 5-10: Regional EC Emissions – 2002& 2018 Inventory

#### Great Sand Dunes National Monument, CO



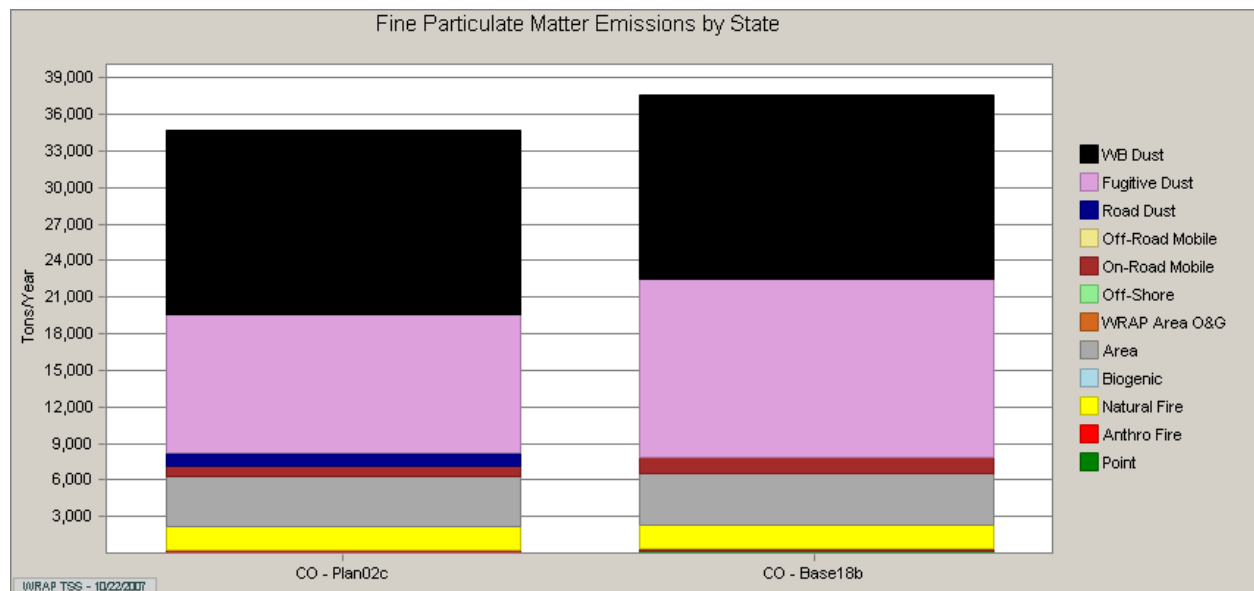
### (11) Colorado Soil Emission Inventory for 2002 & 2018

Soil emissions are comprised of fine particulates under 2.5 microns that are generated mostly by area sources, fugitive dust and windblown dust. Fine particulate matter can remain suspended in the atmosphere for long periods of time and travel long distances. Fine particulates can efficiently scatter the transmission of light that contributes to visibility reduction on a regional scale at our Class I Areas.

In Figure 5-11, the projected statewide soil emission increase is about 8%. Most of the anticipated increase is associated with fugitive dust.

Figure 5-11: Colorado Soil Emissions – 2002 & 2018 Inventory

Colorado Planning and Baseline Emission Inventories			
Source Category	Statewide Soil (fine PM)		
	Plan 02c [tpy]	Base 18b [tpy]	Net Change
Point	6	191	3293%
Area	4,091	4,237	4%
On-Road Mobile	812	1,250	54%
Off-Road Mobile	0	0	0%
Oil & Gas	0	0	0%
Road Dust	1,072	0	-100%
Fugitive Dust	11,394	14,720	29%
Windblown Dust	15,105	15,105	0%
Anthro Fire	253	169	-33%
Natural Fire	1,948	1,948	0%
Biogenic	0	0	0%
<b>Total:</b>	<b>34,681</b>	<b>37,620</b>	<b>8%</b>

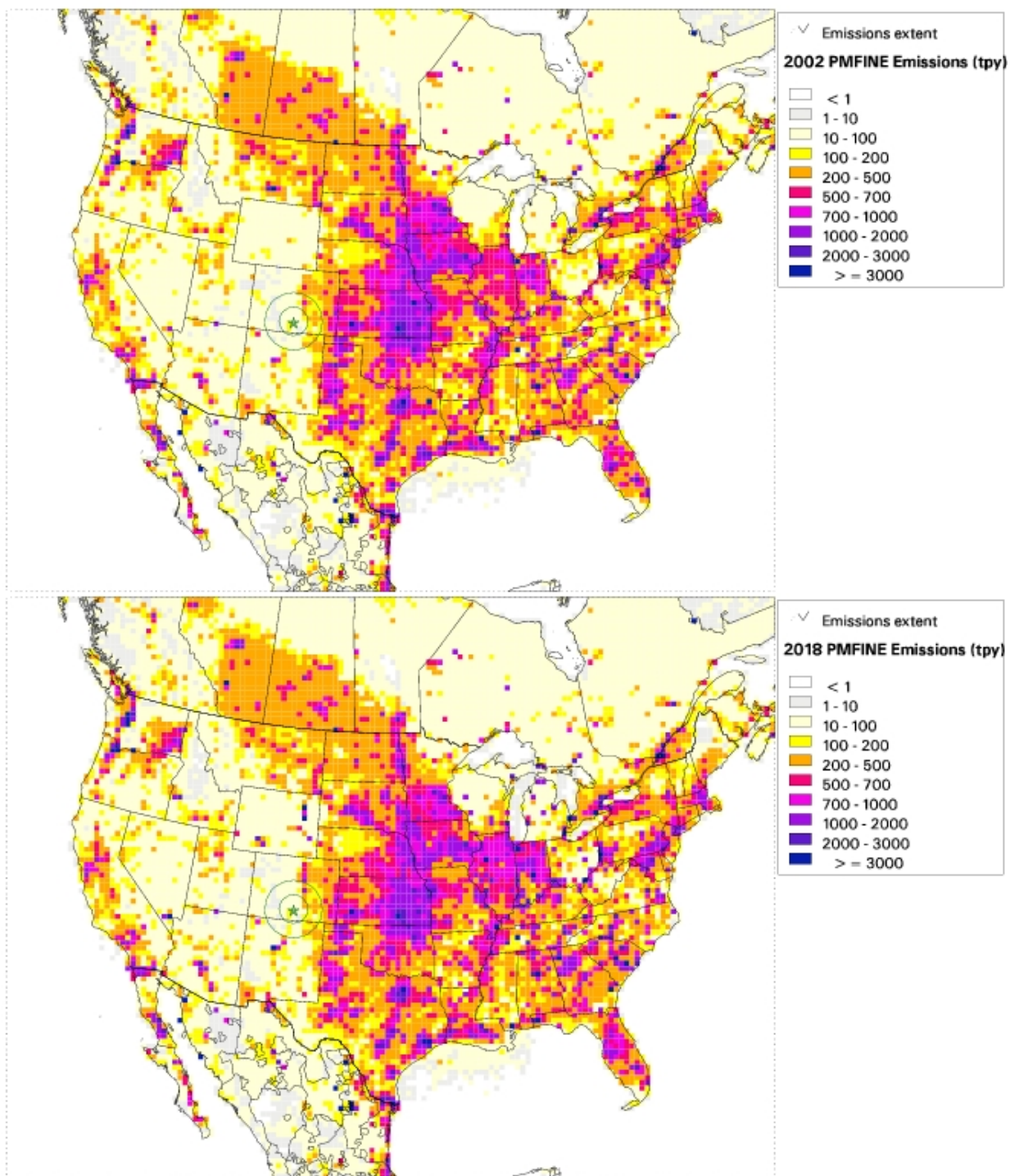


### (12) Regional Map of PM2.5 Emissions for 2002 and 2018

Figure 5-12, provides the plan02c and base18b regional fine soil (fine particulate -PM2.5) emissions with the location of the GRSA1 IMPROVE monitor identified with a green star surrounded by 100 km and 200 km radius concentric circles.

Figure 5-12: Regional PM2.5 Emissions – 2002 & 2018 Inventory

#### Great Sand Dunes National Monument, CO



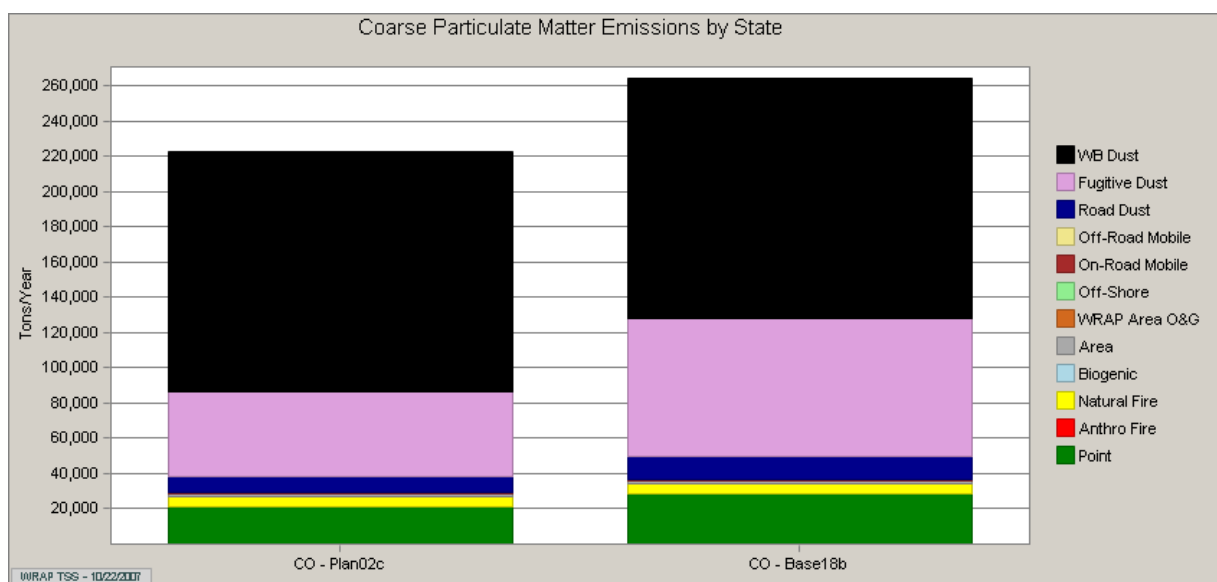
### (13) Colorado Coarse Mass Emission Inventory for 2002 & 2018

Coarse mass (CM) emissions are comprised of particulates with an aerodynamic diameter between 10 and 2.5 microns that are generated mostly by point sources, fugitive dust and windblown dust. Coarse particulate matter can remain suspended in the atmosphere for long periods of time and travel long distances. Coarse particulates scatter the transmission of light that contributes to visibility reduction on a regional scale at our Class I Areas. Sources of coarse particles include construction sites, tilled fields, windblown dust, vehicle traffic, mineral processing facilities, mining and wood burning.

In Figure 5-13, the projected statewide CM emission increase is about 19%. Most of the anticipated increase is associated with fugitive dust.

Figure 5-13: Colorado Coarse Mass Emissions – 2002 & 2018 Inventory

Colorado Planning and Baseline Emission Inventories			
Source Category	Statewide CM		
	Plan 02c [tpy]	Base 18b [tpy]	Net Change
Point	21,096	28,390	35%
Area	1,360	1,388	2%
On-Road Mobile	794	917	15%
Off-Road Mobile	0	0	0%
Oil & Gas	0	0	0%
Road Dust	8,857	13,414	51%
Fugitive Dust	48,470	78,073	61%
Windblown Dust	135,945	135,945	0%
Anthro Fire	51	32	-37%
Natural Fire	5,973	5,973	0%
Biogenic	0	0	0%
<b>Total:</b>	<b>222,546</b>	<b>264,132</b>	<b>19%</b>

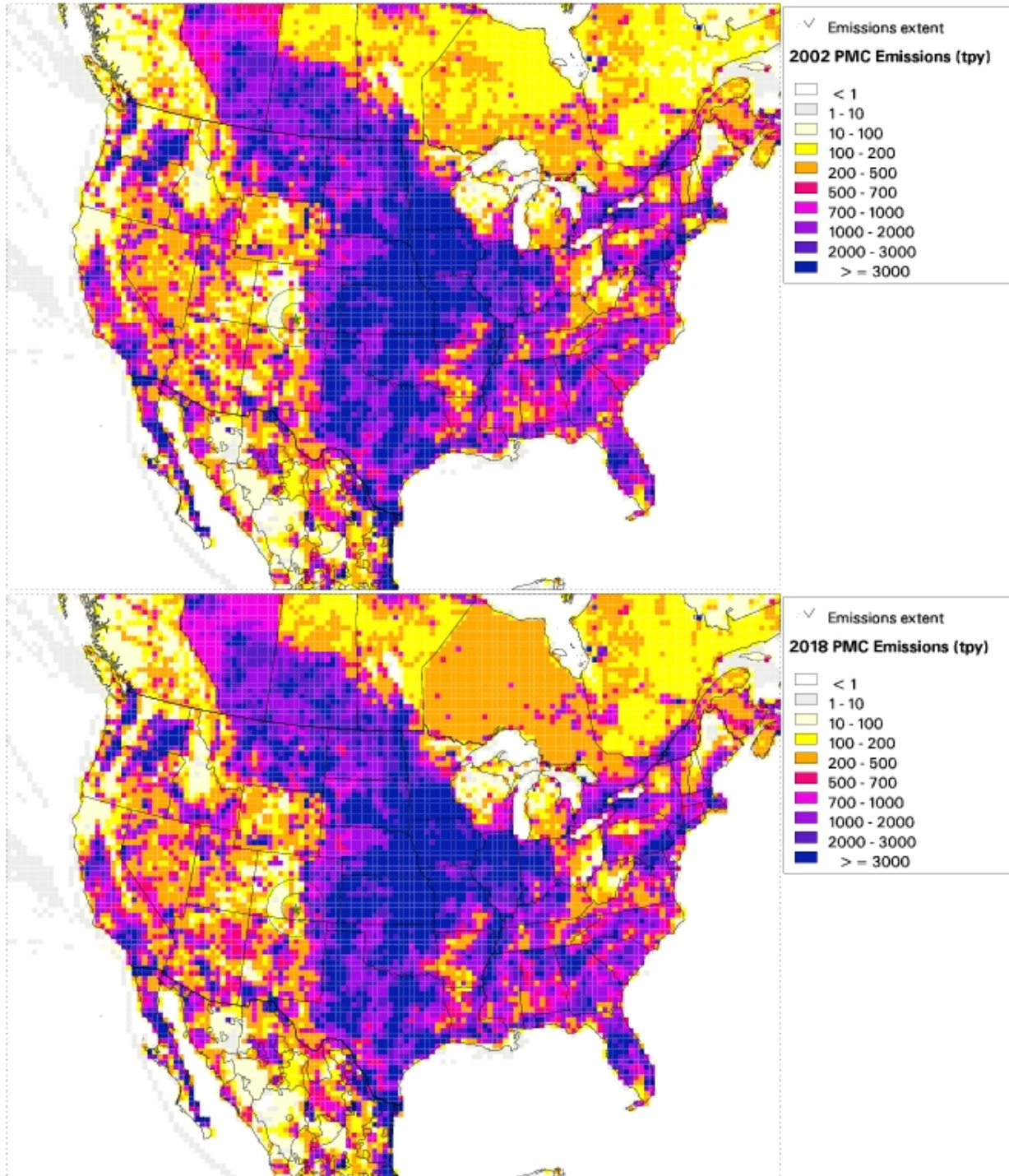


In Figure 5-14, provides the plan02c and base18b regional coarse particulate matter (PMC) emissions with the location of the GRSA1 IMPROVE monitor identified with a green star surrounded by 100 km and 200 km radius concentric circles.

**(14) Regional Map of PMC Emissions for 2002 & 2018**

Figure 5-14: Regional PMC Emissions – 2002 & 2018 Inventory

**Great Sand Dunes National Monument, CO**



## **B. Weighted Emissions Potential (WEP)**

### **(1) Overview**

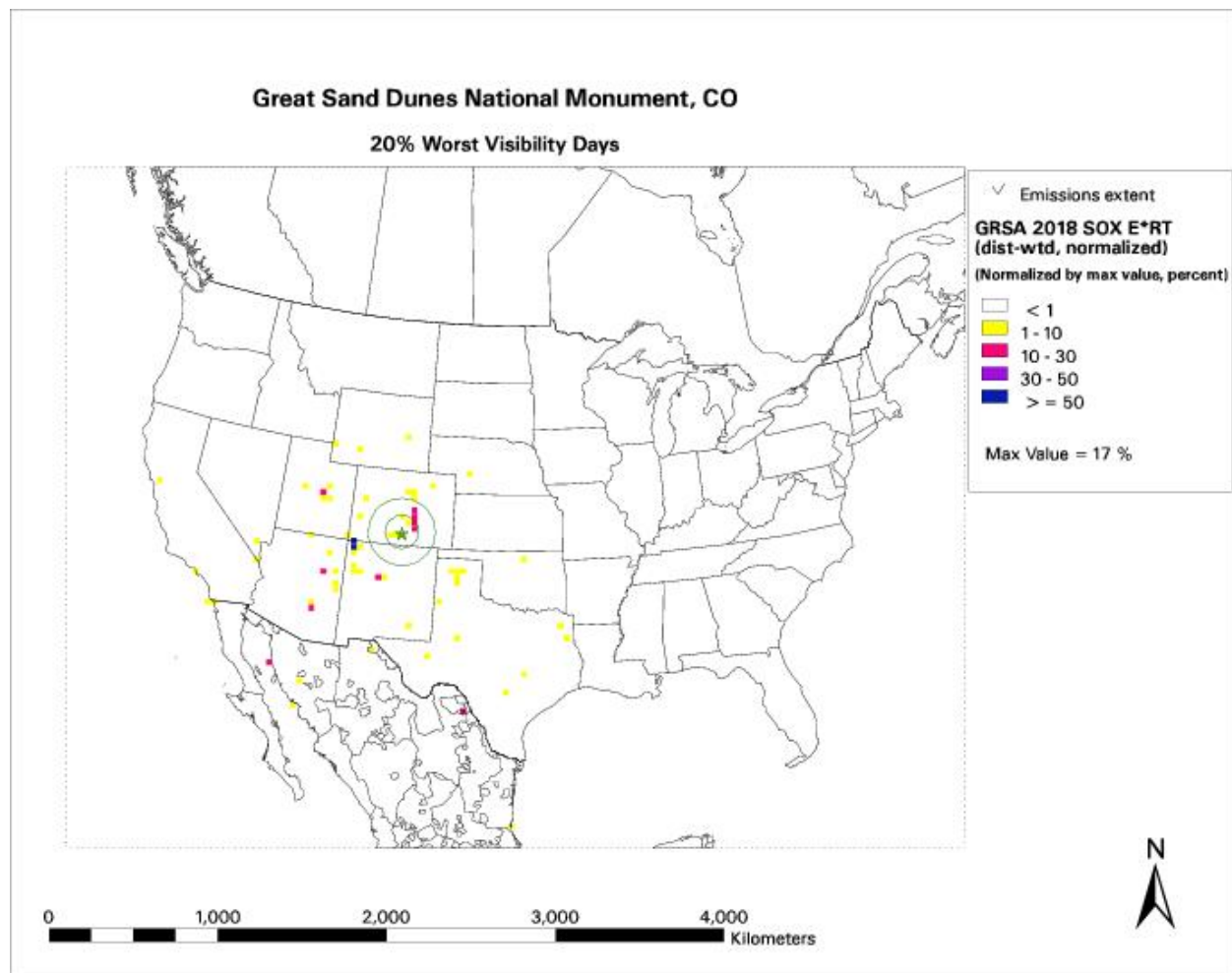
The Weighted Emissions Potential (WEP) tool is an analysis technique that identifies the predominant emission source regions contributing haze-forming pollutants at each Class I area (CIA) based on 5-years of historical meteorology. A map of the seasonal statewide wind patterns is included in Appendix C that provides a general sense of air movement across the state. The CIA specific WEP map for each haze pollutant is determined by multiplying the annual emission inventory (in 36 by 36 km grid cells) for all source categories by the Air Mass Residence Time (2000-04) values. The resultant map provides the distance weighted emissions potential of each grid cell relative to the CIA receptor. Two different modeling simulation emission scenarios (2000-04 Baseline and 2018 Base Case) were used to produce the WEP maps.

It is important to note that this technique does not address secondary particulate formation (e.g. no complex chemistry) or deposition at the CIA receptor. More information on WEP tool can be found in Appendix D.

## (2) Sulfur Oxides - Regional WEP Map for 2018 Worst Days

In Figure 5-15, the location of the GRSA1 IMPROVE monitor is identified with a green star surrounded by 100 km and 200 km radius concentric circles. The areas shaded in different colors identify those grid cells with the potential of contributing SO<sub>x</sub> emissions at GRSA for the worst days in 2018. The areas shaded in darker colors identify the 36 km grid cells that are likely dominant contributors of SO<sub>x</sub> emissions at the class I area whereas the white areas denote those grid cells with negligible emission potential. This analysis provides information on relevant source areas with the potential to contribute SO<sub>x</sub> emissions but the SO<sub>x</sub> WEP doesn't consider particulate deposition or the complex chemical conversion of SO<sub>x</sub> emissions to particulate sulfate.

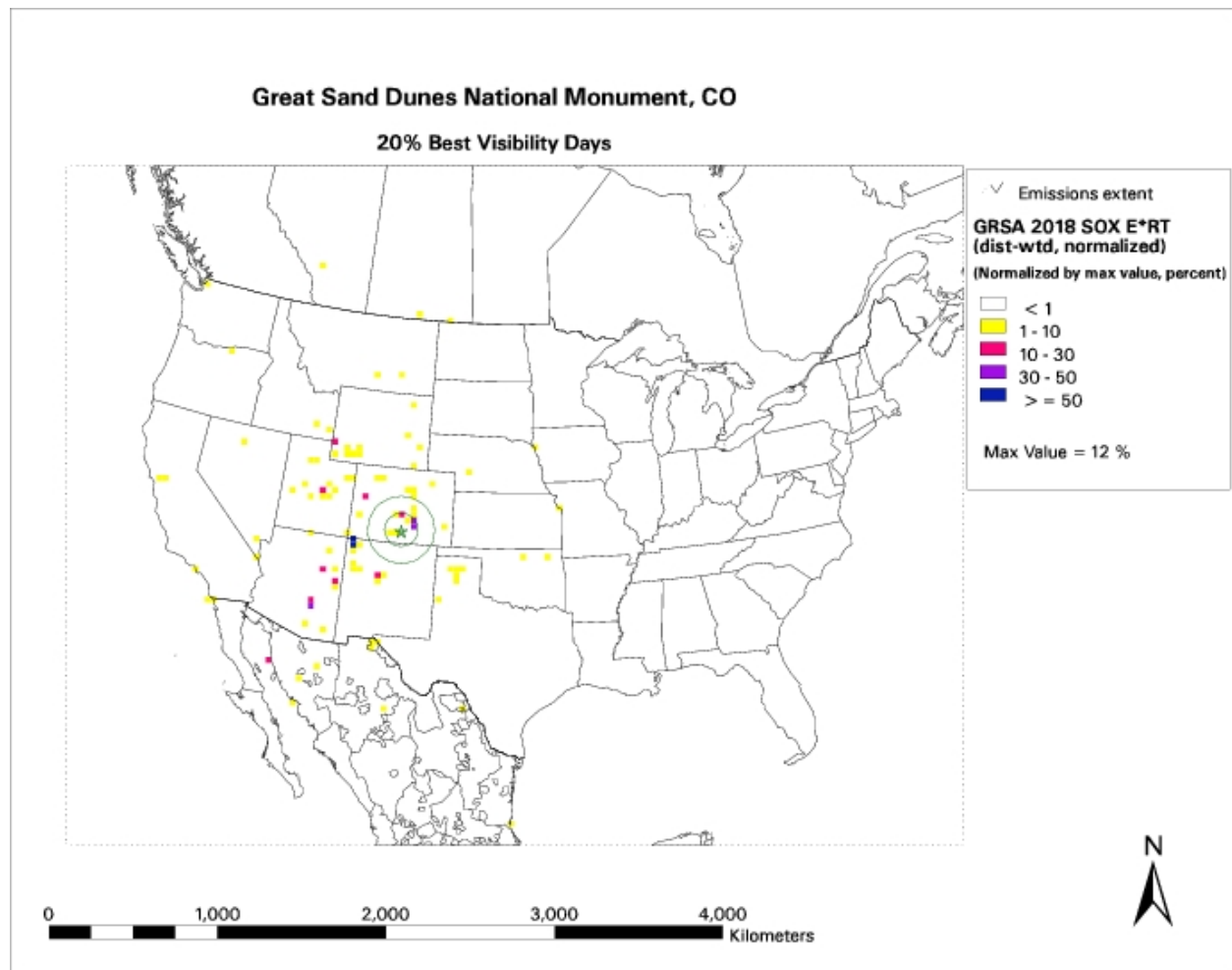
Figure 5-15: Regional SO<sub>x</sub> WEP for 2018 Worst Days



### (3) Sulfur Oxides - Regional WEP Map for 2018 Best Days

In Figure 5-16, the SO<sub>x</sub> WEP max value for the best days (12%) is lower than the worst days (17%) but the distribution of larger emission sources impacting the best days appears to be more widespread.

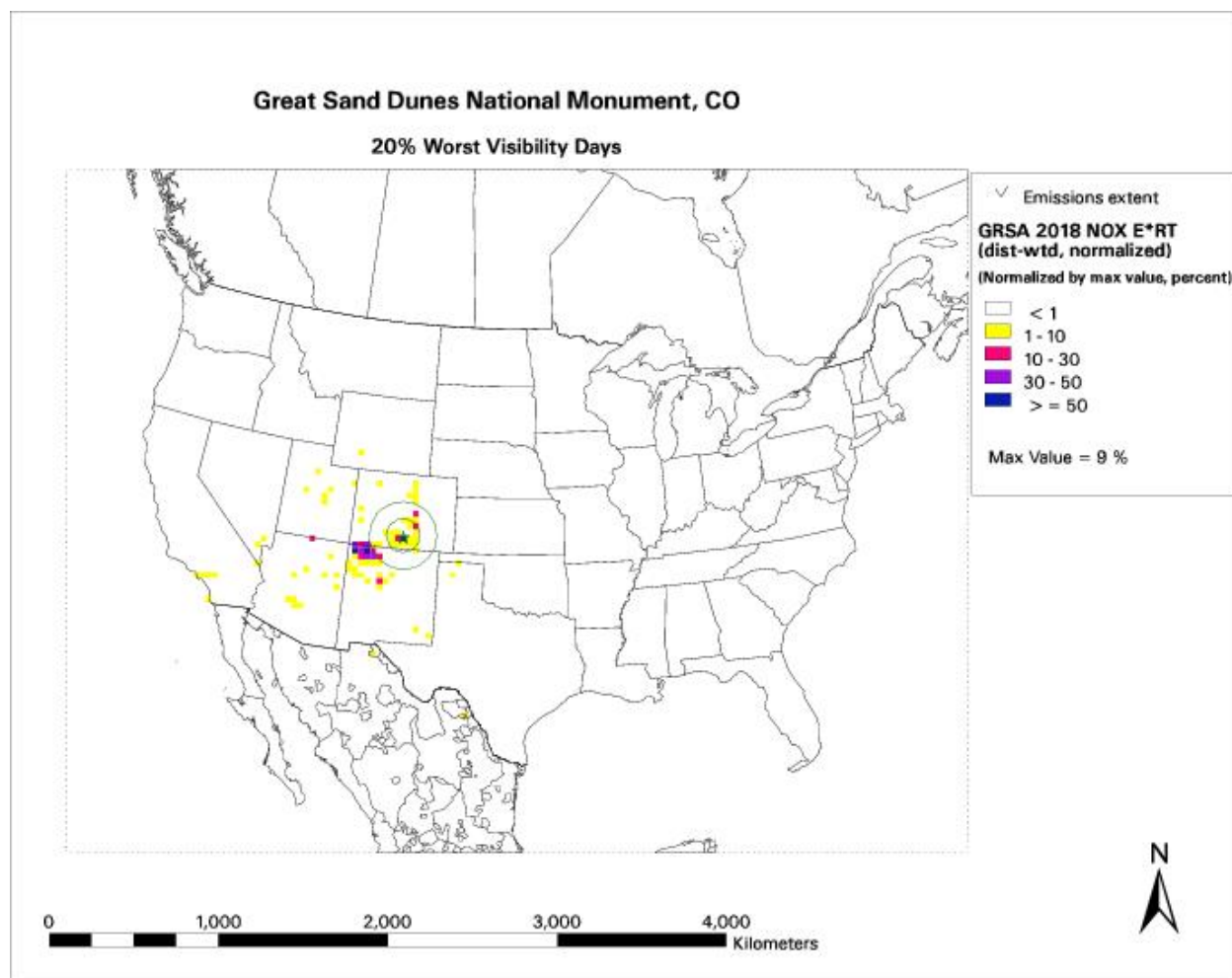
Figure 5-16: Regional SO<sub>x</sub> WEP for 2018 Best Days



#### (4) Nitrogen Oxides - Regional WEP Map for 2018 Worst Days

In Figure 5-17, the location of the GRSA1 IMPROVE monitor is identified with a green star surrounded by 100 km and 200 km radius concentric circles. The areas shaded in different colors identify those grid cells with the potential of contributing NO<sub>x</sub> emissions at GRSA for the worst days in 2018. The areas shaded in darker colors identify the 36 km grid cells that are likely dominant contributors of NO<sub>x</sub> emissions at the class I area whereas the white areas denote those grid cells with negligible emission potential. This analysis provides information on relevant source areas with the potential to contribute NO<sub>x</sub> emissions but the NO<sub>x</sub> WEP doesn't consider particulate deposition or the complex chemical conversion of NO<sub>x</sub> emissions to particulate nitrate.

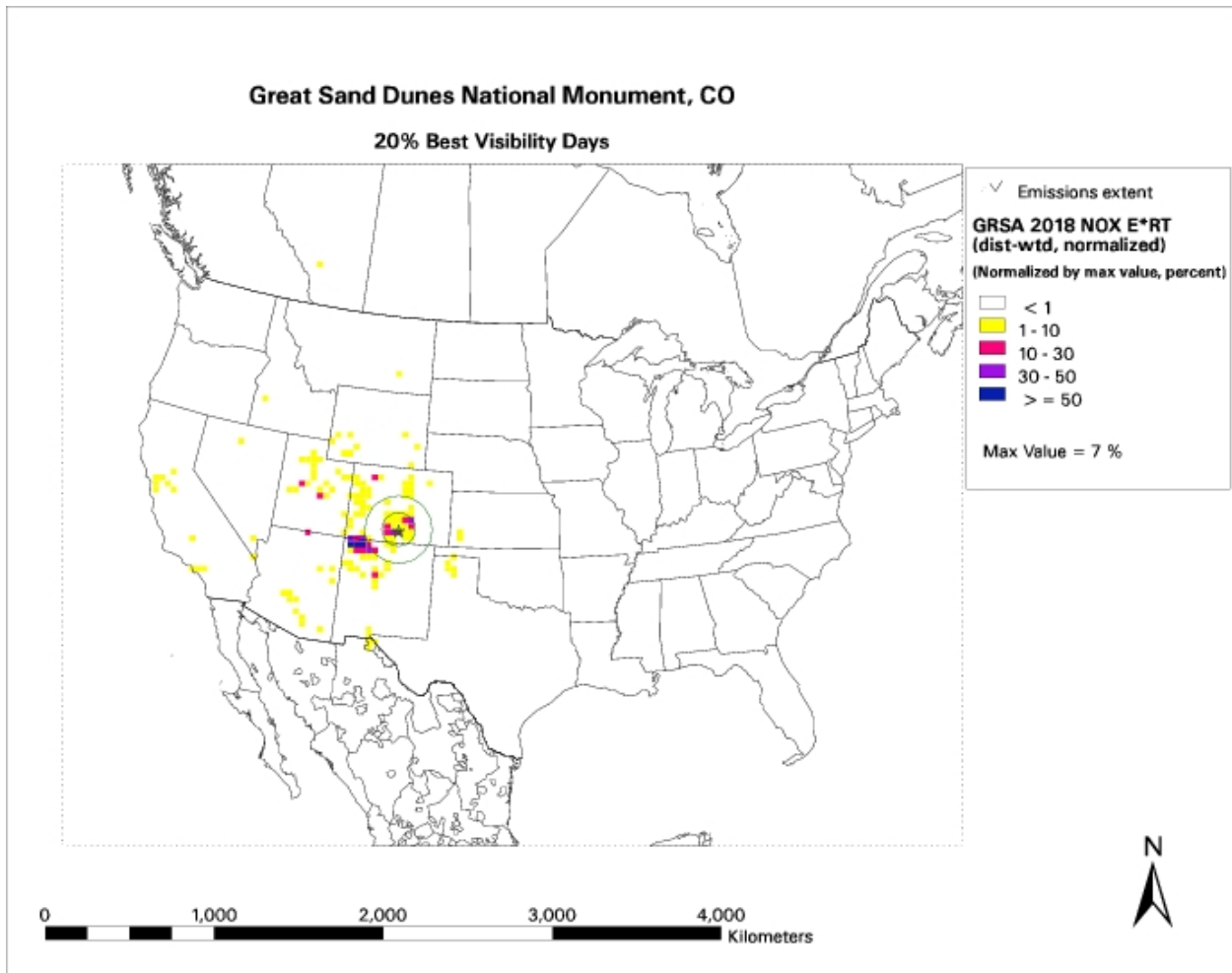
Figure 5-17: Regional NO<sub>x</sub> WEP for 2018 Worst Days



**(5) Nitrogen Oxides - Regional WEP Map for 2018 Best Days**

In Figure 5-18, the NOx WEP max value for the best days (7%) is a little lower than the worst days (9%) but the distribution of larger emission sources impacting the best days appears to be more widespread.

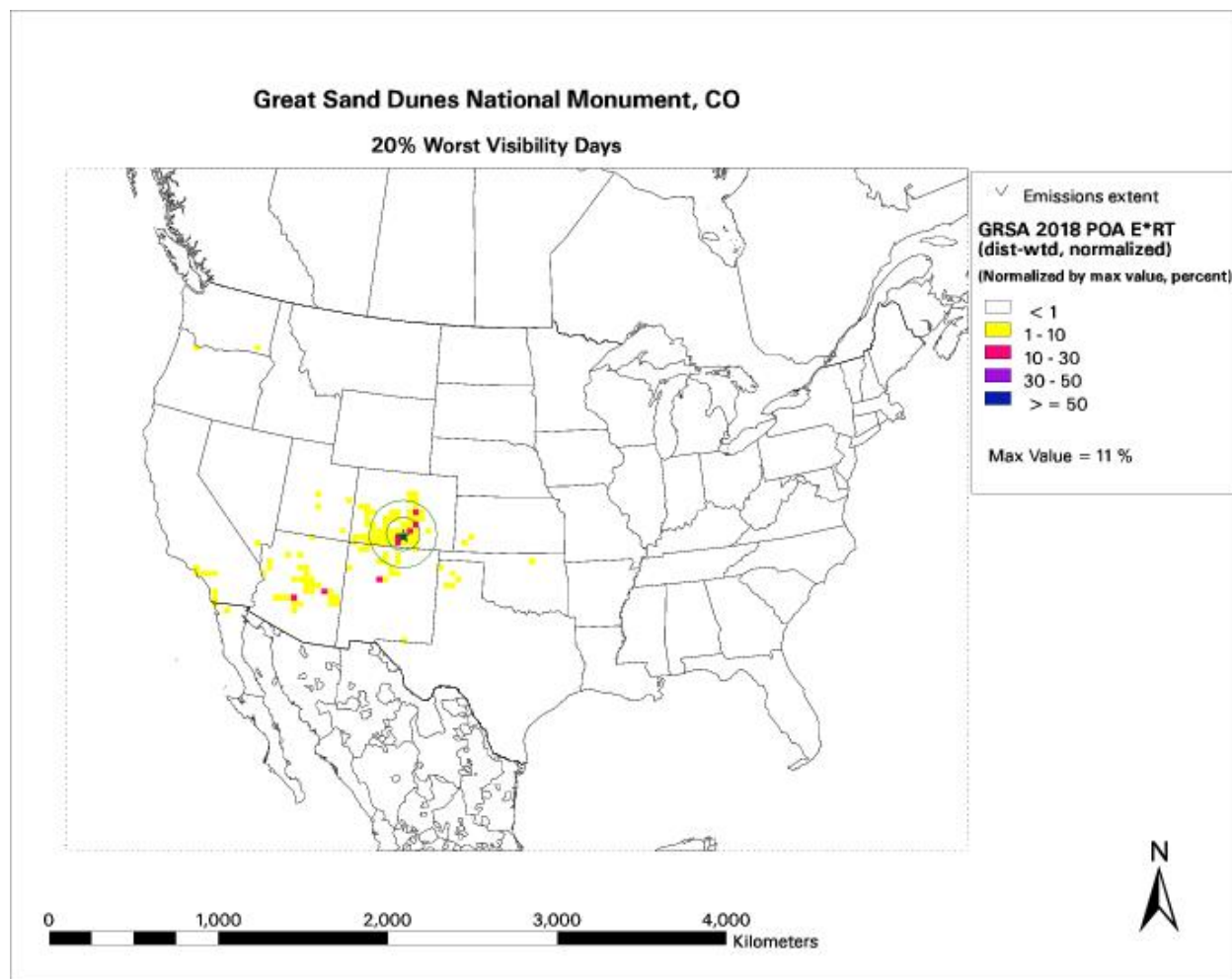
Figure 5-18: Regional NOx WEP for 2018 Best Days



### (6) Primary Organic Aerosol - Regional WEP Map for 2018 Worst Days

In Figure 5-19, the location of the GRSA1 IMPROVE monitor is identified with a green star surrounded by 100 km and 200 km radius concentric circles. The areas shaded in different colors identify those grid cells with the potential of contributing Primary Organic Aerosol (POA) emissions at GRSA for the worst days in 2018. The areas shaded in darker colors identify the 36 km grid cells that are likely dominant contributors of POA emissions at the class I area whereas the white areas denote those grid cells with negligible emission potential. This analysis provides information on relevant source areas with the potential to contribute POA emissions but the POA WEP doesn't consider particulate deposition. Since POA emissions are emitted as a primary particulate organic carbon, the POA WEP doesn't have the limitations of associated with complex chemical particle conversion.

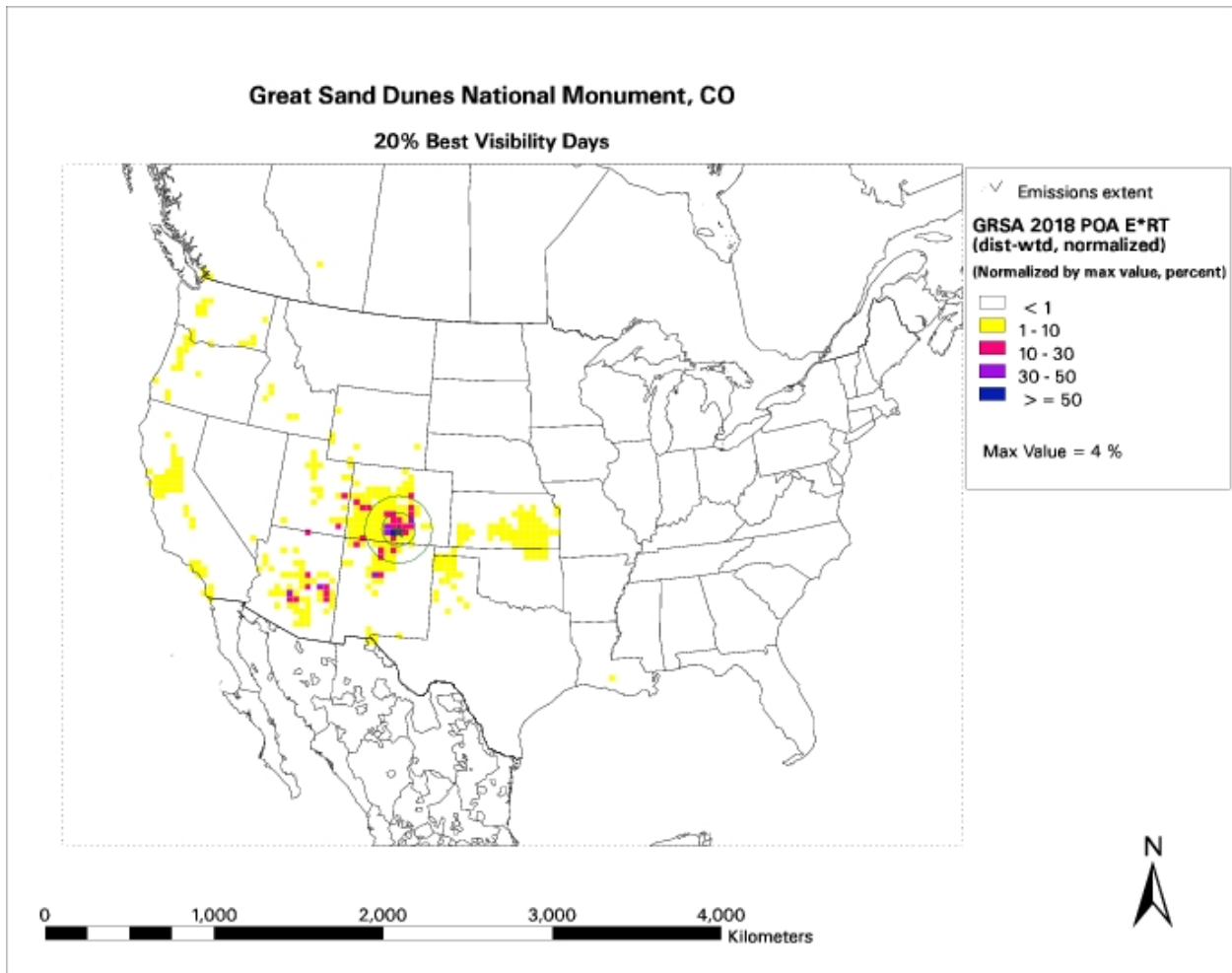
Figure 5-19: Regional POA WEP for 2018 Worst Days



**(7) Primary Organic Aerosol - Regional WEP Map for 2018 Best Days**

In Figure 5-20, the POA WEP max value for the best days (4%) is much lower than worst days (11%) but the distribution of emission sources impacting the best days appears to be much more widespread.

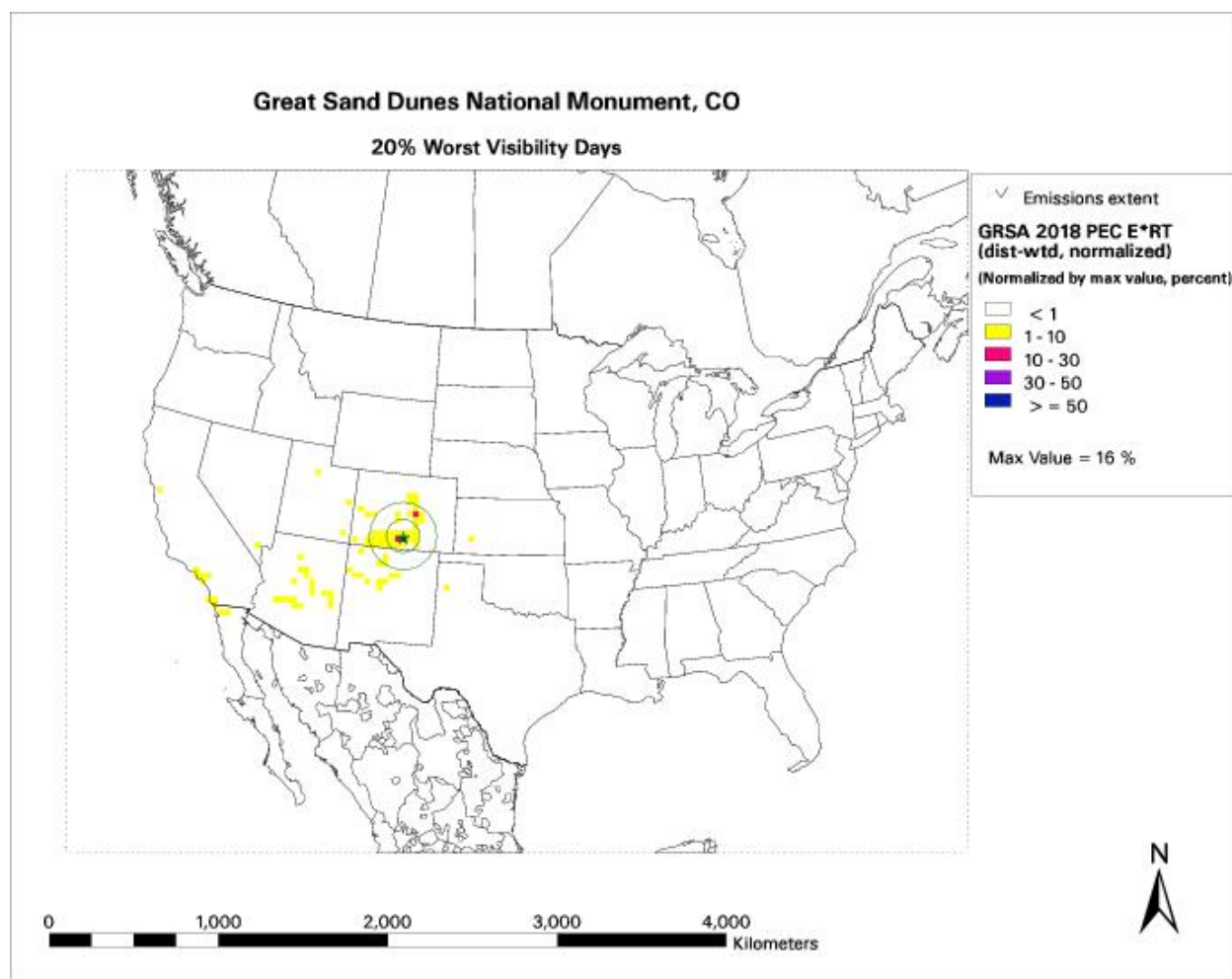
Figure 5-20: Regional POA WEP for 2018 Best Days



### (8) Primary Elemental Carbon - Regional WEP Map for 2018 Worst Days

In Figure 5-21, the location of the GRSA1 IMPROVE monitor is identified with a green star surrounded by 100 km and 200 km radius concentric circles. The areas shaded in different colors identify those grid cells with the potential of contributing Primary Elemental Carbon (PEC) emissions at GRSA for the worst days in 2018. The areas shaded in darker colors identify the 36 km grid cells that are likely dominant contributors of PEC emissions at the class I area whereas the white areas denote those grid cells with negligible emission potential. This analysis provides information on relevant source areas with the potential to contribute PEC emissions but the PEC WEP doesn't consider particulate deposition. Since PEC emissions are emitted as a primary particulate elemental carbon, the PEC WEP doesn't have the limitations of associated with complex chemical particle conversion.

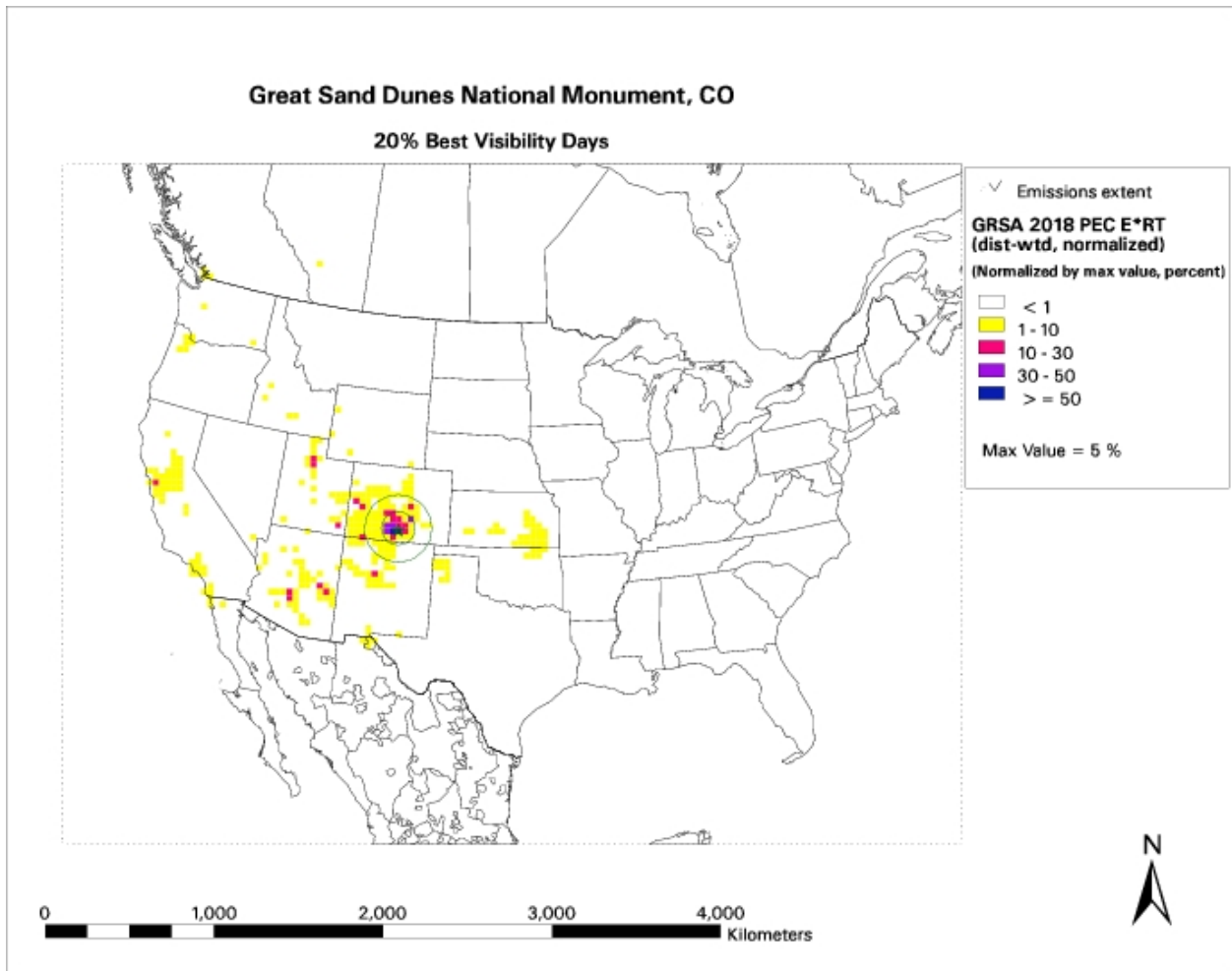
Figure 5-21: Regional PEC WEP for 2018 Worst Days



**(9) Primary Elemental Carbon - Regional WEP Map for 2018 Best Days**

In Figure 5-22, the PEC WEP max value for the best days (5%) is less than 1/3 of the worst days (16%) but the distribution of emission sources impacting the best days appears to be more widespread.

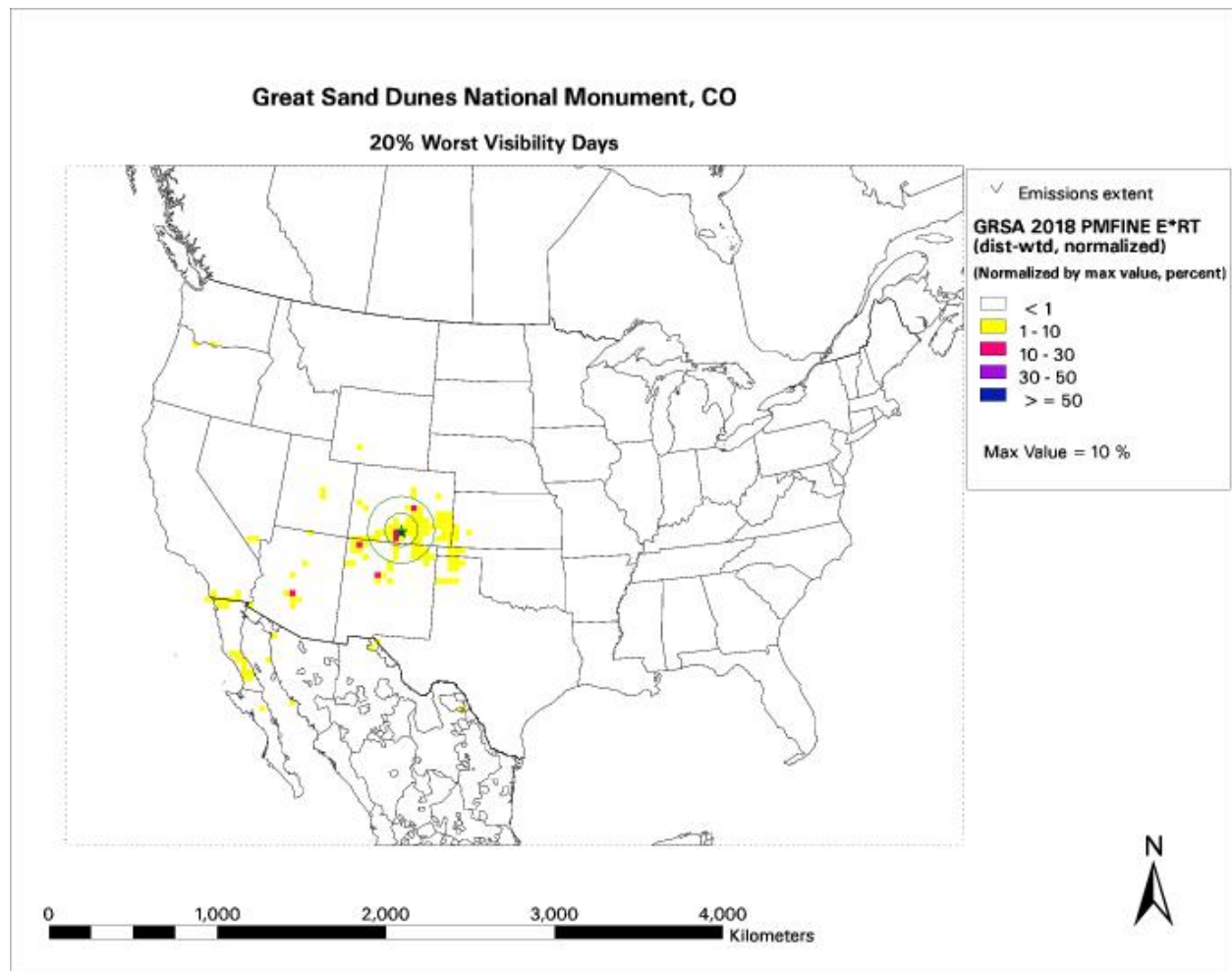
Figure 5-22: Regional PEC WEP for 2018 Best Days



### (10) Particulate Matter Fine - Regional WEP Map for 2018 Worst Days

In Figure 5-23, the location of the GRSA1 IMPROVE monitor is identified with a green star surrounded by 100 km and 200 km radius concentric circles. The areas shaded in different colors identify those grid cells with the potential of contributing fine Particulate Matter (PM<sub>2.5</sub>) emissions at GRSA for the worst days in 2018. The areas shaded in darker colors identify the 36 km grid cells that are likely dominant contributors of PM<sub>2.5</sub> emissions at the class I area whereas the white areas denote those grid cells with negligible emission potential. This analysis provides information on relevant source areas with the potential to contribute PM<sub>2.5</sub> emissions but the PM<sub>2.5</sub> WEP doesn't consider particulate deposition. Since PM<sub>2.5</sub> emissions are emitted as primary fine particulates, the PM<sub>2.5</sub> WEP doesn't have the limitations of associated with complex chemical particle conversion.

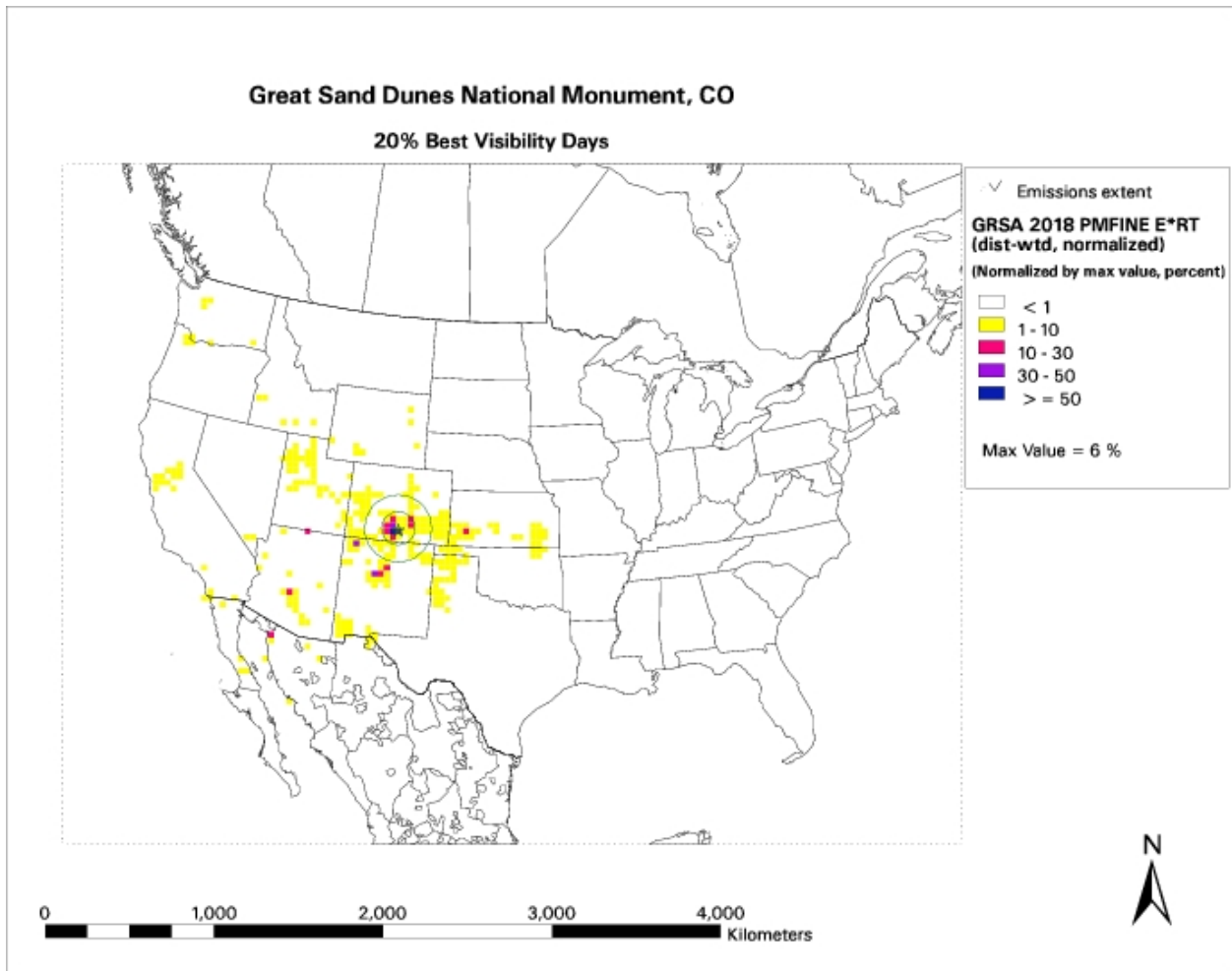
Figure 5-23: Regional PM Fine WEP for 2018 Worst Days



### (11) Particulate Matter Fine - Regional WEP Map for 2018 Best Days

In Figure 5-24, the PM Fine WEP max value for the best days (6%) is almost half of the worst days (10%) but the distribution of emission sources impacting the best days appears to be more widespread.

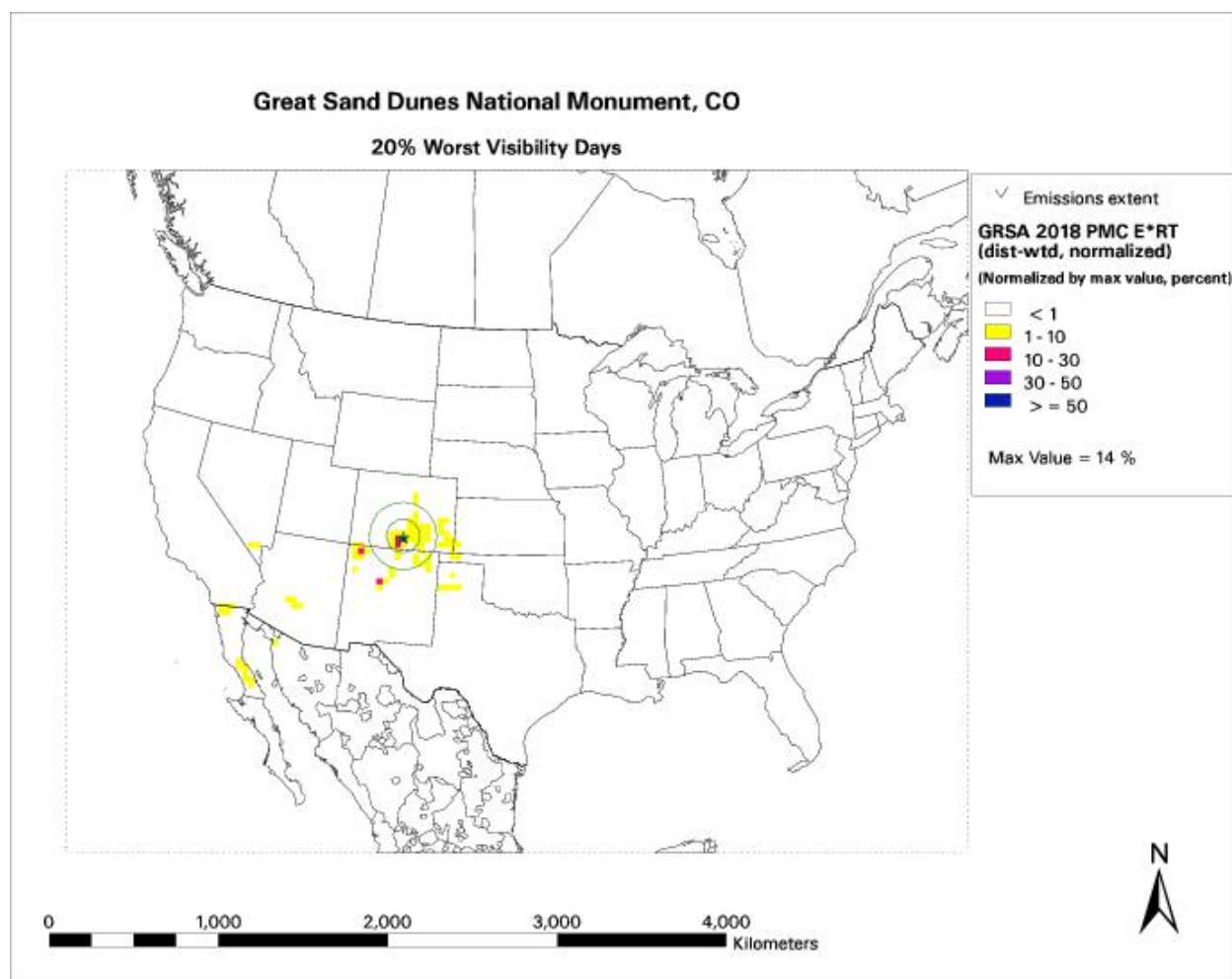
Figure 5-24: Regional PM Fine WEP for 2018 Best Days



## (12) Particulate Matter Coarse - Regional WEP Map for 2018 Worst Days

In Figure 5-25, the location of the GRSA1 IMPROVE monitor is identified with a green star surrounded by 100 km and 200 km radius concentric circles. The areas shaded in different colors identify those grid cells with the potential of contributing coarse Particulate Matter (PMC) emissions at GRSA for the worst days in 2018. The areas shaded in darker colors identify the 36 km grid cells that are likely dominant contributors of PMC emissions at the class I area whereas the white areas denote those grid cells with negligible emission potential. This analysis provides information on relevant source areas with the potential to contribute PMC emissions but the PMC WEP doesn't consider particulate deposition. Since PMC emissions are emitted as primary particulates, the PMC WEP doesn't have the limitations of associated with complex chemical particle conversion.

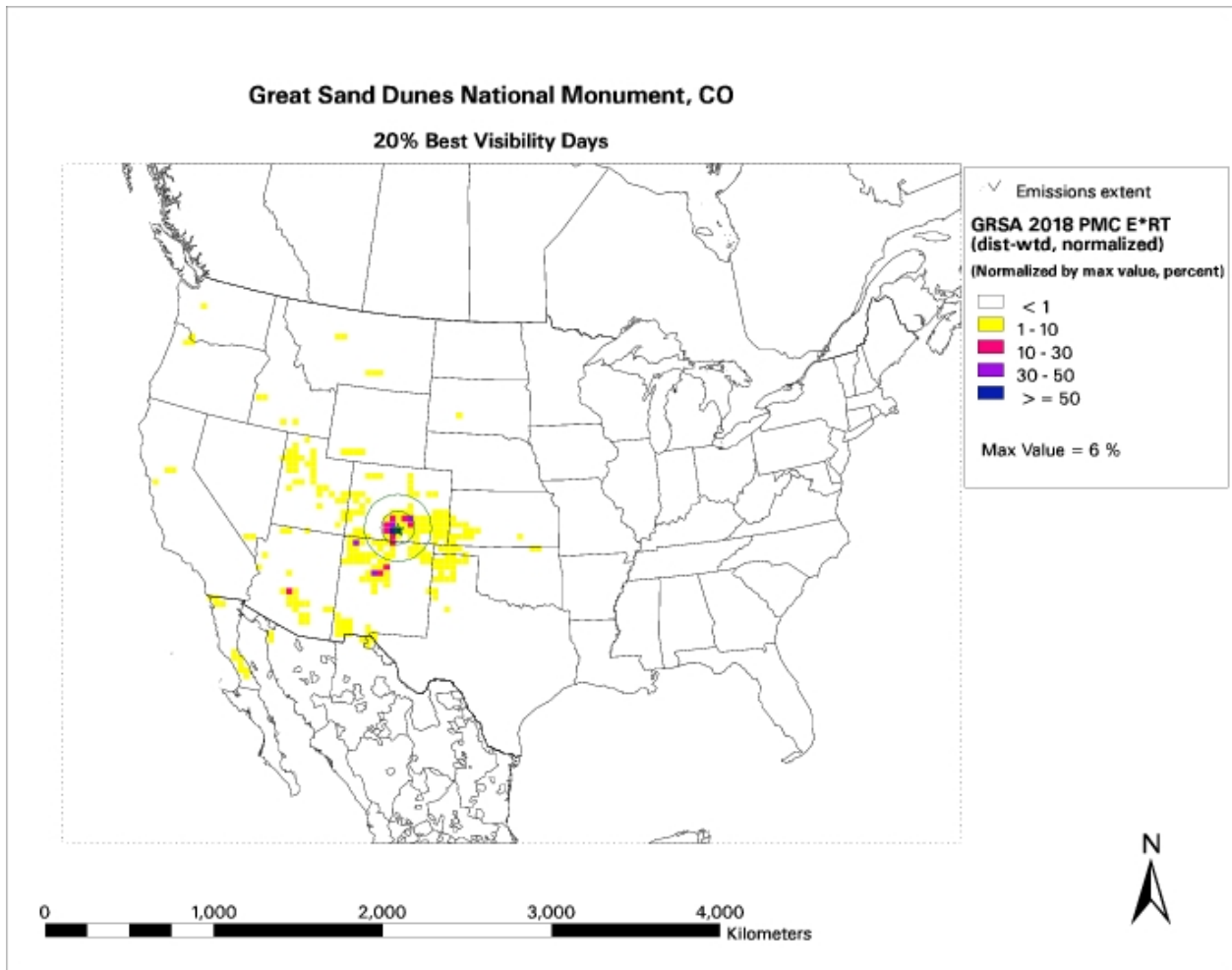
Figure 5-25: Regional PMC WEP for 2018 Worst Days



### (13) Particulate Matter Coarse - Regional WEP Map for 2018 Best Days

In Figure 5-26, the PMC WEP max value for the best days (6%) is less than half of the worst days (14%) but the distribution of larger emission sources impacting the best days appears to be more widespread.

Figure 5-26: Regional PMC WEP for 2018 Best Days



## SECTION 6: REGIONAL VISIBILITY MODELING

### A. Overview

Visibility impairment occurs when fine particulate matter (PM<sub>2.5</sub>) in the atmosphere scatters and absorbs light, thereby creating haze. PM<sub>2.5</sub> can be emitted into the atmosphere directly as primary particulates, or it can be produced in the atmosphere from photochemical reactions of gas-phase precursors and subsequent condensation to form secondary particulates. Examples of primary PM<sub>2.5</sub> include crustal materials and elemental carbon; examples of secondary PM include ammonium nitrate, ammonium sulfates, and secondary organic aerosols (SOA). Secondary PM<sub>2.5</sub> is generally smaller than primary PM<sub>2.5</sub>, and because the ability of PM<sub>2.5</sub> to scatter light depends on particle size, with light scattering for fine particles being greater than for coarse particles, secondary PM<sub>2.5</sub> plays an especially important role in visibility impairment. Moreover, the smaller secondary PM<sub>2.5</sub> can remain suspended in the atmosphere for longer periods and is transported long distances, thereby contributing to regional-scale impacts of pollutant emissions on visibility.

The sources of PM<sub>2.5</sub> are difficult to quantify because of the complex nature of their formation, transport, and removal from the atmosphere. This makes it difficult to simply use emissions data to determine which pollutants should be controlled to most effectively improve visibility. Photochemical air quality models offer opportunity to better understand the sources of PM<sub>2.5</sub> by simulating the emissions of pollutants and the formation, transport, and deposition of PM<sub>2.5</sub>. If an air quality model performs well for a historical episode, the model may then be useful for identifying the sources of PM<sub>2.5</sub> and helping to select the most effective emissions reduction strategies for attaining visibility goals. Although several types of air quality modeling systems are available, the gridded, three-dimensional, Eulerian models provide the most complete spatial representation and the most comprehensive representation of processes affecting PM<sub>2.5</sub>, especially for situations in which multiple pollutant sources interact to form PM<sub>2.5</sub>. For less complex situations in which a few large point sources of emissions are the dominant source of PM<sub>2.5</sub>, trajectory models (such as the California Puff Model [CALPUFF]) may also be useful for simulating PM<sub>2.5</sub>.

### B. Air Quality Models

The WRAP RMC utilized two regulatory air quality modeling systems to conduct all regional haze modeling. A brief discussion of each of these models is provided below.

#### **(1) Community Multi-Scale Air Quality Model**

EPA initially developed the Community Multi-Scale Air Quality (CMAQ) modeling system in the late 1990s. The model source code and supporting data can be downloaded from the Community Modeling and Analysis System (CMAS) Center (<http://www.cmascenter.org/>), which is funded by EPA to distribute and provide limited support for CMAQ users. CMAQ was designed as a “one atmosphere” modeling system to encompass modeling of multiple pollutants and issues, including ozone, PM, visibility, and air toxics. This is in contrast to many earlier air quality models that focused on single-pollutant issues (e.g., ozone modeling by the Urban Airshed Model). CMAQ is an Eulerian model - that is, it is a grid-based model in which the frame of reference is a fixed, three-dimensional (3-D) grid with uniformly sized horizontal grid cells and variable vertical layer thicknesses. The number and size of grid cells and the number and thicknesses of layers are defined by the user, based in part on the size of the modeling domain to be used for each modeling project. The key science processes included in CMAQ are emissions, advection and dispersion, photochemical transformation, aerosol thermodynamics and phase transfer, aqueous chemistry, and wet and dry deposition of trace species. CMAQ

offers a variety of choices in the numerical algorithms for treating many of these processes, and it is designed so that new algorithms can be included in the model. CMAQ offers a choice of three photochemical mechanisms for solving gas-phase chemistry: the Regional Acid Deposition Mechanism version 2 (RADM2), a fixed coefficient version of the SAPRC90 mechanism, and the Carbon Bond IV mechanism (CB-IV).

## **(2) Comprehensive Air Quality Model with Extensions**

The Comprehensive Air Quality Model with extensions (CAMx) model was initially developed by ENVIRON in the late 1990s as a nested-grid, gas-phase, Eulerian photochemical grid model. ENVIRON later revised CAMx to treat PM, visibility, and air toxics. While there are many similarities between the CMAQ and CAMx systems, there are also some significant differences in their treatment of advection, dispersion, aerosol formation, and dry and wet deposition.

## **C. Modeling Performance**

The objective of a model performance evaluation (MPE) is to compare model-simulated concentrations with observed data to determine whether the model's performance is sufficiently accurate to justify using the model for simulating future conditions. There are a number of challenges in completing an annual MPE for regional haze. The model must be compared to ambient data from several different monitoring networks for both PM and gaseous species, for an annual time period, and for a large number of sites. The model must be evaluated for both the worst visibility conditions and for very clean conditions. Finally, final guidance on how to perform an MPE for fine-particulate models is not yet available from EPA. Therefore, the RMC experimented with many different approaches for showing model performance results. The plot types that were found to be the most useful are the following:

- Time-series plots comparing the measured and model-predicted species concentrations
- Scatter plots showing model predictions on the y-axis and ambient data on the x-axis
- Spatial analysis plots with ambient data overlaid on model predictions
- Bar plots comparing the mean fractional bias (MFB) or mean fractional error (MFE) performance metrics
- "Bugle plots" showing how model performance varies as a function of the PM species concentration
- Stacked-bar plots of contributions to light extinction for the average of the best-20% visibility days or the worst-20% visibility days at each site; the higher the light extinction, the lower the visibility

Examples of each of these MPE metrics and analysis products can be found in Tonnesen, G. et al., 2006. The results of the MPE are available from the WRAP RMC website (<http://pah.cert.ucr.edu/aqm/308/eval.shtml>)

### (1) Model Performance for 2002 Worst Days

Figure 6-1, the model performance can be roughly judged by comparing the modeled output (on left) against the monitored IMPROVE data (on right) for the worst days in 2002. As indicated, the model greatly under predicts coarse mass (CM – gray color). Across the WRAP region a similar model under prediction is seen, thus the RMC has concluded that the CMAQ model cannot be used to forecast future CM concentrations.

Figure 6-1: CMAQ Model Performance for GRSA 2002 Worst Days

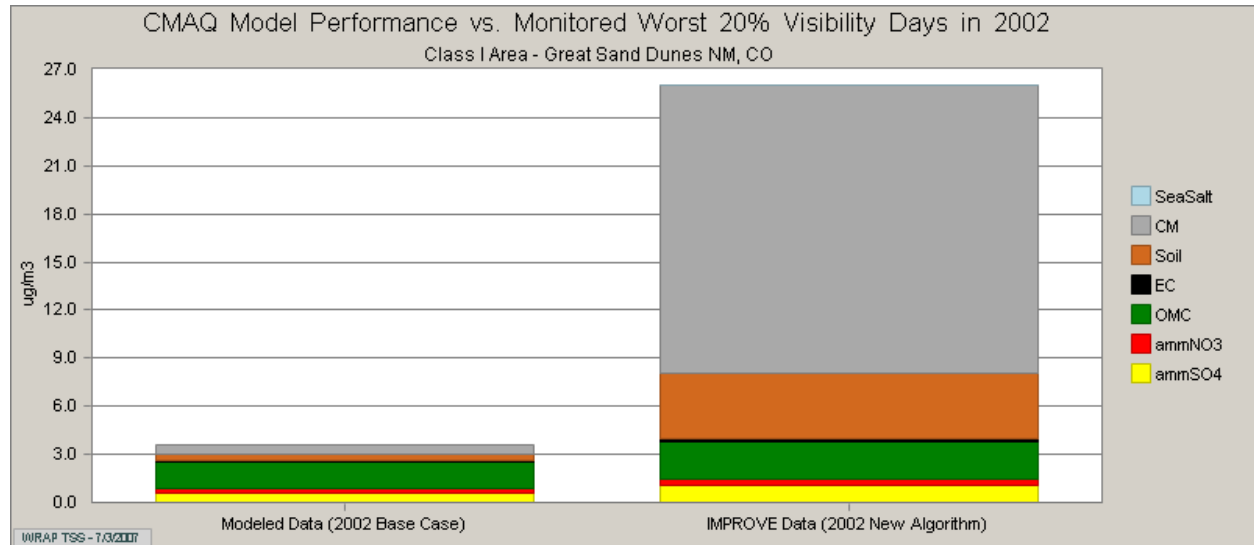
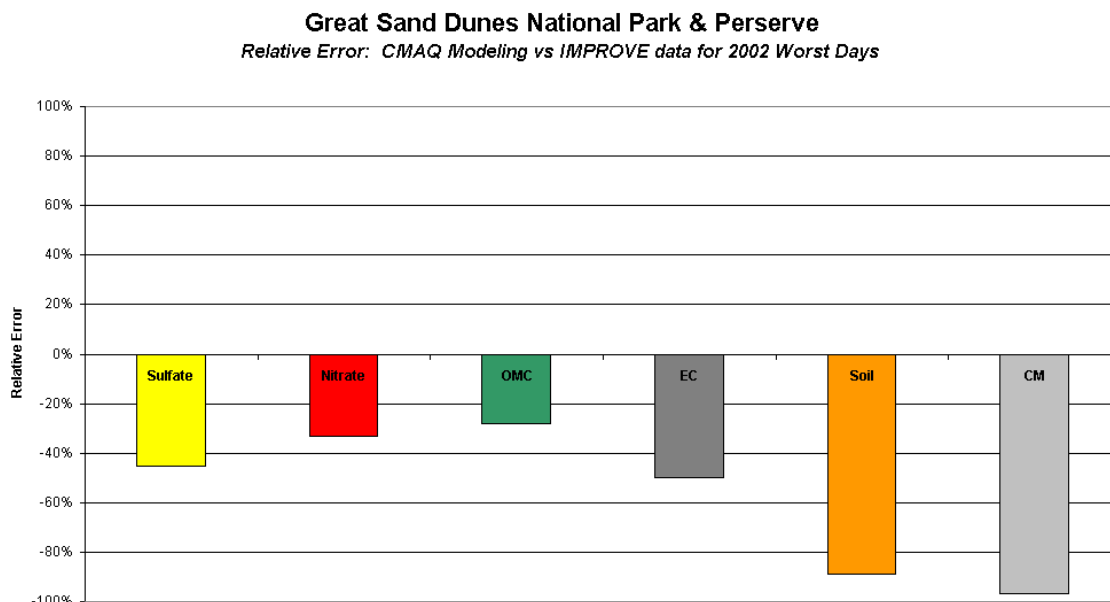


Figure 6-2, indicates that the model under predicts all 6 components of extinction for the worst days at GRSA. The Division has determined that the model performance for the worst days is acceptable for sulfate (-45%), nitrate (-33%), OMC (-28%) and EC (-50%) but is unacceptable for soil (-89%).

Figure 6-2: Relative Error: CMAQ Model vs IMPROVE data for ROMO 2002 Worst Days



## (2) Model Performance for 2002 Best Days

Figure 6-3, the model performance can be roughly judged by comparing the modeled output (on left) against the monitored IMPROVE data (on right) for the best days in 2002. As indicated, the model greatly under predicts coarse mass (CM – gray color). Across the WRAP region a similar model under prediction is seen, thus the RMC has concluded that the CMAQ model cannot be used to forecast future CM concentrations.

Figure 6-3: CMAQ Model Performance for GRSA 2002 Best Days

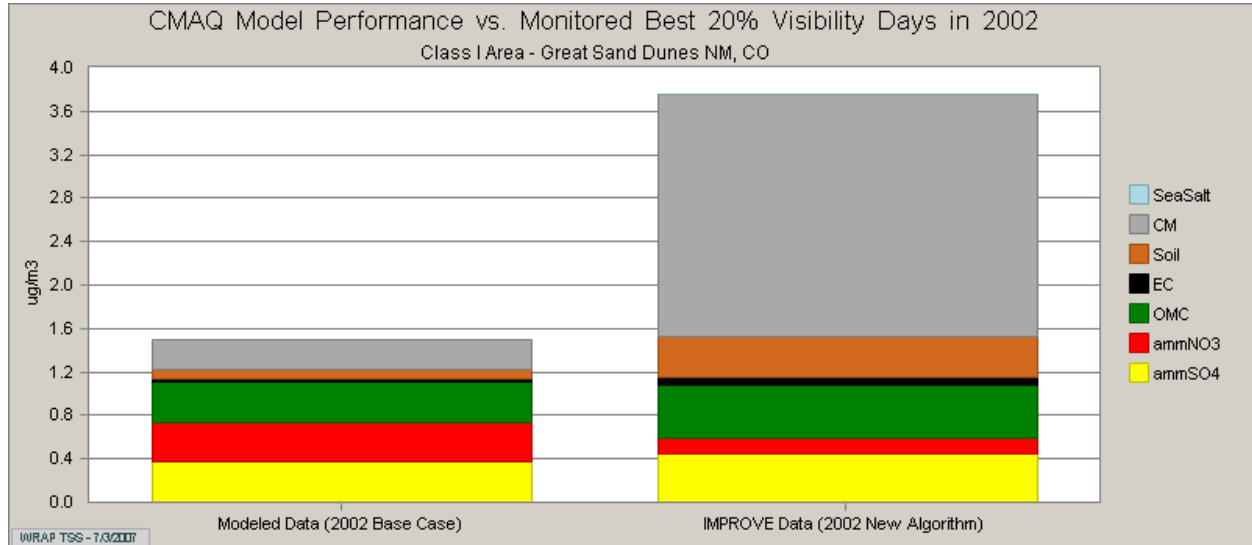
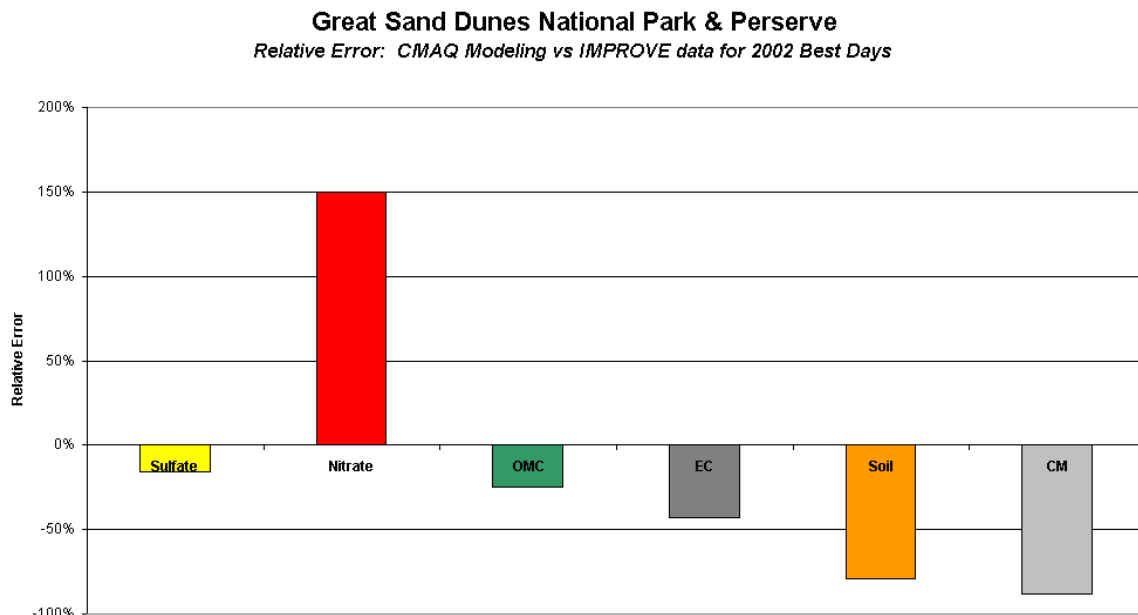


Figure 6-4, indicates that the model produces mixed predictions for the best days at GRSA. The Division has determined that the model performance for the best days is acceptable for sulfate (-15%), OMC (-25%) and EC (-43%) but is marginally acceptable for soil (-79%). The model performance for nitrate (+150%) on the best days is unacceptable.

Figure 6-4: Relative Error: CMAQ Model vs IMPROVE data for ROMO 2002 Best Days

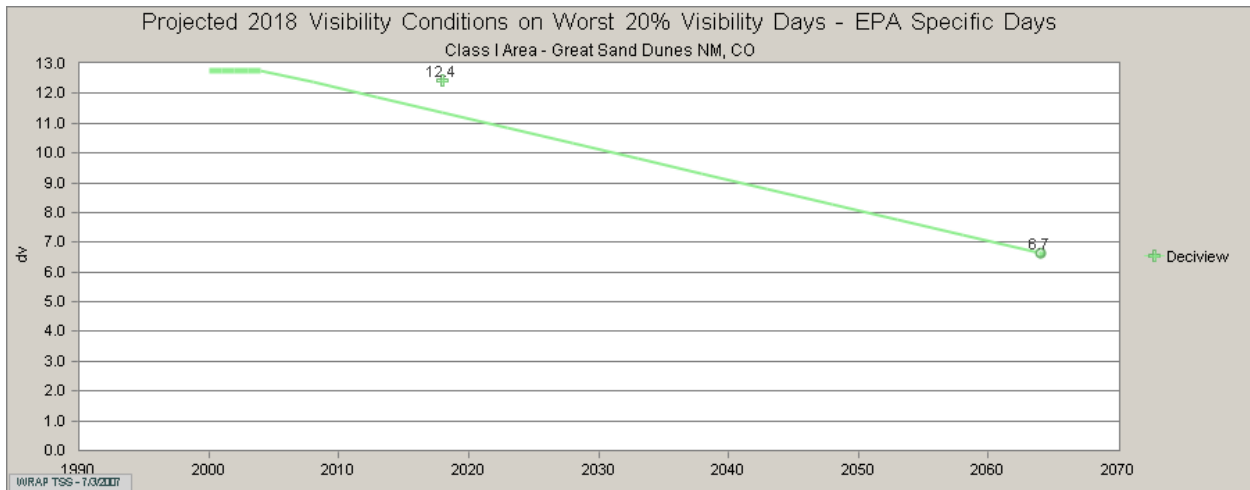


## D. Modeling Projections

### (1) 2018 Worst Days Model Projection using Haze Index Metric

Figure 6-5 indicates the 2018 model projection for the worst days at GRSA using the EPA specific days method is estimated at 12.44 deciviews which is about 23.8% of the 2018 uniform progress goal (11.35 dv). The model projections are based on the 2018(b) emissions inventory, which does include some of Colorado's Best Available Retrofit Technology (BART) emission controls.

Figure 6-5: CMAQ Model Projections in Haze Index for GRSA 2018 Worst Days



### (2) 2018 Worst Days Model Projection using Extinction Metric

Figure 6-6, provides the species-specific glide slopes with the 2018 model projections for the worst days at GRSA using the EPA specific days method. Please note that coarse mass is not included in the figure since model performance is unacceptable.

Figure 6-6: CMAQ Model Projections in Extinction for GRSA 2018 Worst Days

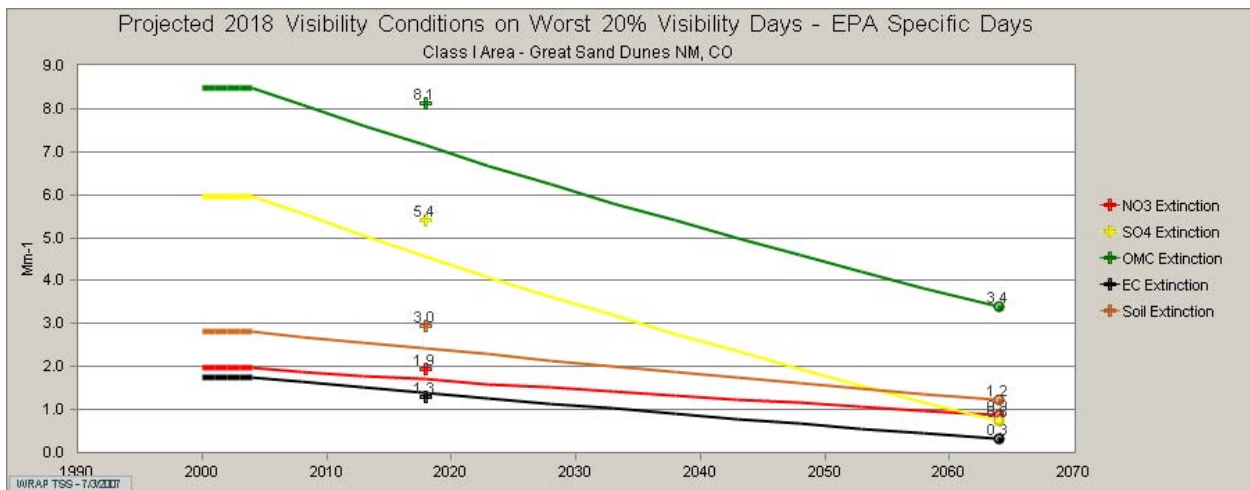


Figure 6-7, indicates the percentage of progress toward the Uniform Progress Goal (UPG) for each species. The 2018 modeling for elemental carbon indicates that it exceeds the UPG by 26% and the glide slope for soil is pretty flat thus a small change is exaggerated when compared to the UPG.

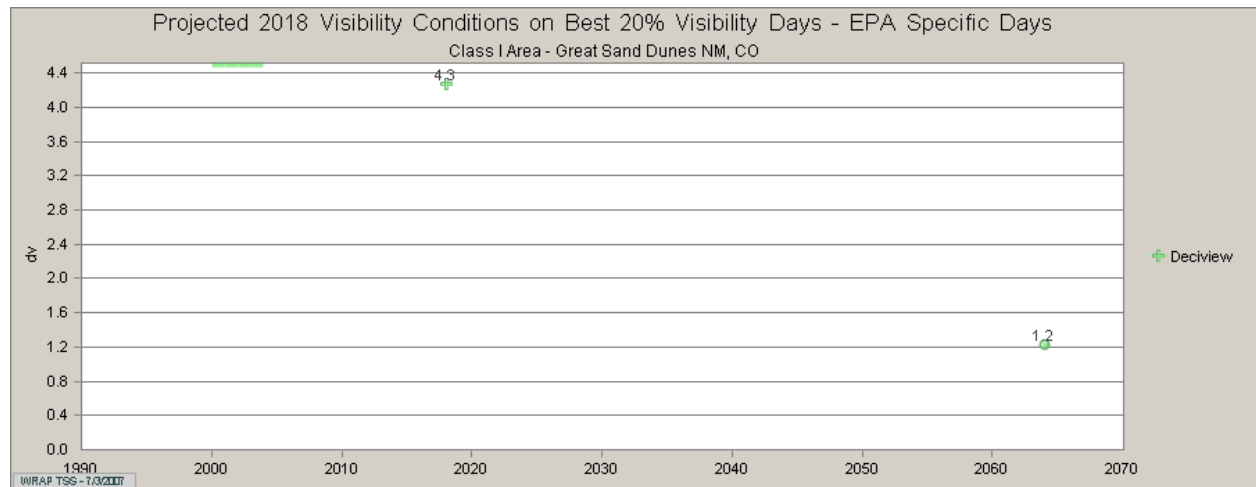
Figure 6-7: Percent Towards Species-Specific UPG for GRSA 2018 Worst Days

Class I Area	2018b Modeled Change in Extinction (from Baseline Period to 2018 UP Goal)					
	Sulfate [%]	Nitrate [%]	Organic Carbon [%]	Elemental Carbon [%]	Fine Soil [%]	Coarse Mass [%]
Great Sand Dunes National Park	40%	12%	25%	126%	-36%	0%

### (3) 2018 Best Days Model Projection using Haze Index Metric

Figure 6-8 indicates the 2018 model projection for the best days at GRSA using the EPA specific days method is estimated at 4.27 deciviews, which is below best days baseline average of 4.5 deciviews. Thus maintaining the best days is forecast for 2018.

Figure 6-8: CMAQ Model Projections in Haze Index for GRSA 2018 Worst Days



# SECTION 7: PM SOURCE APPORTIONMENT TECHNOLOGY (PSAT) MODELING

## A. PSAT Overview

The Regional Modeling Center (RMC) at the University of California – Riverside developed the PSAT algorithm in the Comprehensive Air quality Model with extensions (CAMx) model to assess source attribution. The PSAT analysis is used to attribute particle species, particularly sulfate and nitrate from a specific location within the WRAP modeling domain. The PSAT algorithm applies nitrate-sulfate-ammonia chemistry to a system of tracers or “tags” to track the chemical transformations, transport and removal of emissions.

Each state or region (i.e. Mexico, Canada) is assigned a unique number that is used to tag the emissions from each 36-kilometer grid cell within the WRAP modeling domain. Due to time and computational limitations, only point, mobile, area and fire emissions were tagged.

The PSAT algorithm was also used, in a limited application (e.g. no state or regional attribution), to track natural and anthropogenic species of organic aerosols at each CIA. The organic aerosol tracer tracked both primary and secondary organic aerosols (POA & SOA). Appendix H includes more information on PSAT methodology.

## B. Particulate Sulfate PSAT for Worst Days in 2002 and 2018

Figure 7-1 displays the 2002 and 2018 worst days (in pairs) particulate sulfate concentrations for each source area impacting Great Sand Dunes National Park (GRSA). The chart provides details on the relative source type contribution for a particular source area and the future trend (upward or downward) of each source area. As indicated, the dominant contributors to sulfate at GRSA for the worst days appear to be Colorado, CENRAP (central US) region, Mexico, New Mexico, Pacific Offshore and Arizona. The future 2018 sulfate trends for the worst days are downward for Colorado and CENRAP but increasing for Mexico, New Mexico, PO and Arizona. Point sources (denoted “PT” in blue) appear to be the dominant source of sulfate.

Figure 7-1: Sulfate PSAT - Source Region Bar Chart for Worst Days in 2002 and 2018

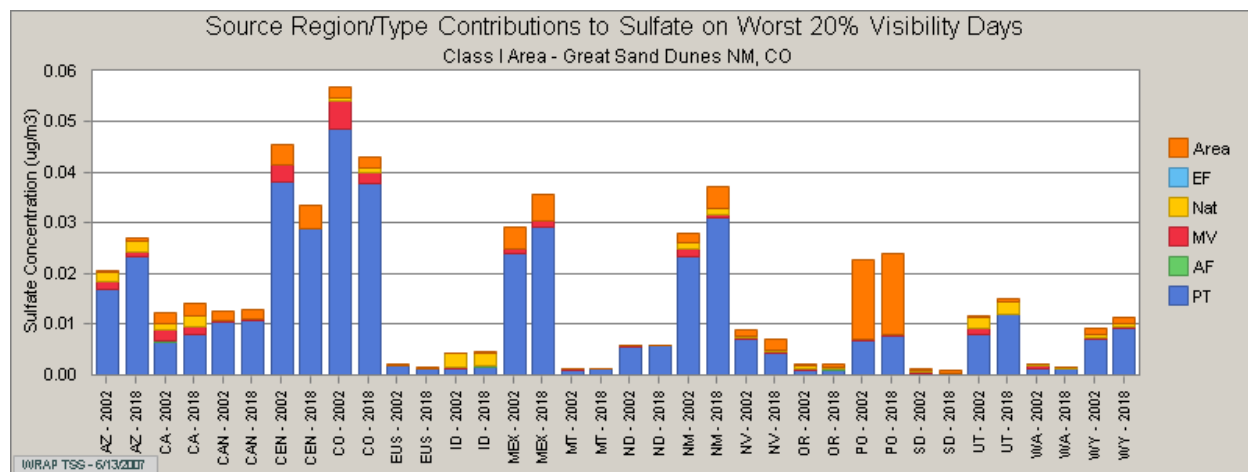
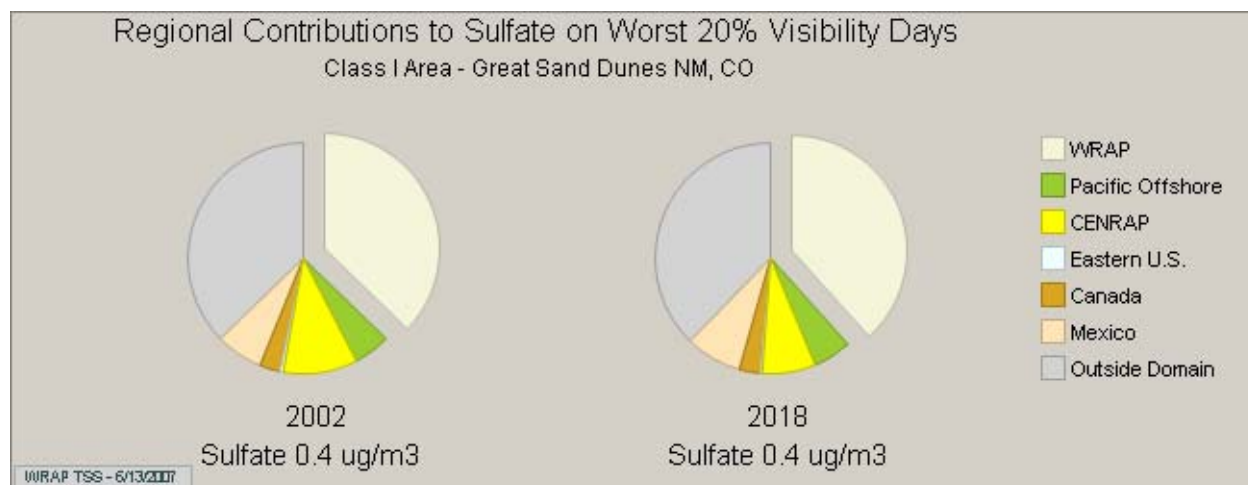


Figure 7-2 displays the 2002 and 2018 worst days sulfate concentrations for each source region impacting GRSA. As indicated, the outside the model domain sulfate sources are as large a contributor as the Western Regional Air Partnership (WRAP) states.

Figure 7-2: Sulfate PSAT - Regional Pie Chart for Worst Days in 2002 and 2018



### C. Particulate Sulfate PSAT for Best Days in 2002 and 2018

Figure 7-3 displays the 2002 and 2018 best days (in pairs) particulate sulfate concentrations for each source area impacting GRSA. The chart provides details on the relative source type contribution for a particular source area and the future trend (upward or downward) of each source area. As indicated, the dominant contributors to sulfate at GRSA for the best days appear to be Colorado, New Mexico, Arizona, Mexico, Utah, Wyoming and CENRAP (central US) region. The future 2018 sulfate trends for the best days are downward for Colorado, New Mexico and CENRAP but increasing for Arizona, Mexico and Wyoming. Point sources (denoted “PT” in blue) appear to be the dominant source of sulfate.

Figure 7-3: Sulfate PSAT - Source Region Bar Chart for Best Days in 2002 and 2018

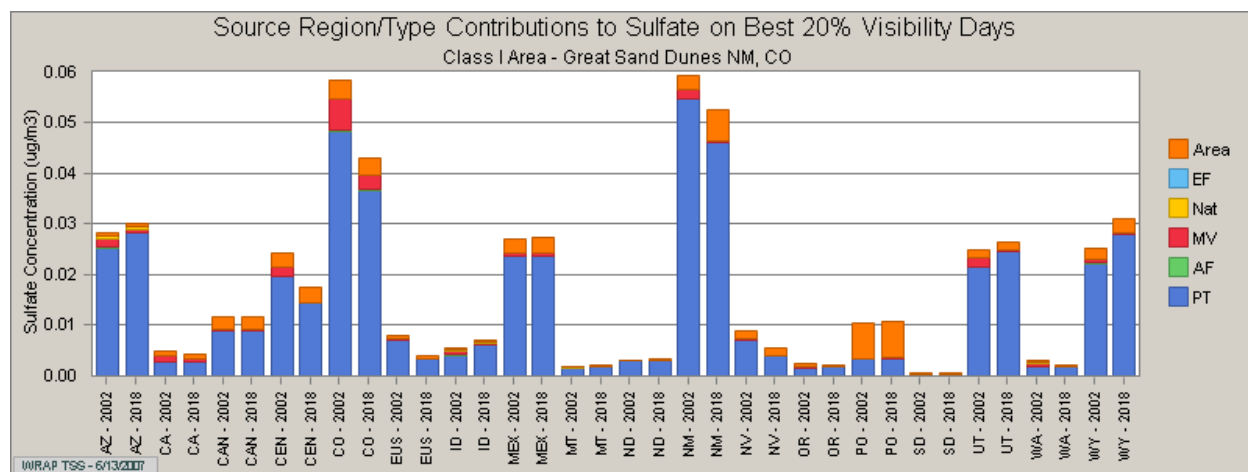
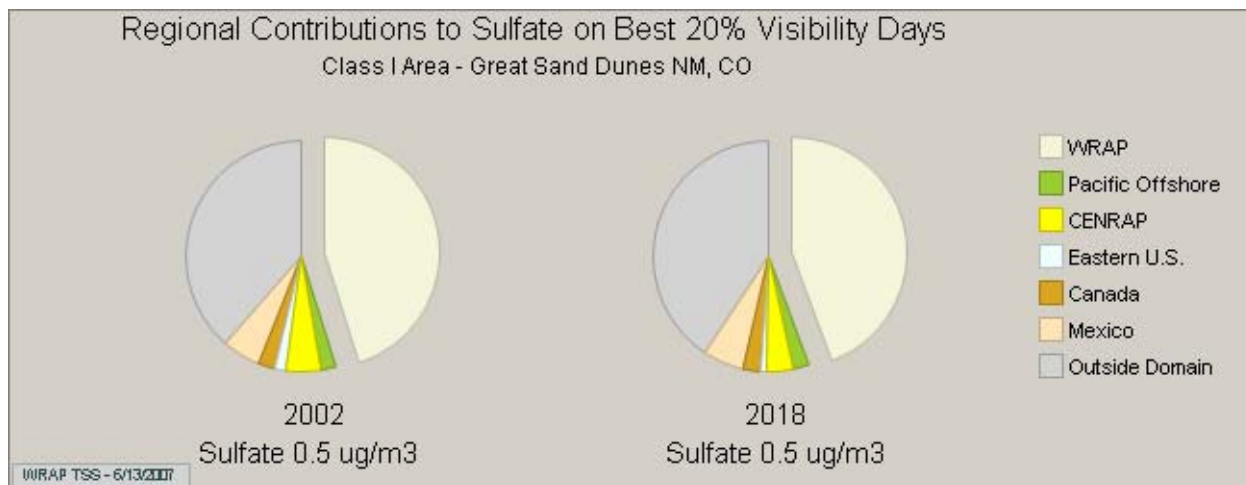


Figure 7-4 displays the 2002 and 2018 best days sulfate concentrations for each source region impacting GRSA. As indicated, the outside the model domain sources are as large a contributor to impacts at GRSA as the Western Regional Air Partnership (WRAP) states. On the best days, sulfate appears to have a higher average concentration than sulfate on the worst days.

Figure 7-4: Sulfate PSAT - Regional Pie Chart for Best Days in 2002 and 2018



### D. Particulate Nitrate PSAT for Worst Days in 2002 and 2018

Figure 7-5 displays the 2002 and 2018 worst days (in pairs) particulate nitrate concentrations for each source area impacting GRSA. The chart provides details on the relative source type contribution for a particular source area and the future trend (upward or downward) of each source area. As indicated, the dominant contributors to nitrate at GRSA for the worst days appear to be New Mexico, Colorado, and CENRAP (central US) region. The future 2018 nitrate trends for the worst days are downward for Colorado and CENRAP but significantly increasing for New Mexico. Point sources (denoted “PT” in blue) along with area (orange color) and mobile sources (denoted “MV” in red) appear to be the dominant sources of nitrate.

Figure 7-5: Nitrate PSAT – Source Region Bar Chart for Worst Days in 2002 and 2018

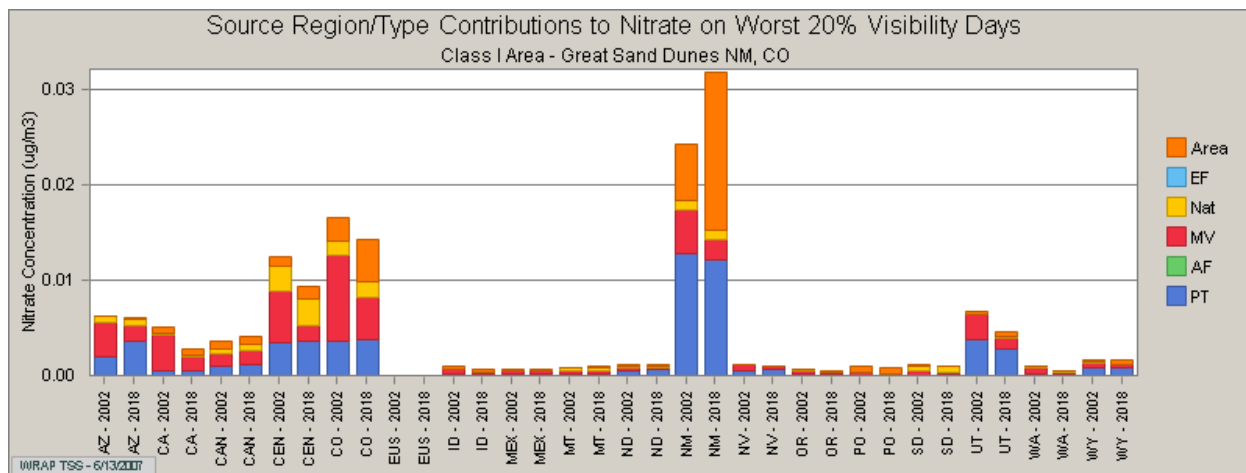
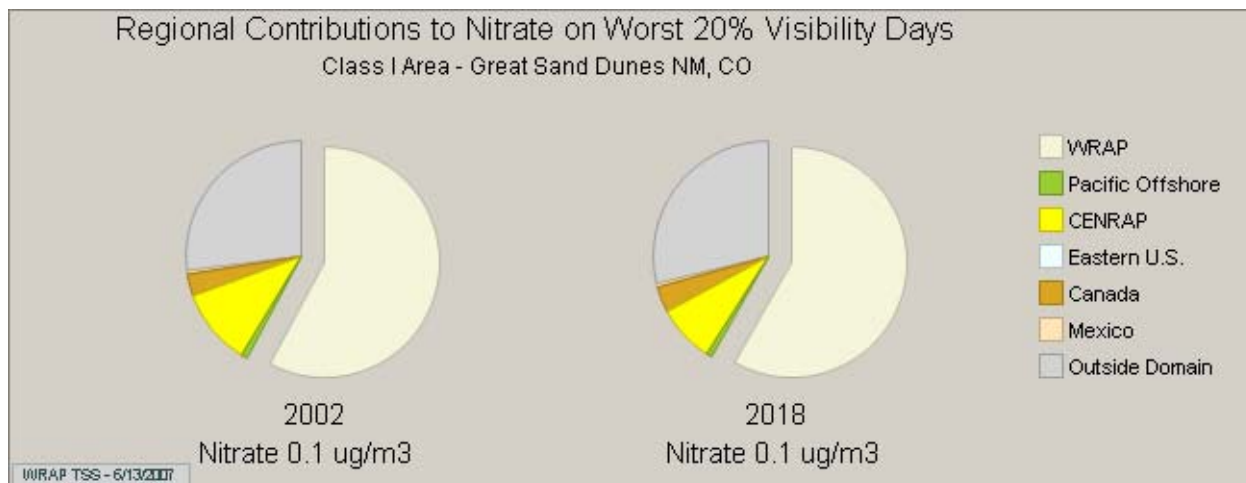


Figure 7-6 displays the 2002 and 2018 worst days nitrate concentrations for each source region impacting GRSA. As indicated, the Western Regional Air Partnership (WRAP) states appear to be the dominant source of nitrate on the worst days.

Figure 7-6: Nitrate PSAT - Regional Pie Chart for Worst Days in 2002 and 2018



### E. Particulate Nitrate PSAT for Best Days in 2002 and 2018

Figure 7-7 displays the 2002 and 2018 best days (in pairs) particulate nitrate concentrations for each source area impacting GRSA. The chart provides details on the relative source type contribution for a particular source area and the future trend (upward or downward) of each source area. As indicated, the dominant contributors to nitrate at GRSA for the best days appear to be Colorado, New Mexico and Utah. The future 2018 nitrate trends for the best days are downward for Colorado and Utah but increasing for New Mexico. Point sources (denoted “PT” in blue) along with area (orange color) and mobile sources (denoted “MV” in red) appear to be the dominant sources of nitrate.

Figure 7-7: Nitrate PSAT – Source Region Bar Chart for Best Days in 2002 and 2018

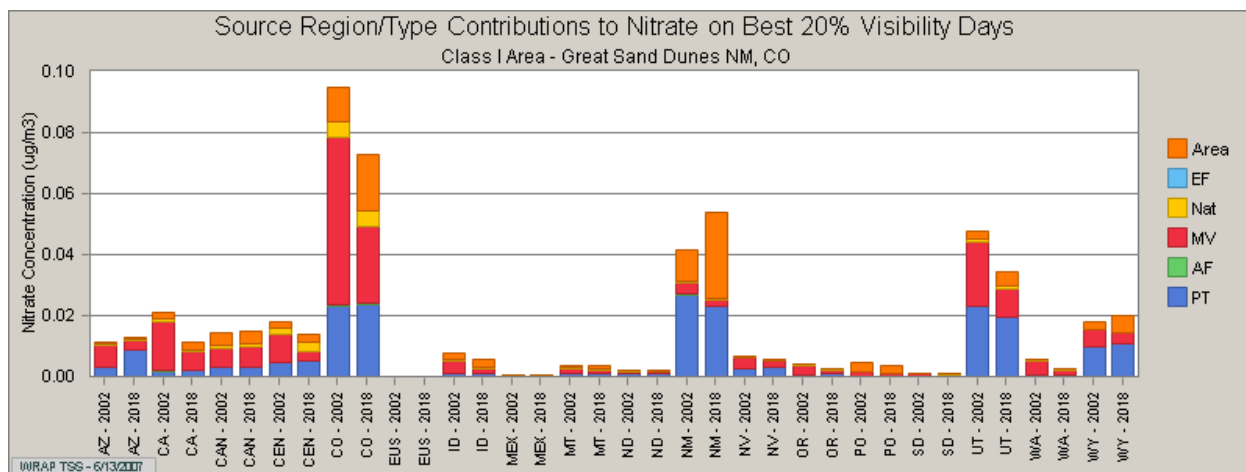
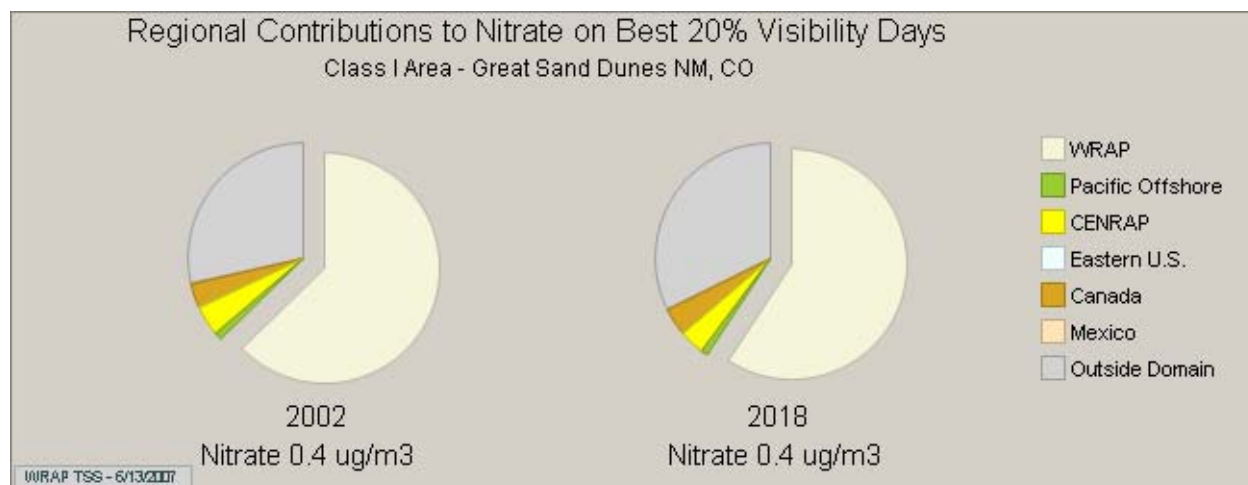


Figure 7-8 displays the 2002 and 2018 best days nitrate concentrations for each source region impacting GRSA. For the best days, the Western Regional Air Partnership (WRAP) states appear to be the dominant source of nitrate. Nitrate on the best days appears to have a higher average concentration over the worst days.

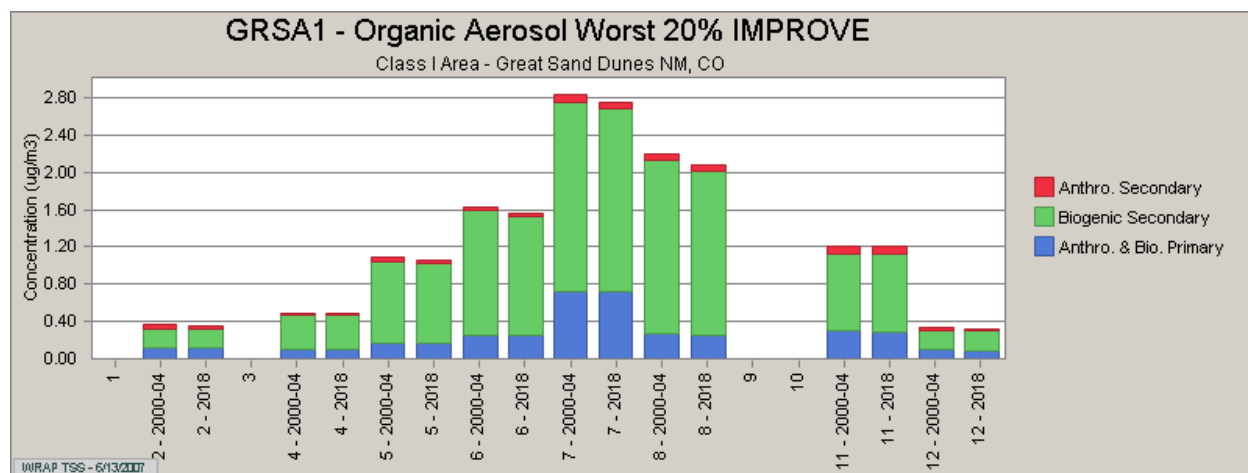
Figure 7-8: Nitrate PSAT - Regional Pie Chart for Best Days in 2002 and 2018



## F. Organic Aerosol PSAT for Worst Days in 2002 and 2018

Figure 7-9 displays the baseline (2000-04) and 2018 monthly (in pairs) organic aerosol concentrations for the worst days at GRSA. The organic aerosol PSAT tracks the following three components: anthropogenic secondary organic aerosol (SOA - red color), biogenic SOA (green color) and anthropogenic/biogenic primary organic aerosol (POA -blue color). The chart provides details on the relative anthropogenic and biogenic contribution each month and the future trend (upward or downward) in 2018.

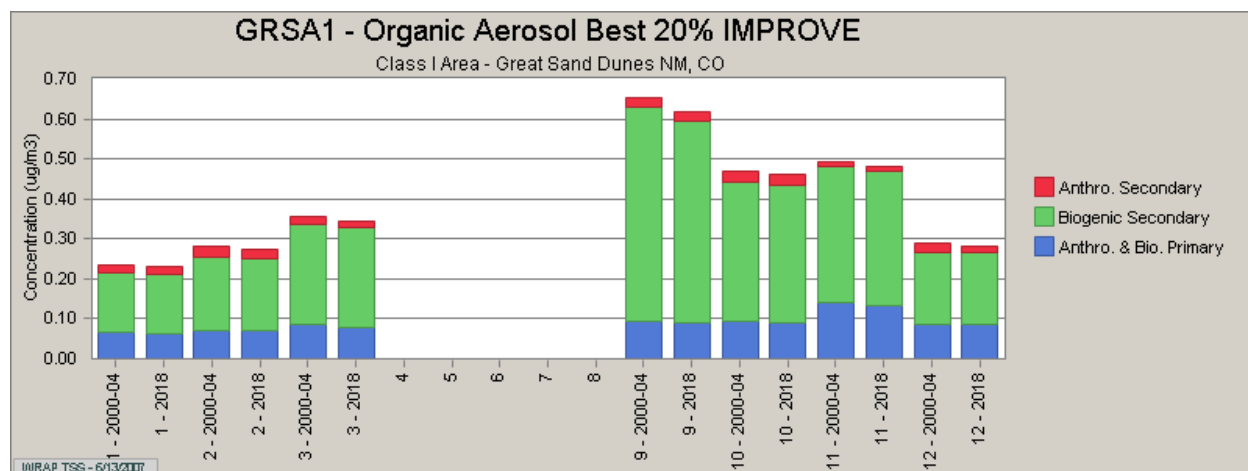
Figure 7-9: Organic Carbon PSAT - Bar Chart for Worst Days in 2002 and 2018



## G. Organic Aerosol PSAT for Best Days in 2002 and 2018

Figure 7-10 displays the baseline (2000-04) and 2018 monthly (in pairs) organic aerosol concentration for the best days at GRSA. The chart provides details on the relative anthropogenic and biogenic contribution each month and the future trend (upward or downward) in 2018. During the baseline period, it is interesting to note that the best days never occur during the summer.

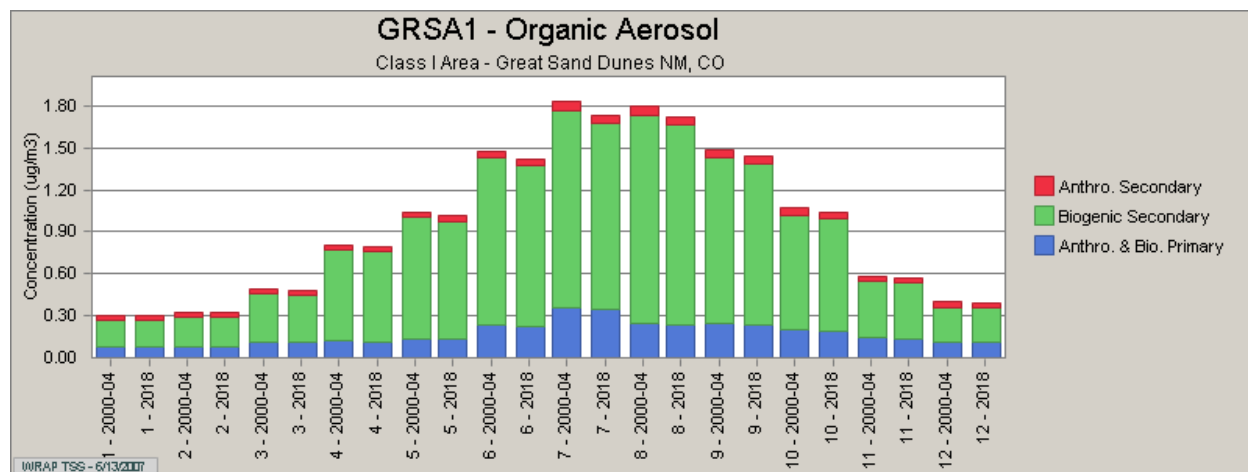
Figure 7-10: Organic Carbon PSAT - Bar Chart for Best Days in 2002 and 2018



## H. Organic Aerosol PSAT for All Days in 2002 and 2018

Figure 7-11 displays the baseline (2000-04) and 2018 monthly (in pairs) organic aerosol concentration for the all days at GRSA. This chart indicates that biogenic SOA (green color) is the dominant source of organic carbon, which occurs at much higher concentrations during the warmer months, which corresponds to the seasons when wildfires typically occur.

Figure 7-11: Organic Carbon PSAT - Bar Chart for All Days in 2002 and 2018



## **SECTION 8: EMISSIONS TRACE**

### **A. ET Overview**

The emissions trace is a tool that graphically combines the information from the PSAT, WEP, and emissions inventory with the statewide stationary source and area source pivot tables. The emissions trace is specific to each class I area for each pollutant (e.g. sulfate, nitrate, organic carbon, elemental carbon, fine soil and coarse mass). The emissions trace focuses on the worst days to allow for easy identification of Colorado sources and the percentage contribution of each category of emissions.

The gray bars identify the source of information displayed in each column. For example “2018 EC WEP” is shorthand for the elemental carbon weighted emissions potential for 2018 or the “2018 POA EI” means the primary organic aerosol emissions inventory for 2018, both of these are discussed in Section 5. All the information from the emissions trace is available to the public and can be found on the WRAP TSS website.

The light green colored bars denote natural sources of secondary particulates, which are fairly common for organic carbon. The light yellow bars denote natural and anthropogenic sources of primary particulates, which are common for elemental carbon, soil and coarse mass. The light blue bars denote anthropogenic sources of secondary particulates, which are common for sulfate and nitrate.

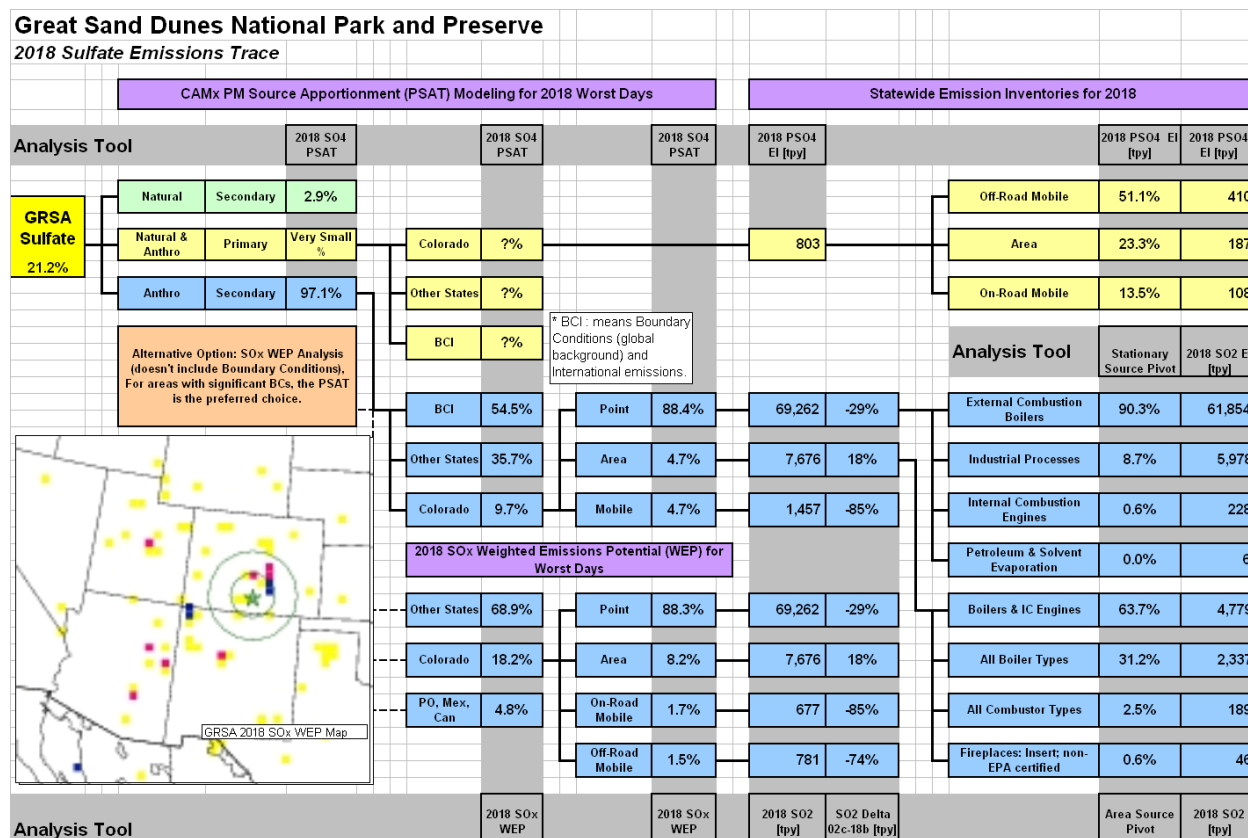
For some particulates such as sulfate, nitrate and organic carbon, the WRAP performed two different analysis techniques, the PSAT and WEP. The PSAT analysis better characterizes sulfate, nitrate and OC, since secondary particle formation dominates these components of extinction. As discussed earlier, the PSAT module of the CAMx model addresses complex chemistry and particle deposition, which is an important for estimating secondary particulates, particularly for sulfate and nitrate. The WEP analysis for sulfate, nitrate and OC are included on the emissions trace for purposes of comparison and are indicated by the dashed lines. It is important to note that the WEP does not address complex chemistry or particle deposition and does not consider intercontinental particle transport, which helps explain the differences between the PSAT and WEP apportionment of contributing sources.

## B. Sulfate Emissions Trace for 2018 Worst Days

In Figure 8-1, the sulfate emissions trace for Great Sand Dunes National Park (GRSA) indicates that sulfate comprises 21.2% of visibility extinction with about 97.1% of sulfate is human-caused with the majority (54.5%) coming from outside the modeling domain and from international sources. Colorado's contribution is about 9.7%, which is mainly from point sources (88.4%). The regional 2018 SO<sub>x</sub> WEP map indicates that SO<sub>x</sub> emissions from the Front Range and Four Corners are the predominant source regions contributing sulfate at GRSA. From the 2002 baseline, Colorado point sources are expected to reduce SO<sub>2</sub> emissions by 29% in 2018. These reductions are from the implementation of Best Available Retrofit Technology (BART) on specific point sources. In 2018, area source emissions are expected to increase by 18%, which is due to increases in population and growth in the oil & gas industry. The 85% reduction in mobile sources is due to clean fuel standards.

The modeled sulfate projection (see Section 6 D.2) indicates fair progress (40%) towards the 2018 UPG. The GRSA sulfate emissions trace indicates that although Colorado is a relatively minor contributor (<10%), the Division may conduct additional future analysis to determine if additional Colorado SO<sub>2</sub> controls are practical.

Figure 8-1: Sulfate Emissions Trace for 2018 Worst Days

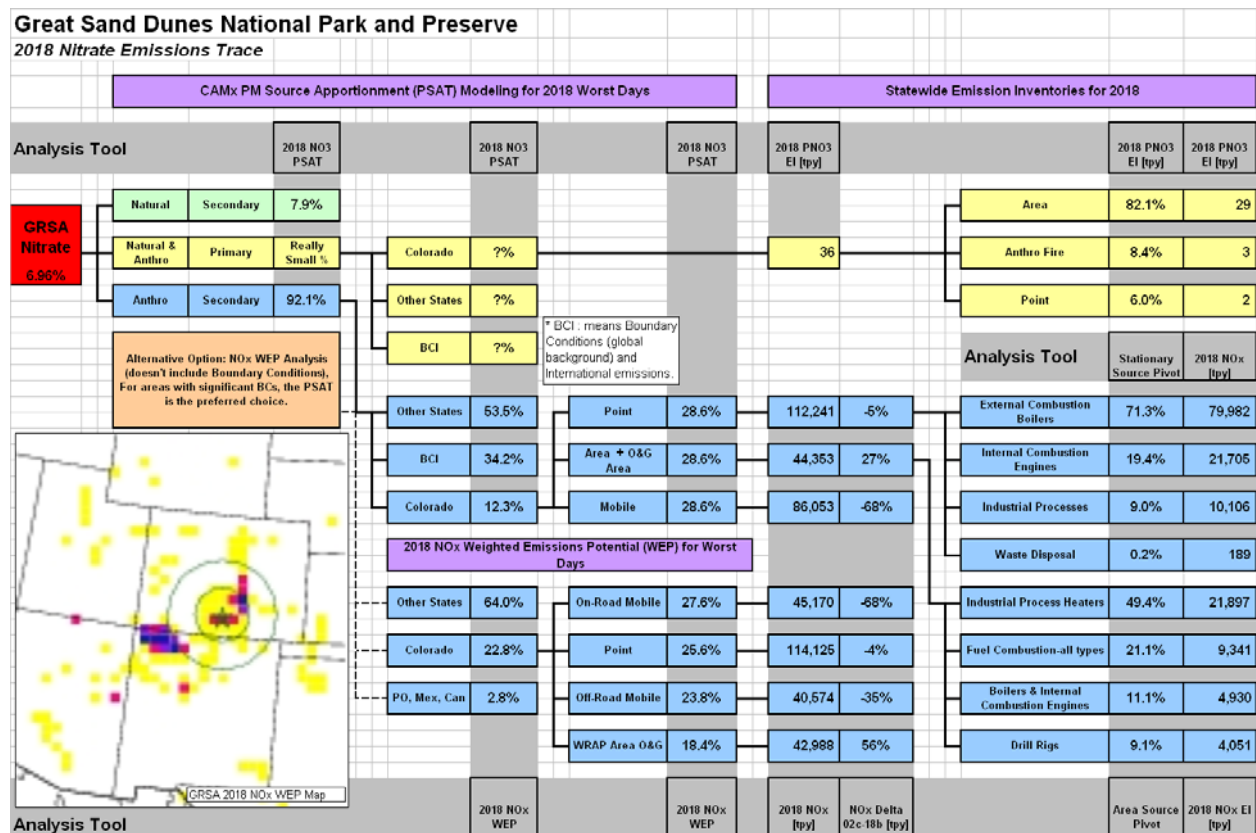


### C. Nitrate Emissions Trace for 2018 Worst Days

In Figure 8-2, the nitrate emissions trace for Great Sand Dunes National Park (GRSA) indicates that nitrate comprises 6.96% of visibility extinction with about 92.1% of nitrate is human-caused with the majority (53.5%) coming from surrounding states and over 34% from outside the modeling domain and from international sources. Colorado's contribution to GRSA nitrate is about 12.3%, which are evenly distributed between point (28.6%) area (28.6%) and mobile (28.6%) sources. The regional 2018 NOx WEP map indicates that NOx emissions from the Southern Front Range and Four Corners area are the predominant source regions contributing nitrate at GSDNP. From the 2002 baseline, Colorado point sources are expected to reduce NOx emissions by 5% in 2018. These reductions are from the implementation of Best Available Retrofit Technology (BART) on specific point sources. In 2018, area source emissions are expected to increase by 27%, which is due to increases in population and growth in the oil & gas industry. The 68% reduction in mobile sources is due to federal Tier II emission standards on motor vehicles.

The modeled nitrate projection (see Section 6 D.2) indicates poor progress (12%) towards the 2018 UPG. The GRSA nitrate emissions trace indicates that although Colorado is a relatively minor contributor (<11%), the Division may conduct additional future analysis to determine if additional Colorado NOx controls are practical.

Figure 8-2: Nitrate Emissions Trace for 2018 Worst Days



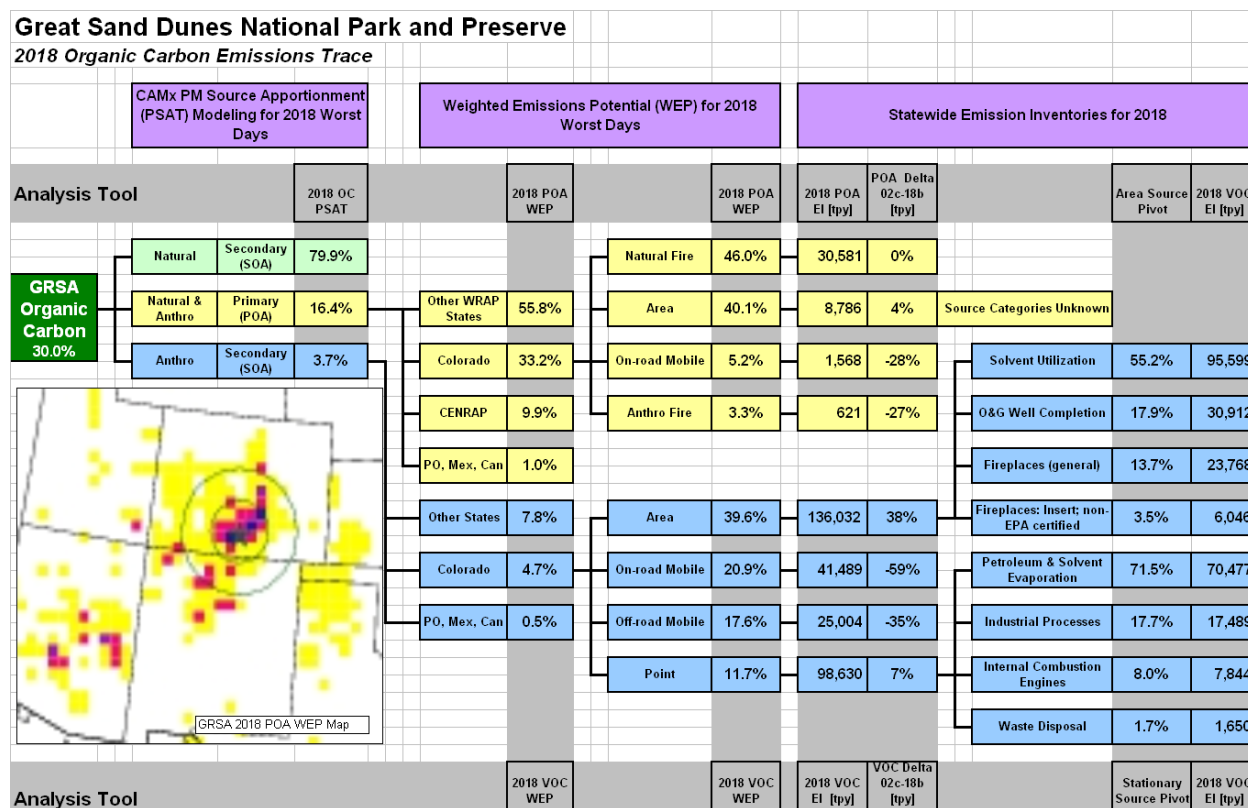
## D. Organic Carbon Emissions Trace for 2018 Worst Days

In Figure 8-3, the organic carbon (OC) emissions trace for Great Sand Dunes National Park (GRSA) indicates that OC comprises 30% of visibility extinction with the majority of OC (about 80%) is natural secondary organic aerosol (SOA) that originates from wildfires with another 3.7% of SOA is directly attributable anthropogenic emissions. Primary Organic Aerosol (POA) accounts for about 16.4%, which is from both natural sources and human-caused sources. Colorado contributes about 33.2% of the POA with the majority originating from natural fires (46%) and area sources (40%). The regional 2018 POA WEP map indicates a wide distribution of POA emissions with higher contributions from developed areas.

The anthropogenic portion of VOC emissions are tracked under the anthropogenic SOA trace, which contributes about 3.7% to organic carbon particulates. Other states appear to be the dominant contributor of anthropogenic SOA at 7.8%. Unfortunately, the WRAP did not produce VOC WEP maps for organic carbon.

The modeled OC projection (see Section 6 D.2) indicates poor progress (25%) towards the 2018 UPG. The GRSA OC emissions trace indicates that the majority of OC appears to be natural SOA (80%) with Colorado anthropogenic POA & SOA contributions under 6% including 2% from unknown area sources of POA. Considering Colorado's relatively minor contribution to OC and the uncertainty of significant source contributors, the Division has determined that further analysis of potential statewide POA and VOC emission controls may not be practical at this time.

Figure 8-3: Organic Carbon Emissions Trace for 2018 Worst Days

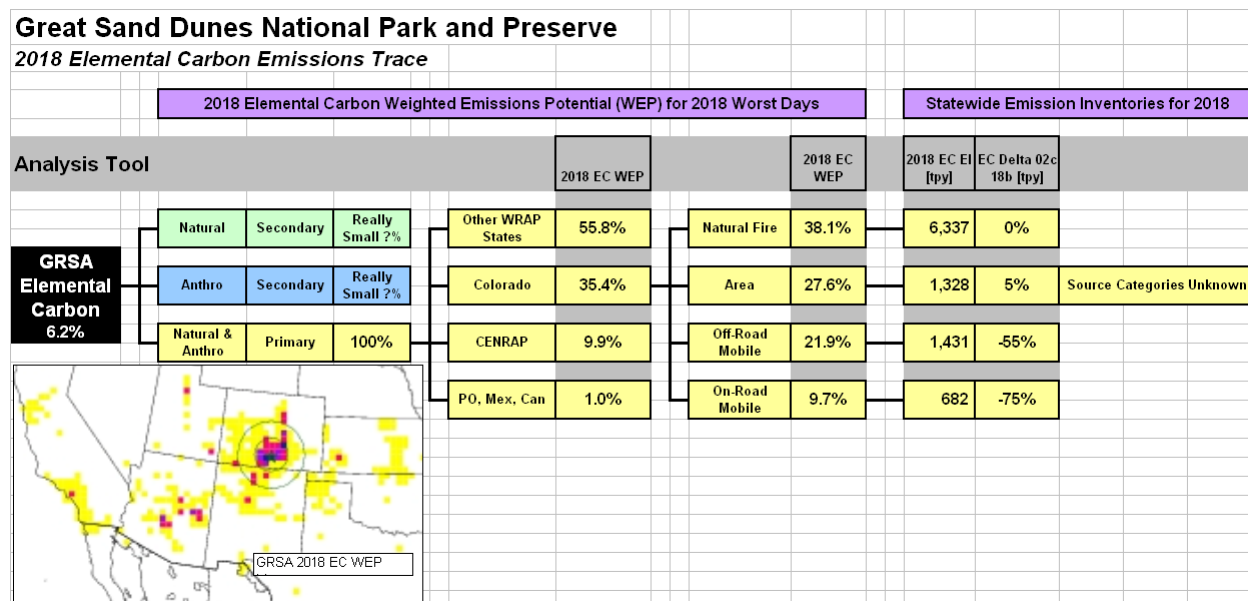


## E. Elemental Carbon Emissions Trace for 2018 Worst Days

In Figure 8-4, the elemental carbon (EC) emissions trace for Great Sand Dunes National Park (GRSA) indicates that EC comprises 6.2% of visibility extinction with all EC in the form of primary particulates. Colorado's contribution is about 35.4%, which is mainly from wildfire (38.1%), area (27.6%), off-road mobile sources (21.9%) and on-road mobile sources (9%). Other WRAP states contribute about 55.8%, CENRAP (9.9%) and Pacific offshore, Mexico & Canada contributing about 1%. The regional 2018 EC WEP map indicates concentrations of EC emissions from the southern Front Range and the San Luis Valley area are contributing EC at GRSA. The reductions in off-road and on-road mobile, 55% and 75% respectively, are due to federal clean fuel standards and Tier II vehicle emission standards.

The modeled EC projection (see Section 6 D.2) indicates excellent progress (126%) that exceeds the 2018 UPG. Since elemental carbon emissions are not currently inventoried by the Division but based on modeled estimates for area, mobile and fire source categories, the Division has determined that further analysis of potential emission controls on EC sources may not be practical at this time.

Figure 8-4: Elemental Carbon Emissions Trace for 2018 Worst Days

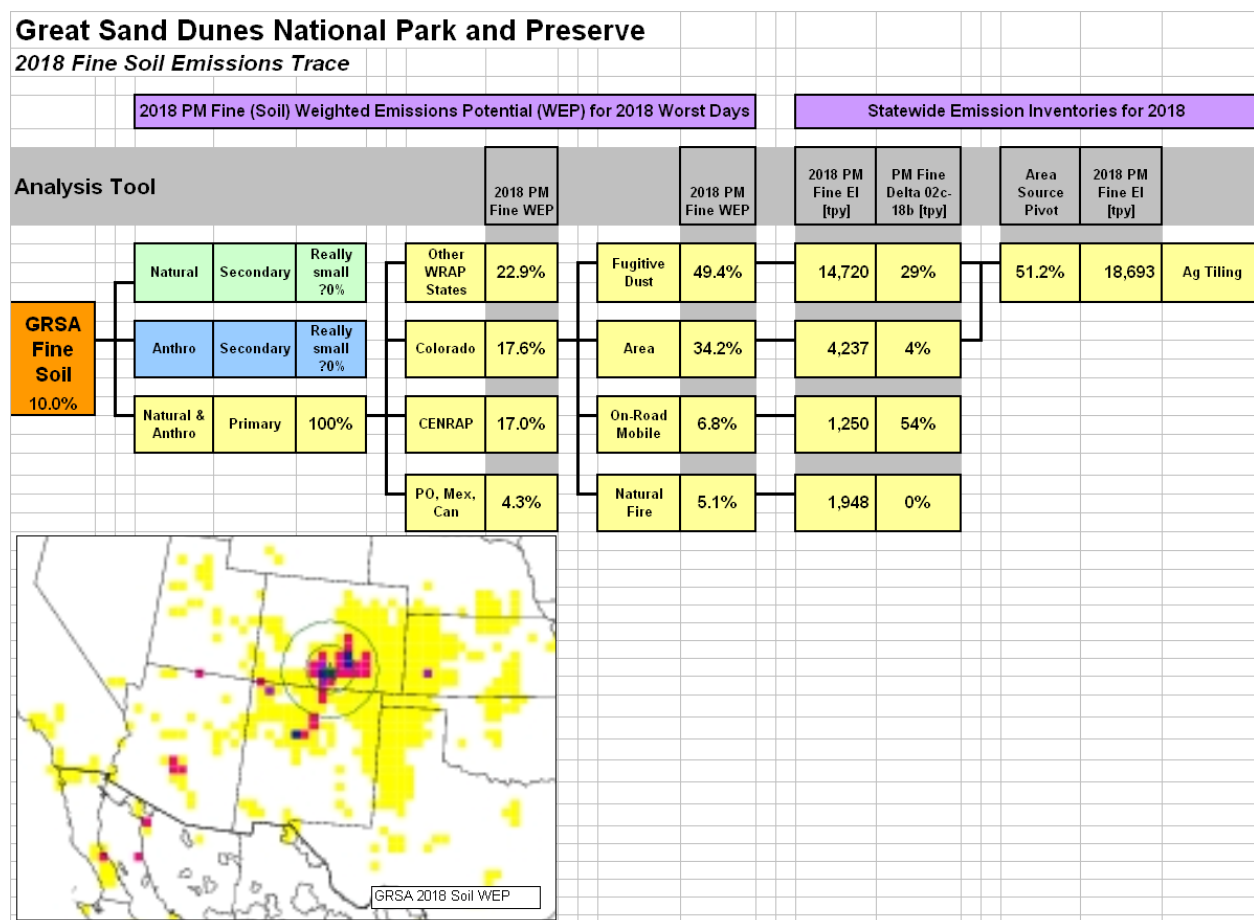


## F. Fine Soil Emissions Trace for 2018 Worst Days

In Figure 8-5, the fine soil emissions trace for Great Sand Dunes National Park (GRSA) indicates that soil comprises 10% of visibility extinction with all soil in the form of primary particulates. Colorado's contribution is about 17.6%, which is mainly from fugitive dust (49.4%) and area sources (34.2%). Other WRAP states contribute about 22.9%, CENRAP 17%, with Pacific offshore, Mexico & Canada contributing about 4.3%. The regional 2018 soil WEP map indicates concentrations of fine soil emissions from the San Luis Valley, southern Front Range, and Four-Corners area are contributing to fine soil impacts at GRSA.

The modeled soil projection (see Section 6 D.2) indicates degradation (-36%) in 2018, although, the high relative modeling error (about 89%) contributes to the uncertainty in the model results. The Division has determined that further analysis of potential emission controls on sources of soil (PM Fine) may not be practical at this time because most of Colorado's soil emissions are from sources (fugitive dust & area) with very uncertain emission inventories.

Figure 8-5: Fine Soil Emissions Trace for 2018 Worst Days

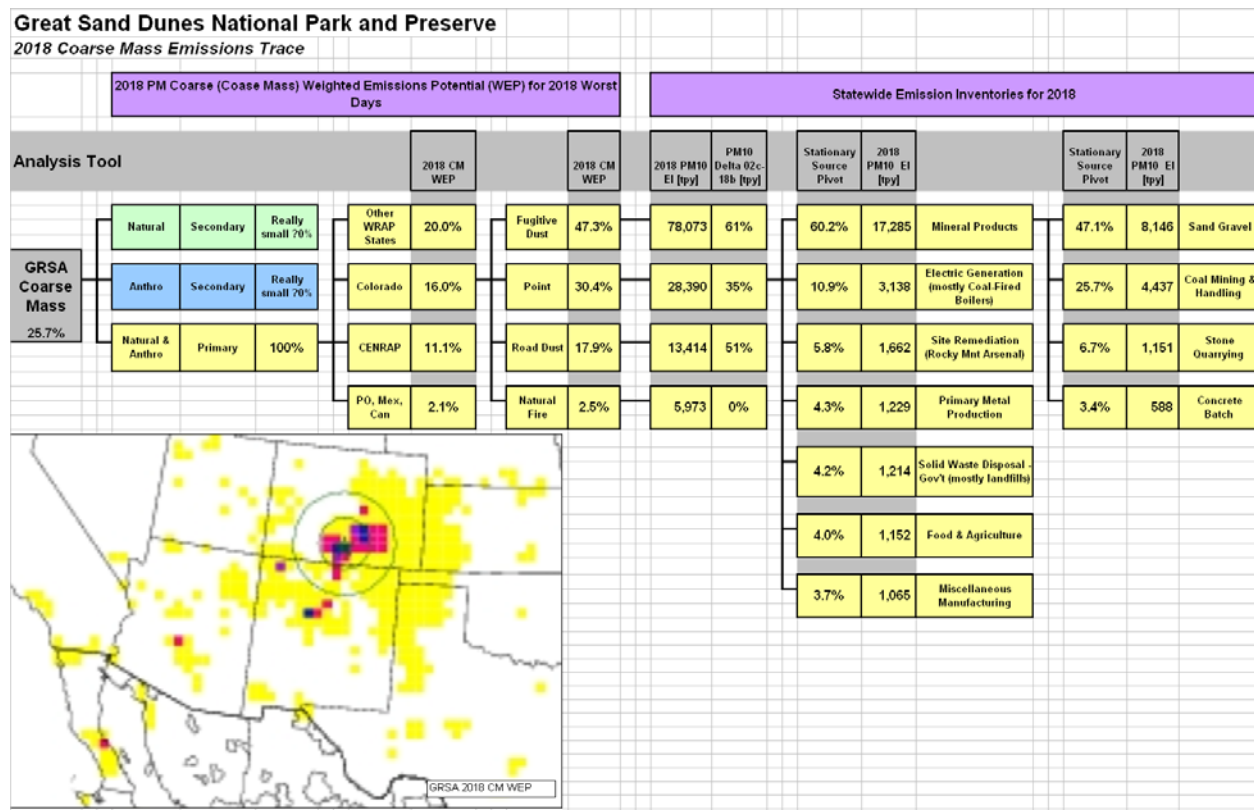


## G. Coarse Mass Emissions Trace for 2018 Worst Days

In Figure 8-6, the Coarse Mass (CM) emissions trace for Great Sand Dunes National Park (GRSA) indicates that CM comprises 25.7% of visibility extinction with all CM in the form of primary coarse particulates. Colorado's contribution is about 16%, which is mainly from fugitive dust (47.3%), point sources (30.4%), and road dust (17.9%). Other WRAP states contribute about 20%, CENRAP 11.1%, with Pacific offshore, Mexico & Canada contributing about 2.1%. The regional 2018 CM WEP map indicates concentrations of CM emissions from the San Luis Valley are contributing to CM impacts at GRSA.

The Division has determined that coarse mass emissions from construction activities and controlled burning will be evaluated under the long-term strategy (LTS). As discussed in Section 6, the model performance for CM across the WRAP region is unacceptable, thus no forecast of CM extinction can be made for 2018. Without model projections, the Division is unable to evaluate the effectiveness of potential emission controls on contributing source categories. Thus, it is impossible to know what is "reasonable" if the benefit (degree of deciview improvement) of such controls cannot be determined at a particular CIA. Under the Regional Haze Rule, the Division is required to develop a long-term strategy (LTS) that must consider measures to mitigate the impacts of construction activities and smoke management techniques for agricultural and forestry management purposes.

Figure 8-6: Coarse Mass Emissions Trace for 2018 Worst Days



# APPENDICES

## Appendix A: IMPROVE Monitoring Program

In the mid-1980's, the IMPROVE program (Interagency Monitoring of Protected Visual Environments) was established to measure visibility impairment in mandatory Class I areas throughout the United States. The monitoring sites are operated and maintained through a formal cooperative relationship between the EPA, National Park Service, U.S. Fish and Wildlife Service, Bureau of Land Management, and U.S. Forest Service. In 1991, several additional organizations joined the effort: State and Territorial Air Pollution Program Administrators and the Association of Local Air Pollution Control Officials, Western States Air Resources Council, Mid-Atlantic Regional Air Management Association, and Northeast States for Coordinated Air Use Management.

### IMPROVE Program Objectives

- ◆ Establish current visibility and aerosol conditions in mandatory Class I areas,
- ◆ Identify chemical species and emission sources responsible for existing human-made visibility impairment,
- ◆ Document long-term trends for assessing progress towards the national visibility goals,
- ◆ With the enactment of the Regional Haze Rule, to provide regional haze monitoring representing all visibility-protected federal Class I areas where practical.

The data collected at these sites are used by land managers, industry planners, scientists, public interest groups, and air quality regulators to better understand and protect the visual air quality resource in Class I areas. Most importantly, the IMPROVE Program scientifically documents the visual air quality of their wilderness areas and national parks.

## Appendix B: Photographic Images of Visibility

### Overview

In 1995, the IMPROVE (Interagency Monitoring of Protected Visual Environment) Steering Committee formed a consensus, that five years of scene monitoring yields sufficient examples of most visual air quality conditions. To secure a representative set of observed air quality conditions for each scene-monitoring site, a series of slides is selected from the period of record and archived on CD-ROM. This series of slides makes up the historical photographic archive and consists of:

- A spectrum series of regional haze visibility conditions observed at the site for each monitored time of day.
- Selected visibility and meteorological episodes or events observed during the period of record (including wildfire, winter inversions, and/or regional haze impacts).
- Selected layered haze events observed during the period of record.
- Specific slides that show scenic views of the vista and observations of meteorological interest during the period of record.
- Historical slide selections requested by the IMPROVE Steering Committee and/or other air quality managers that depict visibility conditions for project-specific reports or public presentations.

### Image Selection Process

The total number of slides selected for each historical archive depends on the vista, the variability in visual air quality, the period of record, and completeness of the slide database. Final sets can vary from 50 to 150 slides. Final images are selected and assigned to gallery archive types (accessed at the left) as follows:

- Spectrum series slides consist of selected clear sky days that represent a range of visibility conditions from good to bad for selected monitoring periods. Slides with fog and other weather-related occurrences or evident layered hazes are not included. Impaired visibility is most often apparent by the loss of color, texture or contrast of scenic features. Each series also contains slides showing a uniform haze, which degrades visibility evenly across the scene.

Using slide densitometry measurements, known target distances, and estimated inherent contrast measurements; the visual range (km) is estimated for each slide of the series. All values are rounded for precision. Associated extinction ( $Mm^{-1}$ ) and haziness (dv) values are calculated. Representative cumulative frequency summaries for each image are provided for sites that also have IMPROVE aerosol-monitoring instrumentation.

- Episode series slides are chosen to represent regional or layered haze conditions that continue for a period greater than an isolated event (2 or more days). These can often be attributed to wildfires, long-term periods of air stagnation, plumes, or winter inversions in the region.
- Layered haze slides depict ground-based or elevated layered haze, or some combination thereof described as multiple haze layers. Layered hazes occur when pollutants are released into a stable atmosphere with little or no vertical mixing. The pollutants form a layer of haze that continues to develop as long as the air mass above remains stagnant. Layers can form near the ground and are known as ground-based layered hazes. Layers that are not in contact with the ground are described as elevated layered hazes. Layered

hazes are usually associated with emissions that are local in nature as opposed to pollutants that are transported over hundreds of kilometers.

- Scenic slides represent special scenic qualities such as interesting cloud formations, pristine conditions, snow-covered scenes or meteorological observations.
- Historical selections include any slide data that has been used to depict visibility conditions in project-specific reports or public presentations. Base slides used for the modeling application WinHaze Visual Air Quality Modeler, and the header image used for HTML-formatted Web pages of this historical archive are also included in historical selections.

Historical slide archives for each site are reproduced digitally to Kodak Photo Cd (PCD) format and transferred to a Kodak Gold CD. Master historical photographic archives produced for each site contain 4 JPEG resolutions of each selected image (Image Gallery); graphic images of the monitoring location and site vistas (Site Specifications); as well as associated cumulative frequency summaries, tables, and/or data listings (Spectrum Frequencies).

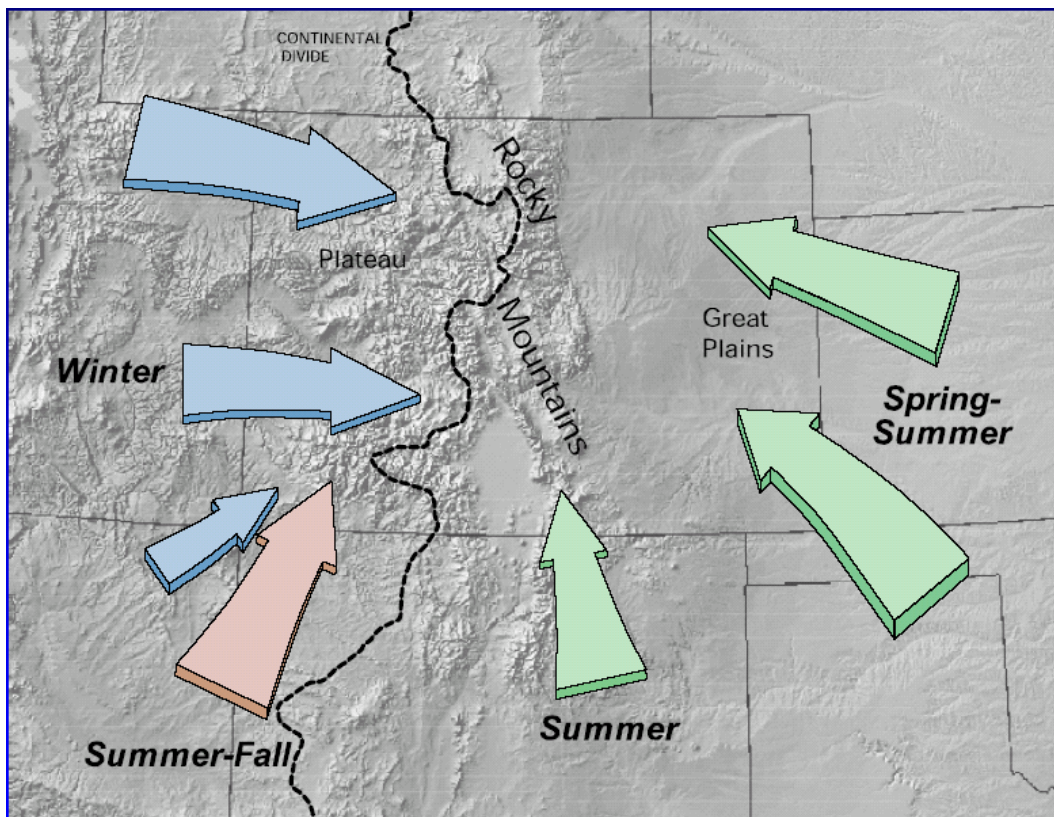
## Appendix C: Seasonal Wind Patterns

While all winds are the movement of air mostly parallel to the Earth's surface, they come in a variety of forms including global, synoptic, mesoscale and microscale. Global winds are the result of global circulation patterns that include trade winds and the jet stream. Synoptic winds are regional winds that are associated with large-scale events such as warm and cold fronts, and are part of what makes up everyday weather. Mesoscale winds typically arise and fade over time-periods too short and over geographic regions too narrow to predict with any long-range accuracy. Microscale winds take place over very short durations of time (seconds – minutes) in areas comprising tens of acres.

Mountain and valley breezes are mesoscale winds resulting from heating (due to solar radiation) and cooling of the land surface. In the case of a valley wind, the radiated ground heats air next to a mountain slope in the daytime while colder, denser air farther away from the mountain slope settles down upon the warmer air forcing it to move up the mountain slope. At night, the opposite movement occurs. The air on the mountain slope gradually cools and becomes heavier than the surrounding air and drains down into the valley. Mountain winds are usually stronger than valley winds.

Figure D -1 depicts the synoptic (regional) wind patterns for the various seasons in Colorado. The influence of mountain and valley winds for a particular Class I area are not addressed in the below map.

Figure D-1: Airflow into Colorado



Source: Nolan Doesken, state climatologist

## **Appendix D: Weighted Emissions Potential**

### **Introduction**

The Weighted Emissions Potential analysis (WEP) was developed as a screening tool for states to decide which source regions have the potential to contribute to haze formation at specific Class I areas, based on both the 2002 and 2018 emissions inventories. This method does not produce highly accurate results because, unlike the air quality model and associated PSAT analysis, it does not account for chemistry and removal processes. Instead, it relies on an integration of gridded emissions data, back trajectory residence time data, a one-over-distance factor to approximate deposition, and a normalization of the final results. Residence time over an area is indicative of general flow patterns, but does not necessarily imply the area contributed significantly to haze at a given receptor. Therefore, users are cautioned to view the WEP as one piece of a larger, more comprehensive weight of evidence analysis.

### **Emissions Data Inputs**

The emissions data used were the annual, 36km grid SMOKE-processed, model-ready emissions inventories provided by the WRAP Regional Modeling Center (RMC). The analysis was performed for nine (9) pollutants (maps were generated for all but the last three):

- Sulfur oxides
- Nitrogen oxides
- Organic carbon
- Elemental carbon
- Fine particulate matter
- Coarse particulate matter
- Ammonia
- Volatile organic carbon
- Carbon monoxide.

The following source categories for each pollutant were identified and preserved through the analysis:

- Biogenic
- Natural fire
- Point
- Area
- WRAP oil and gas
- Off-shore
- On-road mobile
- Off-road mobile
- Road dust
- Fugitive dust

- Windblown dust
- Anthropogenic fires

### **Residence Time Inputs**

The back trajectory residence times were provided by the WRAP Causes of Haze Assessment (COHA). The COHA project used NOAA’s HYSPLIT model to generate eight (8) back trajectories daily for each WRAP Class I area for the entire five-year baseline period (2000-04). The major model parameters selected for this analysis are presented in Table 1. From these individual trajectories, residence time fields were generated for one-degree latitude by one-degree longitude grid cells. Residence time analysis computes the amount of time (e.g., number of hours) or percent of time an air parcel is in a horizontal grid cell. Plotted on a map, residence time is shown as percent of total hours in each grid cell across the domain, thus allowing an interpretation of general air flow patterns for a given Class I area. The residence time fields for the 20% worst and best IMPROVE-monitored extinction days were selected for the WEP analysis to highlight the potential emissions sources during those specific periods.

Table 1

Back Trajectory Model Parameters Selected for WEP Analysis

Model Parameter	Value
Trajectory duration	192 hours (8 days) backward in time
Top of model domain	14,000 meters
Vertical motion option	used model data
Receptor height	500 meters
Meteorological Field	EDAS and FNL (location dependent)

### **Integration of Emissions and Residence Time Data**

The WEP analysis consisted of weighting the annual gridded emissions (by pollutant and source category) by the worst and best extinction days residence times for the five-year baseline period. To account for deposition along the trajectories, the result was further weighted by a one-over-distance factor, measured as the distance in km between the centroid of each emissions grid cell and the centroid of the grid cell containing the Class I area monitoring site under investigation. (The “home” grid cell of the monitoring site was weighted by one fourth of the 36km grid cell distance, or one-over-9km, to avoid a large response in that grid cell.) The resulting weighted emissions field was normalized by the highest grid cell to ease interpretation.

An example series of maps illustrating the WEP analysis is presented in Figure 1. This example shows the annual emissions for NOx across the domain, the specific residence time pattern for the 20% worst monitored days at a Class I area, and the resulting weighted emissions map. Both the 2002 and 2018 cases are presented. Interpretation of the results should focus on which grid cells (or larger regions) have significant potential to affect the Class I area, and on changes between 2002 and 2018.

An example of associated bar charts showing the estimated contribution by source category and region is presented in Figure 2. It is important to note that these charts show normalized values with no direct connection to original emissions values. Interpretation of the results should focus on the relative contributions by each source category and region, and the changes between 2002 and 2018.

### **Caveats**

The WEP is not a rigorous, stand-alone analysis, but a simple, straightforward use of existing data. As such, there are several caveats to keep in mind when using WEP results as part of a comprehensive weight of evidence analysis:

- This analysis does not take into account any emissions chemistry.
- While actual emissions may vary considerably throughout the year, this analysis pairs up annual emissions data with 20% worst/best extinction days residence times – this is likely most problematic for carbon and dust emissions, which can be highly episodic.
- Coarse particle and some fine particle dust emissions tend not to be transported long distances due to their large mass.
- The WEP results are unitless numbers, normalized to the largest-valued grid cell. Effective use of these results requires an understanding of actual emissions values and their relative contribution to haze at a given Class I area.

## Appendix E: Standard Aerosol-Type Equations

This section addresses the equations for calculating aerosol types, e.g. sulfate, organic, soil, from elemental concentrations.

The following table lists the standard formulae and assumptions applied to IMPROVE sampler measurements to derive the principal fine aerosol species, reconstructed fine mass, and coarse mass. The brackets indicate the mass concentration of the aerosol species or element. For a detailed discussion on these aerosol type equations see Malm et al, 1994, Chapter 2 of the 2000 IMPROVE report and Chapter 2 of the 1996 IMPROVE report

SPECIES	Abbreviation	FORMULA	ASSUMPTIONS
Ammonium Sulfate	SULFATE	4.125[S]	All elemental S is from sulfate. All sulfate is from ammonium sulfate.
Ammonium Nitrate	NITRATE	1.29[NO <sub>3</sub> ]	Denuder efficiency is close to 100%. All nitrate is from ammonium nitrate.
total Organic Carbon	OC	OC1+OC2+OC3+OC4+OP (see definitions below)	
Organic Mass by Carbon	OMC	1.4 * OC	Average organic molecule is 70% carbon.
Organic Carbon by Hydrogen	OCH	(11 * (H - 0.25 * S))	Assumes all sulfur is ammonium sulfate and there is no hydrogen from nitrate. Organic mass is equal to 1.4*OCH
Light Absorbing Carbon	LAC	EC1+EC2+EC3-OP (see definitions below)	
Fine Soil	SOIL	2.2[Al]+2.49[Si]+1.63[Ca] +2.42[Fe]+1.94[Ti]	[Soil K]=0.6[Fe]. FeO and Fe <sub>2</sub> O <sub>3</sub> are equally abundant. A factor of 1.16 is used for MgO, Na <sub>2</sub> O, H <sub>2</sub> O, CO <sub>2</sub> .
ReConstructed Fine Mass	RCFM	[SULFATE]+[NITRATE] +[LAC]+[OMC]+[SOIL]	Represents dry ambient fine aerosol mass for continental sites.
Coarse Mass	CM	[PM <sub>10</sub> ] - [PM <sub>2.5</sub> ]	Consists only of insoluble soil particles.

**Ammonium Sulfate (NH<sub>4</sub>SO<sub>4</sub>):** The sulfur on the Teflon filter is always present as sulfate (SO<sub>4</sub>). In most cases the sulfate is fully neutralized ammonium sulfate, which is 4.125 times the sulfur concentration. The sulfate at Eastern sites during the summer is not always fully neutralized resulting in acidic aerosol. If 100% of the sulfur were sulfuric acid, the correct sulfate mass would be 74% of the calculated (NH<sub>4</sub>)<sub>2</sub>SO<sub>4</sub>.

**Organic Carbon:** Aerosol samples collected on quartz filters are analyzed at Desert Research Institute for carbon using the Thermal Optical Reflectance (TOR) combustion method. The sample is heated in steps and the evolved CO<sub>2</sub> is measured at each step. The first four steps take place in a pure helium atmosphere to prevent combustion. The carbon released in these steps (OC1-OC4) is interpreted as being evaporated organics. 2% O<sub>2</sub> is introduced at 550 °C and more carbon is released. During the pure-helium stage, some of the organic material has been charred (pyrolyzed), darkening the filter (decreasing its reflectivity). The filter starts to lighten when oxygen is introduced oxidizing the char. The carbon that has been recorded in the oxygen stage when the filter returns to its original reflectivity is interpreted as pyrolyzed organics, (OP). The carbon evolved after the filter has returned to its initial reflectance is interpreted as elemental (E1-E3). For a full description, see [Chow et al.](#), in Atmospheric Environment. 27A, 1185-1201, (1993).

Carbon Components as a Function of Temperature and Added Oxygen.					
<i>Fraction</i>	<i>Pyrolyzed Fraction</i>	<i>Temperature Range</i>	<i>Atmosphere</i>	<i>Reflectance vs. Initial</i>	
O1		ambient to 120°C	100% He	at initial	
O2		120 - 250°C		100% He	under initial
O3		250 - 450°C			
O4		450 - 550°C			
E1	OP	remains at 550°C	98% He 2% O <sub>2</sub>		over initial
E2		550 - 700°C			
E3		700 - 800°C			

**Organic Mass by Carbon (OMC):** The organic mass is the sum of the low temperature organics and pyrolyzed organics multiplied by a factor of 1.4:  $OMC=1.4 * (OC1+OC2+OC3+OC4+OP)$  where the factor 1.4 is used to adjust the organic carbon mass (OC) for other elements assumed to be associated with the organic carbon molecule.

**Light-Absorbing Carbon (LAC):** This is the sum of elemental carbon fractions. The pyrolyzed fraction is subtracted. Preliminary analyses indicate that some of the O4 fraction may absorb light, and that OP may overestimate the pyrolytic mass.

**Organic Carbon by Hydrogen (OCH):** The hydrogen on the Teflon filter is associated with sulfate, organics, nitrate, and water. Since the PIXE analysis is done in vacuum, all water will volatilize. Also it is assumed that no significant hydrogen from nitrate remains. If it is further assumed that the sulfate is fully neutralized ammonium sulfate, the organic carbon concentration can be estimated by subtracting the hydrogen from sulfate and multiplying the difference by a constant representing the fraction of hydrogen:

$$OCH = 11*(H-0.24*S)$$

The sulfur factor, H/S ratio, for ammonium sulfate is  $8/32 = 0.25$ . The C/OM ratio is 11 and operationally defined by forcing OCH to equal OC. Comparison of OCH to OC is used in data validation procedures and OCH is used to estimate organic mass when carbon is not explicitly measured.

The OCH calculation is invalid when (1) there is high nitrate relative to sulfate, as at sites near Los Angeles and San Francisco, and (2) the sulfur is not present as ammonium sulfate. This latter includes sites with marine sulfur, and sites in the eastern United States with unneutralized sulfate. The main advantage of using OCH at valid sites is that its precision is better than that for OC during periods of low organic, e.g. winter in the West. At sites in the East, OCH is often low because of unneutralized sulfate, and imprecise because of the high sulfate relative to organic.

**Light-Absorbing Carbon (LAC):** This is the sum of elemental carbon fractions. The pyrolyzed fraction is subtracted. Preliminary analyses indicate that some of the O4 fraction may absorb light, and that OP may overestimate the pyrolytic mass.

**Soil (SOIL):** This is a sum of the soil-derived elements (Al, Si, K, Ca, Ti, Fe) along with their normal oxides ( $Al_2O_3$ ,  $SiO_2$ ,  $CaO$ ,  $K_2O$ ,  $FeO$ ,  $Fe_2O_3$ ,  $TiO_2$ ). The variable does not depend on the type of soil, such as sediment, sandstone, or limestone. One fine element, K, however, may partly derive from smoke as well as soil. Smoke potassium is eliminated from the calculation using Fe as a surrogate. This is discussed in nonsoil potassium below.

**Nonsoil Potassium (KNON):** Fine potassium has two major sources, soil and smoke, with the smoke potassium on much smaller particles than the soil potassium. The potassium in coarse particles will be solely produced from soil. The soil potassium is estimated from the measured concentration of Fe and the ratio of K/Fe of 0.6 measured on coarse samples (2.5 to 15  $\mu m$ ) collected between 1982 and 1986. This ratio depends on the soil composition and varies slightly from site to site. If the ratio were slightly smaller (say 0.5), the KNON values will be negative when there is no smoke influence. The residual potassium,  $K - 0.6 * Fe$ , is then assumed to be produced by smoke. The burning of most organic fuels will produce potassium vapor. During transport, this vapor will transform into fine particles. The KNON parameter is not a quantitative measure of the total smoke mass, since the ratio of nonsoil potassium to total smoke mass will vary widely, depending on the fuel type and the transport time. However, the KNON parameter can be used as an indicator of a nonsoil contribution for samples with large KNON. In some situations, there may be some fine Fe from industrial sources, which could cause occasional smoke episodes to be lost.

## Appendix F: Procedure for Reconstructing Light Extinction

The light-extinction coefficient,  $b_{ext}$  (expressed as inverse megameters, 1/Mm), is the sum:

$$\text{Equation (F-1):} \quad b_{ext} = b_{scat} + b_{abs} = b_{sg} + b_{sp} + b_{ag} + b_{ap}$$

Where  $b_{scat}$  is the sum of scattering by gases and scattering by particles, and  $b_{abs}$  is the sum of absorption by gases and particles. Scattering by gases in the atmosphere,  $b_{sg}$ , is described by the Rayleigh scattering theory [VandeHulst, 1981] and will be referred to as Rayleigh scattering. The IMPROVE program assumes a standard value of 10 1/Mm. Scattering by particles,  $b_{sp}$ , is caused by both fine and coarse aerosol species and is the largest contributor to total light extinction in most locations [Malm et al., 1994a]. Absorption due to gases,  $b_{ag}$ , is primarily due to nitrogen dioxide ( $\text{NO}_2$ ) and is assumed to be negligible because almost all monitoring sites are in rural locations [Trijonis and Pitchford, 1987]. Absorption by particles,  $b_{ap}$ , is caused primarily by carbon containing particles.

A particle in the atmosphere can be a mix (internal mixture) of various aerosol species, or in some cases its compositional structure may be restricted to one species (external mixture) such as  $(\text{NH}_4)_2\text{SO}_4$ . Furthermore, an internally mixed aerosol such as organic/ammoniated sulfate/water particle can be externally mixed from wind-blown dust particles. Whether an aerosol is internally or externally mixed, it scatters and/or absorbs a specific fraction of radiant energy impinging on it. Following the suggestion of White [1986], an aerosol scattering/extinction per unit mass ratio will be referred to as specific scattering/extinction, as in specific gravity.

Most routine aerosol monitoring programs and many special study visibility characterization programs were designed to measure bulk aerosol species mass concentrations such as sulfates, nitrates, carbonaceous material, and selected elements [Heisler et al., 1980; Malm et al., 1994b; Tombach and Thurston, 1994; Watson et al., 1990; Macias et al., 1981]. They were not designed to determine the microphysical and chemical characteristics of these species.

The inherent limitations of estimating aerosol optical properties from bulk aerosol measurements have been addressed, at least in part, by a number of authors. For instance, Ouimette and Flagan [1982] have shown, from basic theoretical considerations, that if an aerosol is mixed externally or if in an internally mixed aerosol the index of refraction is not a function of composition or size, and the aerosol density is independent of volume, then:

$$\text{Equation (F-2)} \quad b_{ext} = \sum_i \alpha_i m_i$$

Where  $\alpha_i$  is the specific scattering or absorption efficiency and  $m_i$  is the mass of the individual species.

Malm and Kreidenweis [1997] demonstrated from a theoretical perspective, that specific scattering of mixtures of organics and ammoniated sulfates were insensitive to the choice of internal or external mixtures. Sloane [1983, 1984, 1986], Sloane and Wolff [1985], and more recently Lowenthal et al. [1995], Malm [1998], and Malm et al. [1997] have shown that differences in estimated specific scattering between external and internal model assumptions are usually less than about 10%. In the absence of detailed microphysical and chemical structure of ambient aerosols, the above studies demonstrate that a reasonable estimate of aerosol extinction can be achieved by assuming each species is externally mixed.

However, the issue of water uptake by hygroscopic species must be addressed. Implicit to the use of Equation (F-2) is an assumed linear relationship between aerosol mass and extinction. It is well known that sulfates and other hygroscopic species form solution droplets that increase in size as a function of relative humidity (RH). Therefore, if scattering is measured at various relative humidities the relationship between measured scattering and hygroscopic species mass can be quite nonlinear. A number of authors have attempted to linearize the model, in an empirical way, by multiplying the hygroscopic species by such a factor as  $1/(1-RH)$  to account for the presence of water mass [White and Roberts, 1977; Malm et al., 1986]. However, Malm et al. [1989] and Gebhart and Malm [1989] proposed a different approach. They multiplied the hygroscopic species by a relative humidity scattering enhancement factor,  $f(RH)$ , that is calculated on a sampling-period-by-sampling-period basis using Mie theory and an assumed size distribution and laboratory measured aerosol growth curves.

Measurements of hygroscopic species growth as a function of relative humidity show that species such as ammonium sulfate show zero growth until a relative humidity, referred to as the deliquescent relative humidity, is reached where they spontaneously form a solution droplet that is in equilibrium with water molecules in the ambient atmosphere. Conversely, when the relative humidity is decreased from some value greater than 80% the solution droplet retains water below the deliquescent point to a relative humidity where all water is spontaneously given up. This point is referred to as the crystallization relative humidity.

However, because the growth factor and light-scattering efficiency for ambient aerosols has previously been observed to be rather smooth, [Sloane 1983, 1984, 1986; Wexler and Seinfeld, 1991; Waggoner et al., 1981; Day et al., 2000; Malm et al. 2000] a "best estimate" for the sulfates and nitrates species growth, the laboratory growth curves, as measured by Tang [1996] were smoothed between the deliquescence and crystallization points. Malm [1998] and Malm et al., [1997] have demonstrated that in both the East (Great Smoky Mountains National Park) and West (Grand Canyon National Park) the best estimate growth model, in combination with measured size distributions, yields an  $f_T(RH)$  function that results in good agreement between measured and reconstructed scattering for particles less than 2.5  $\mu\text{m}$ .

Therefore, the following equation is used to estimate reconstructed particle scattering:

*Equation (F-3):*

$$b_{scat} = (3)f_T(RH)[SULFATE] + (3)f_T(RH)[NITRATE] + (4)f_{org}(RH)[OMC] + (1)[SOIL] + (0.6)[CM] + 10$$

See Aerosol-Type Equations for definitions of the species in equation F-3

The brackets indicate the species concentration, 3  $\text{m}^2/\text{g}$  is the dry specific scattering for ammonium sulfate and ammonium nitrate, 4  $\text{m}^2/\text{g}$  for organic carbon, and 1  $\text{m}^2/\text{g}$  and 0.6  $\text{m}^2/\text{g}$  are the respective scattering efficiencies for soil and coarse mass. The efficiencies for fine soil and coarse mass are taken from a literature review by Trijonis and Pitchford [1987].

A dry scattering efficiency of 3  $\text{m}^2/\text{g}$  is a nominal scattering efficiency based on a literature review by Trijonis et al. [1988, 1990] and a review by White [1990]. Trijonis' best estimate for ammonium sulfate and ammonium nitrate is 2.5  $\text{m}^2/\text{g}$  with an error factor of 2, while for organics it is 3.75  $\text{m}^2/\text{g}$  again with an error factor of 2. White took a somewhat different approach in that he reviewed 30 studies in which particle scattering and mass were measured. He then estimated a high and low scattering efficiency by using mass measurements to prorate the measured extinction. For ammonium sulfate, the low estimate was arrived at by assuming sulfates, nitrates, and organics scatter twice as efficiently as all other species, and for the high estimate he assumed that only the ammonium sulfate was twice as efficient. His low and high ammonium sulfate mass scattering efficiencies for the rural west were 3.0 and 3.7  $\text{m}^2/\text{g}$ , respectively. For organics his low estimate assumes organics and other non-sulfate species

scatter half as efficiently as ammonium sulfate, and for the high estimate he assumes organics are three, and ammonium sulfate twice as efficient at scattering light as other species. His low and high estimates for organic mass scattering coefficients are 1.8 and 4.1 m<sup>2</sup>/g. More recently, Malm et al. [1996] demonstrated that an assumption of dry specific scattering values given in Equation (F-3) yielded good agreement between measured and reconstructed extinction across the entire IMPROVE monitoring network.

Various functions for the hygroscopicity of organics have been proposed. Assumptions must not only be made about the solubility of organics but also on the fraction of organics that are soluble. It should be noted, models that treat water uptake for non ideal multicomponent solutions using theoretical and semi-theoretical thermodynamic relationships have been developed and have been applied to both visibility and climate forcing problems [Saxena and Peterson, 1981; Pilinis et al., 1995; Saxena et al., 1986, 1993]. The correct treatment of the hygroscopicity of species in multicomponent mixtures—especially organic species—remains problematic, not only because of the lack of suitable mixture thermodynamic data but also because of the lack of information about other critical mixture properties. Given the variety of organic species, it is possible that a geographic variation in organic species exists, with large fractions of soluble species occurring in certain parts of the continent and much smaller fractions in other areas. However, field experiments and subsequent data analysis at Great Smoky Mountains and Grand Canyon National Parks [Malm et al., 1997; Malm and Kreidenweis, 1996 Malm et al., 2000] and, more generally, data collected in the IMPROVE Network [Malm et al., 1996] show that to within the uncertainty of the measurements and modeling assumptions, organics are not or are only weakly hygroscopic. Therefore,  $f_{org}(RH)$  for organics was set equal to one.

Equation (F-3) has been shown to give a good estimation of scattering for particles less than 2.5 μm, however, estimating extinction requires a knowledge of particle absorption. Mass absorption efficiencies of carbon vary by more than a factor of two as do direct measurements. Horvath [1993] has reviewed the measurement of absorption, while Fuller et al. [1999] has theoretically explored the variability of absorption efficiency as a function of carbon morphology. Although absorption can be estimated in a variety of ways, there is no one method that is generally accepted by the scientific community. For purposes of this report, carbon absorption is estimated using:

Equation (F-4): 
$$b_{abs} = 10[LAC]$$

Where  $b_{abs}$  is particle absorption, LAC is the concentration of light-absorbing carbon as measured using the Thermal Optical Reflectance (TOR) analysis scheme [Chow et al., 1993], and 10 is the specific absorption for LAC, which has been used by a number of scientists [Horvath, 1993].

Because aerosol concentrations are derived from averages over long periods, the light scattering due to soluble species is derived using hourly RH values less than or equal to 98%, as given by the following equation:

Equation (F-5): 
$$b_{scat} = \alpha F_T \overline{C}$$

Where  $\overline{C}$  is the average species concentration,  $\alpha$  is the specific scattering, and

Equation (F-6): 
$$F_T = f_T(RH)$$

Using Equation (F-3), extinction budgets for a time interval may be calculated by replacing  $f_T(RH)$  with  $F_T$  and by using the average concentration of each species over the same time

interval as the mass concentration. Using the data from sites with collocated optical and RH data, a polynomial curve was fitted to the annual and seasonal data as defined by:

$$\text{Equation (F-7): } F = b_0 + b_1(100/(100-RH)) + b_2(100/(100-RH))^2$$

Where  $b_0 = 0.33713$ ,  $b_1 = 0.58601$ , and  $b_2 = 0.09164$  with an R-square of 0.93 annually. Figure F-1 shows the fitted curve plotted against annual average RH for IMPROVE sites with collocated RH data. Table F-1 lists the regression results for annual and seasonal averaging periods. For those sites without collocated optical and RH data, the annual factors can be calculated using Equation (F-7) and estimates of annual average RH. (Five significant figures are used in the curve fit program used for this report and therefore are included here for reference.)

Figure F-1: Best-fit relation between a site's annual average RH and its annual average RH correction factor.

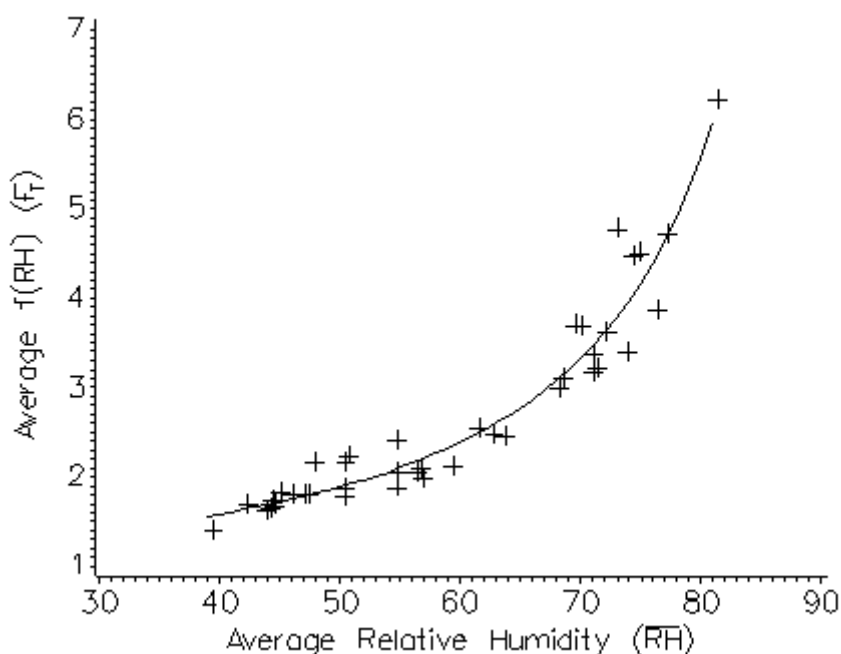
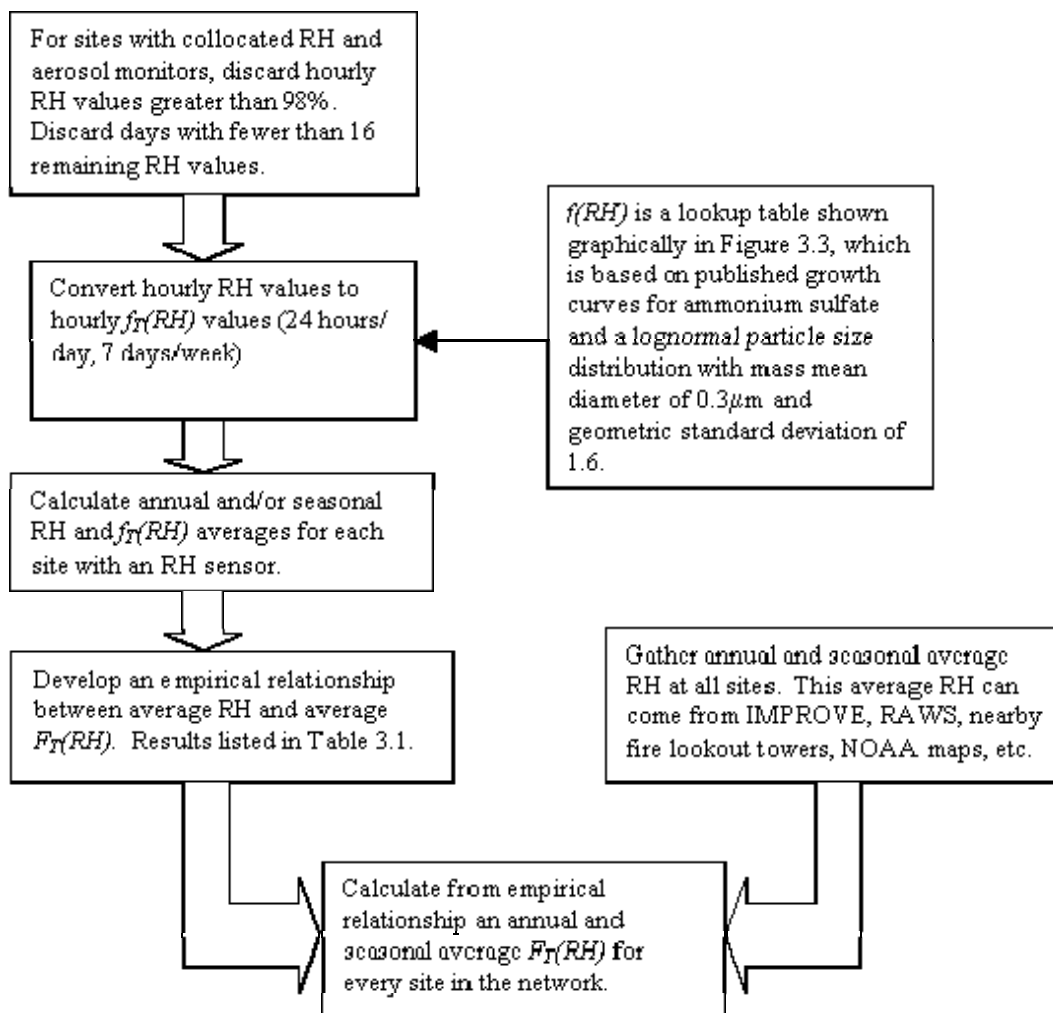


**Table F-1:** Parameters of the best-fit equation relating the relative humidity light-extinction correction factors ( $F_T$ ) to seasonal and annual average site relative humidity ( $F = b_0 + b_1(1/(1-RH)) + b_2(1/(1-RH))^2$ ).

Season	$b_0$	$b_1$	$b_2$	$R^2$
Spring	-0.01097	0.78095	0.080147	0.93
Summer	-0.18614	0.99211	---	0.91
Autumn	-0.24812	1.01865	0.01074	0.93
Winter	0.34603	0.81984	---	0.77
<b>ANNUAL</b>	0.33713	0.58601	0.09164	0.93

Figure F-2 is a flowchart, which details the process used to account for the effects of relative humidity at those sites with or without relative humidity sensors.

Figure F-2: The process by which IMPROVE data is used to develop site-specific seasonal and annual RH correction factors.



The extinction reconstruction process starting with the raw IMPROVE data through to the extinction calculation can be summarized:

1. At those sites with collocated RH sensors and particle monitors, discard hourly RH values greater than 98% and discard days with less the 16 RH values.
2. Convert the hourly RH to  $f(RH)$  values using the “smoothed” ammonium sulfate  $f_T(RH)$  versus RH lookup table shown graphically in Figure G-3.
3. Calculate annual and/or seasonal RH and  $f(RH)$  averages ( $F_T$ ) [Equation (G-6)].
4. Develop an empirical relationship between average RH and average  $F_T(RH)$  [Eq. (G-7)].
5. For the desired time period (annual or seasonal) find the average of the following species: ammonium sulfate, ammonium nitrate, organics, light-absorbing carbon, fine soil, and coarse mass.

6. Using these averages calculate average reconstructed aerosol extinction according to the following equation (referred to as the old IMPROVE equation):

Equation (F-8): OLD IMPROVE EQUATION:

$$b_{ext} = (3)F_T(RH) [Sulfate] + (3)F_T(RH) [Nitrate] + (4)[OMC] + (10)[LAC] + (1)[Soil] + (0.6) [CM] + 10$$

or

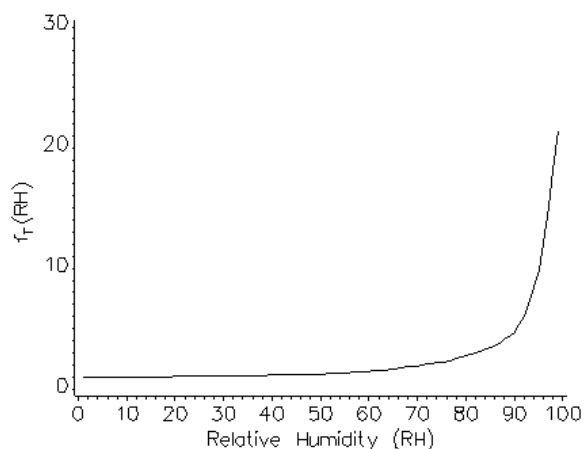
$$b_{ext} \approx 3 \times f(RH) \times [Sulfate] + 3 \times f(RH) \times [Nitrate] + 4 \times [Organic Mass] + 10 \times [Elemental Carbon] + 1 \times [Fine Soil] + 0.6 \times [Coarse Mass] + 10$$

Where the parameters enclosed in the brackets are the average concentrations of each species.

The use of a 98% RH cut point is somewhat arbitrary, but it was chosen to allow for the likelihood that above 98%, precipitation would obscure visibility without regard to pollutant concentrations, and as an expedient measure because  $f_T(RH)$  is infinite at 100% RH. The same  $f_T(RH)$  was used in the first and second IMPROVE reports [Sisler et al., 1993; Sisler, 1996]. However, the assumptions used for estimating this curve will be investigated in light of more recent growth and particle size distribution data.

There are two ways reconstructed extinction is calculated in this report that are different from the 1996 IMPROVE report. First, the factor  $f(RH)$  that accounts for the relative humidity effects on hygroscopic aerosols has been upgraded with new relative humidity data from additional relative humidity monitoring sites and second, absorption is estimated from measurements of light-absorbing carbon rather than from transmission measurements of filter media. Therefore, some differences in aerosol extinction between this and the 1996 report are due to changes other than levels of aerosol mass concentration.

Figure F-3: RH factors ( $f_T(RH)$ ) derived from Tang's ammonium sulfate growth curves smoothed between the crystallization and deliquescence points.



In 2005-06, researchers updated the light-extinction equation using with a more robust data set resulting in the “New IMPROVE Equation”.

Equation (F-9):      NEW IMPROVE EQUATION:

$$\begin{aligned} b_{ext} \approx & 2.2 \times f_S (RH) \times [\text{Small Sulfate}] + 4.8 \times f_L (RH) \times [\text{Large Sulfate}] \\ & + 2.4 \times f_S (RH) \times [\text{Small Nitrate}] + 5.1 \times f_L (RH) \times [\text{Large Nitrate}] \\ & + 2.8 \times [\text{Small Organic Mass}] + 6.1 \times [\text{Large Organic Mass}] \\ & + 10 \times [\text{Elemental Carbon}] \\ & + 1 \times [\text{Fine Soil}] \\ & + 1.7 f_{SS} (RH) \times [\text{Sea Salt}] \\ & + 0.6 \times [\text{Coarse Mass}] \\ & + \text{Rayleigh scattering (Site Specific)} \\ & + 0.33 [\text{NO}_2 \text{ (ppb)}] \end{aligned}$$

Where

$$[\text{Large Sulfate}] = \frac{[\text{Total Sulfate}]}{20} \times [\text{Total Sulfate}], \text{ for } [\text{Total Sulfate}] < 20$$

$$[\text{Large Sulfate}] = [\text{Total Sulfate}], \text{ for } [\text{Total Sulfate}] \geq 20$$

$$[\text{Small Sulfate}] = [\text{Total Sulfate}] - [\text{Large Sulfate}]$$

Nitrate and Organic are split using the same process

The primary changes of the new IMPROVE equation are the sulfate, nitrate and organic carbon are differentiated into large and small size fractions, organic compound mass to organic carbon mass ratio changed from 1.4 to 1.8, sea salt is added as a component of extinction (Sea Salt = 1.8 x [Chlorine]), Rayleigh scattering is calculated for the monitoring site elevation & annual mean temperature (ranges from 8Mm<sup>-1</sup> at 10,000' to 12Mm<sup>-1</sup> at sea level) and NO<sub>2</sub> light absorption in the visible is included for sites that have such data (not routinely available at IMPROVE sites)

Visibility expressed as reconstructed deciview (dv) can now be calculated. The deciview is a visibility metric based on the light-extinction coefficient that expresses incremental changes in perceived visibility [Pitchford and Malm, 1994]. Because the deciview expresses a relationship between changes in light extinction and perceived visibility, it can be useful in describing visibility trends. A 1-dv change is about a 10% change in extinction coefficient, which is a small but perceptible scenic change under many circumstances. The deciview is defined by the following equation:

$$dv = 10 \ln(b_{ext}/10)$$

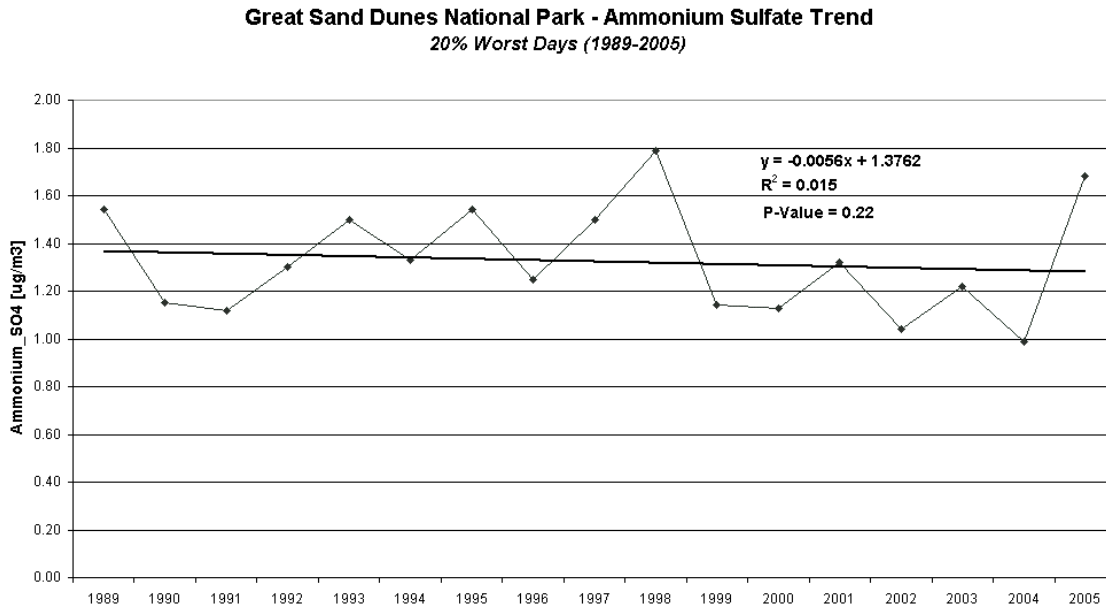
Where the deciview scale is near zero for pristine atmosphere (dv = 0 for Rayleigh condition at about 1.8 km elevation) and increases as visibility is degraded.

# Appendix G: Pollutant Statistical Trends

## Ammonium Sulfate Trend

Figure G-1 indicates a slight downward trend in ammonium sulfate and a statistical analysis of the data indicates that the trend is not statistically significant.

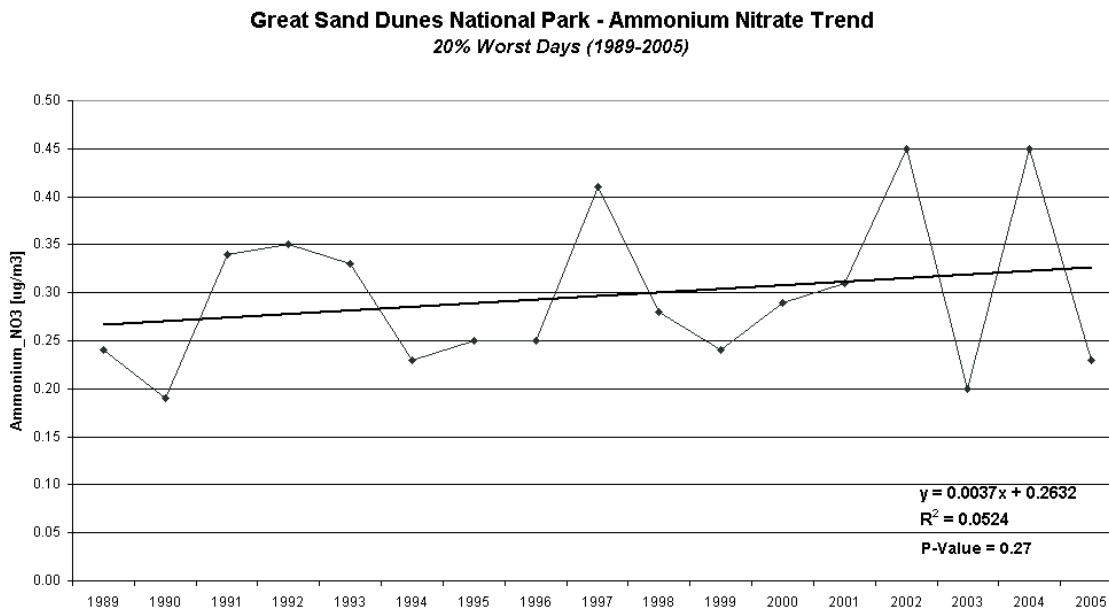
Figure G -1: Ammonium Sulfate Trend



## Ammonium Nitrate Trend

Figure G-2 indicates a slight upward trend in ammonium nitrate and a statistical analysis of the data indicates that the trend is not statistically significant.

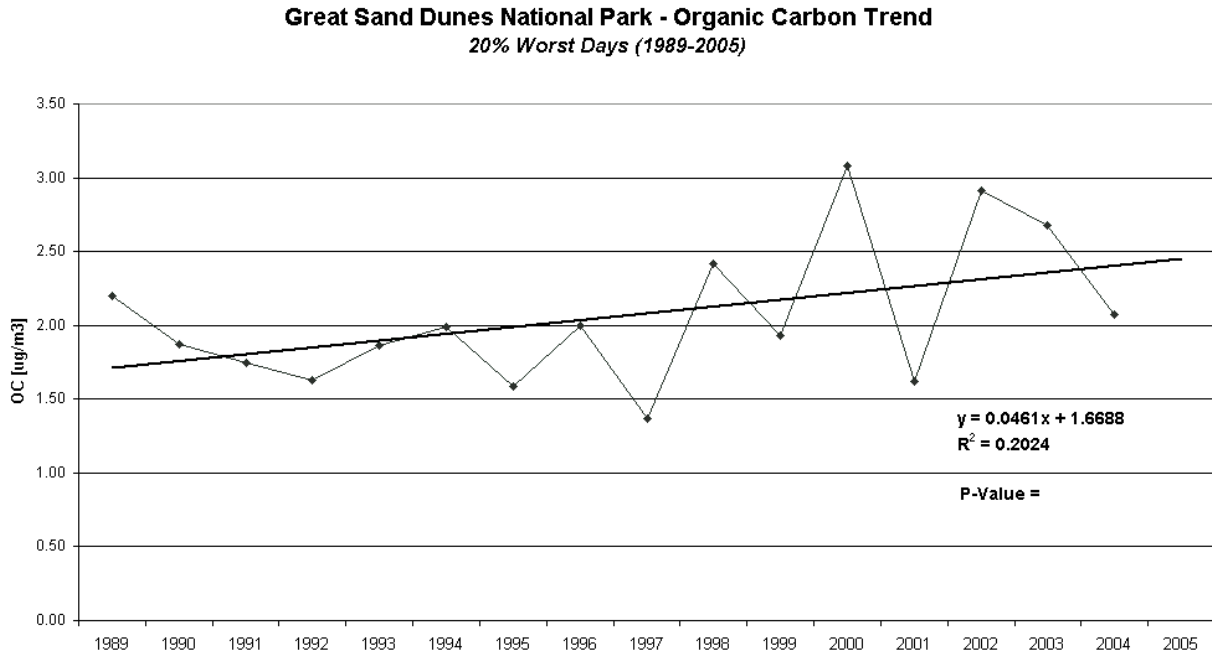
Figure G -2: Ammonium Nitrate Trend



**Organic Carbon Trend**

Figure G-3 indicates an upward trend in organic carbon and a statistical analysis of the data could not be completed due to missing OC data for 2005.

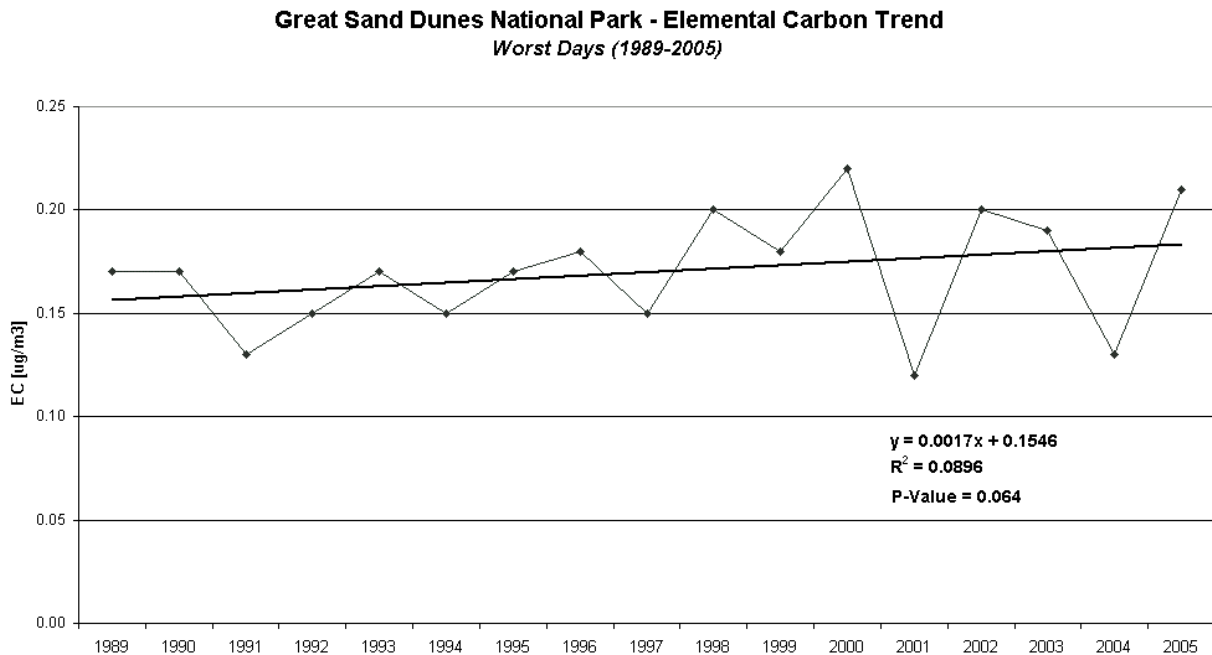
Figure G -3: Organic Carbon Trend



**Elemental Carbon Trend**

Figure G-4 indicates a slight upward trend in elemental carbon and a statistical analysis of the data indicates that the trend is probably statistically significant.

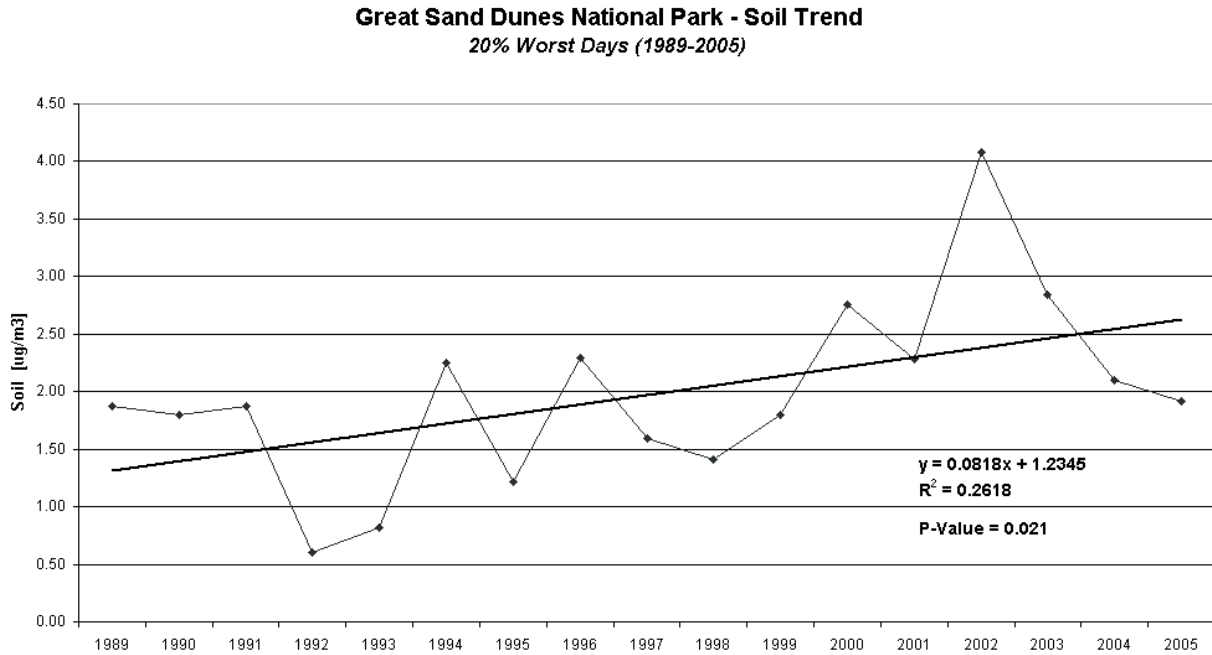
Figure G -4: Elemental Carbon Trend



**Soil Trend**

Figure G-5 indicates a significant upward trend in soil and a statistical analysis of the data indicates that the trend is statistically significant (if P-Value < 0.05, or 95% level of certainty).

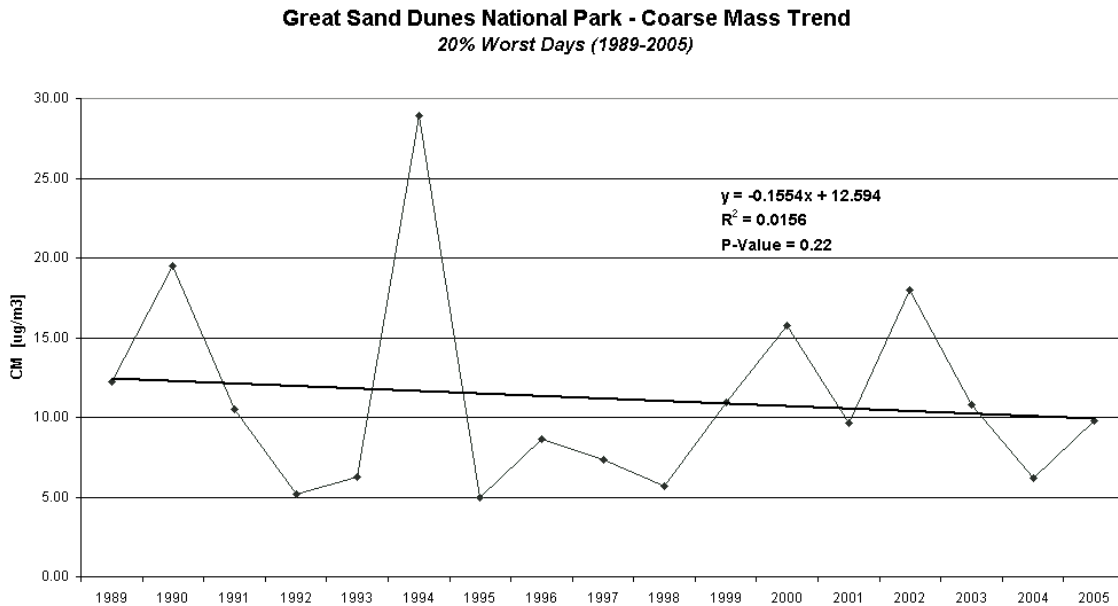
Figure G -5: Soil Trend



**Coarse Mass Trend**

Figure G-6 indicates a downward trend in coarse mass and a statistical analysis of the data indicates that the trend is not statistically significant.

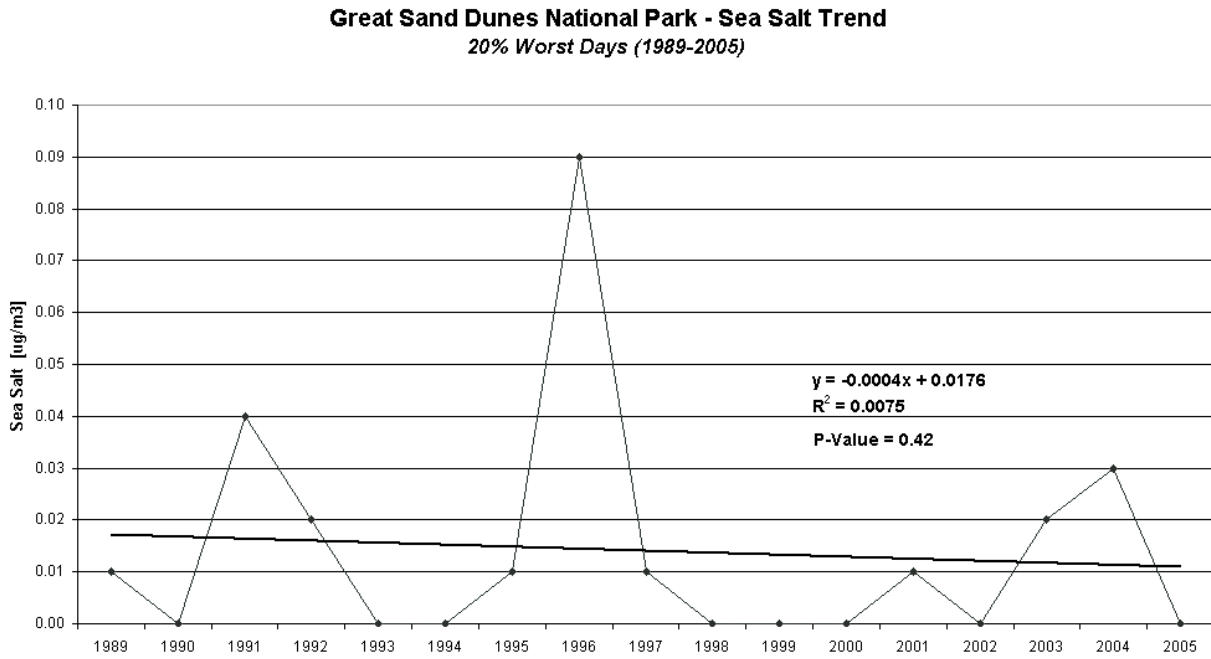
Figure G -6: Coarse Mass Trend



**Sea Salt Trend**

Figure G-7 indicates the trend in sea salt concentrations and a statistical analysis of the data indicates that the trend is not statistically significant. Sea salt is not typically included in our technical visibility analysis since the concentrations are so small in Colorado.

Figure G-7: Sea Salt Trend



## **Appendix H: PM Source Apportionment Technology (PSAT) Modeling**

### **Development History**

Impairment of visibility in Class I areas is caused by a combination of local air pollutants and regional pollutants that are transported long distances. To develop effective visibility improvement strategies, the WRAP member states and tribes need to know the relative contributions of local and transported pollutants, and which emissions sources are significant contributors to visibility impairment at a given Class I area.

A variety of modeling and data analysis methods can be used to perform source apportionment of the PM observed at a given receptor site. Model sensitivity simulations have been used in which a “base case” model simulation is performed and then a particular source is “zeroed out” of the emissions. The importance of that source is assessed by evaluating the change in pollutants at the receptor site, calculated as pollutant concentration in the sensitivity case minus that in the base case. This approach is known as a “brute force” sensitivity because a separate model run is required for each sensitivity test.

An alternative approach is to implement a mass-tracking algorithm in the air quality model to explicitly track for a given emissions source the chemical transformations, transport, and removal of the PM that was formed from that source. Mass tracking methods have been implemented in both the CMAQ and CAMx air quality models. Initial work completed by the RMC during 2004 used the CMAQ Tagged Species Source Apportionment (TSSA) method. Unfortunately, there were problems with mass conservation in the version of CMAQ used in that study, and these affected the TSSA results. A similar algorithm has been implemented in CAMx, the PM Source Apportionment Technology (PSAT). Comparisons of TSSA and PSAT showed that the results were qualitatively similar, that is, the relative ranking of the most significant source contributors were similar for the two methods. However, the total mass contributions differed. With separate funding from EPA, UCR has implemented a version of TSSA in the new CMAQ release (v4.5) that corrects the mass conservation error, but given the uncertainty of the availability of this update, the CAMx/PSAT source apportionment method was used for the WRAP modeling analysis.

The main objective of applying CAMx/PSAT is to evaluate the regional haze air quality for conditions typical of the 2000-04 baseline period (Plan02c) and future-year 2018 (Base18b) conditions. These results are used

- to assess the contributions of different geographic source regions (e.g., states) and source categories to current (2000-04) and future (2018) visibility impairment at Class I areas, to obtain improved understanding of (1) the causes of the impairment and (2) which states are included in the area of influence (AOI) of a given Class I area;
- to determine which source categories contributing to the AOI for each Class I area are changing, and by how much, between the 2000-04 and 2018 base case, by varying only controllable anthropogenic emissions between the 2 PSAT simulations; and
- to identify the source regions and emissions categories that, if controlled to lower emissions rates than the 2018 base case levels, would produce the greatest visibility improvements at a Class I area.

### **CAMx/PSAT**

The PM Source Apportionment Technology performs source apportionment based on user-defined source groups. A source group is the combination of a geographic source region and an

emissions source category. Examples of source regions include states, nonattainment areas, and counties. Examples of source categories include mobile sources, biogenic sources, and elevated point sources; PSAT can even focus on individual sources. The user defines a geographic source region map to specify the source regions of interest. He or she then inputs each source category as separate, gridded low-level emissions and/or elevated-point-source emissions. The model then determines each source group by overlaying the source categories on the source region map. For further information, please refer to the white paper on the features and capabilities of PSAT

([http://pah.cert.ucr.edu/aqm/308/reports/PSAT\\_White\\_Paper\\_111405\\_final\\_draft1.pdf](http://pah.cert.ucr.edu/aqm/308/reports/PSAT_White_Paper_111405_final_draft1.pdf)), with additional details available in the CAMx user's guide (ENVIRON, 2005; <http://www.camx.com>).

PM source apportionment modeling was performed for aerosol sulfate (SO<sub>4</sub>) and aerosol nitrate (NO<sub>3</sub>) and their related species (e.g., SO<sub>2</sub>, NO, NO<sub>2</sub>, HNO<sub>3</sub>, NH<sub>3</sub>, and NH<sub>4</sub>). The PSAT simulations include 9 tracers, 18 source regions, and 6 source groups. The computational cost for each of these species differs because additional tracers must be used to track chemical conversions of precursors to the secondary PM species SO<sub>4</sub>, NO<sub>3</sub>, NH<sub>4</sub>, and secondary organic aerosols (SOA). Table 1 summarizes the computer run time required for each species. The practical implication of this table for WRAP is that it is much more expensive to perform PSAT simulations for NO<sub>3</sub> and especially for SOA than it is to perform simulations for other species.

**Table H-1: Benchmarks for PSAT computational costs\* for each PM species**

Species	No. of Species Tracers	RAM Memory	Disk Storage per Day	Run Time with 1 CPU
SO <sub>4</sub>	2	1.6 GB	1.1 GB	4.7 h/day
NO <sub>3</sub>	7	1.7 GB	2.6 GB	13.2 h/day
SO <sub>4</sub> and NO <sub>3</sub> combined	9	1.9 GB	3.3 GB	16.8 h/day
SOA	14	6.8 GB	Not tested	Not tested
Primary PM species	6	1.5 GB	3.0 GB	10.8 h/day

\*Run time is for one day (01/02/2002) on the WRAP 36-km domain

Two annual 36-km CAMx/PSAT model simulations were performed: one with the Plan02c typical-year baseline case and the other with the Base18b future-year case. It is expected that the states and tribes will use these results to assess the sources that contribute to visibility impairment at each Class I Area, and to guide the choice of emission control strategies. The RMC web site includes a full set of source apportionment spatial plots and receptor bar plots for both Plan02b and Base18b. These graphical displays of the PSAT results, as well as additional analyses of these results are available on the TSS under <http://vista.cira.colostate.edu/tss/Tools/ResultsSA.aspx>

**CAMx/PSAT Configuration for 2002 and 2018 Modeling**

PSAT source apportionment simulations for 2000-04 baseline period and 2018 base case were performed using CAMx v4.30. Table 2 lists overall specifications for the PSAT simulations. The domain setup was identical to the standard WRAP CMAQ modeling domain. The CAMx/PSAT run-time options are shown in Table 3. The CAMx/PSAT computational cost for one simulation day with source tracking for sulfate (SO<sub>4</sub>) and nitrate (NO<sub>3</sub>) is approximately 14.5 CPU hours with an AMD Opteron CPU. The source regions used in the PSAT simulations are shown in Figure 1 and Table 4. The six emissions source groups are described in Table 5. The development of these emissions data are described in more detail below.

The annual PSAT run was divided into four seasons for modeling. The initial conditions for the first season (January 1 to March 31, 2002) came from a CENRAP annual simulation. For the other three seasons, we allowed 15 model spin-up days prior to the beginning of each season. Based on the chosen set of source regions and groups, with nine tracers, and with a minimum requirement of 87,000 point sources and a horizontal domain of 148 by 112 grid cells with 19 vertical layers, the run-time memory requirement is 1.9 GB. Total disk storage per day is approximately 3.3 GB. Although the RMC's computation nodes are equipped with dual Opteron CPUs with 2 GB of RAM and 1 GB of swap space, the high run-time memory requirements prevented running PSAT simulations using the OpenMP shared memory multiprocessing capability implemented in CAMx.

**Table H-2: WRAP 2002 CAMx/PSAT specifications**

WRAP PSAT Specs	Description
Model	CAMx v4.30
OS/compiler	Linux, pgf90 v.6.0-5
CPU type	AMD Opteron with 2 GB of RAM
Source region	18 source regions; see Figure 4.1 and Table 4.4
Emissions source groups	Plan02b, 6 source groups; see Table 4.5
Initial conditions	From CENRAP (camx.v4.30.cenrap36.omp.2001365.inst.2)
Boundary conditions	3-h BC from GEOS-Chem v2

**Table H-3: WRAP CAMx/PSAT run-time options**

WRAP PSAT specs	Description
Advection solver	PPM
Chemistry parameters	CAMx4.3.chemparam.4_CF
Chemistry solver	CMC
Plume-in-grid	Not used
Probing tool	PSAT
Dry/wet deposition	TRUE (turned on)
Staggered winds	TRUE (turned on)

**Table H-4: WRAP CAMx/PSAT source regions cross-reference table**

Source Region ID	Source Region Description <sup>1</sup>	Source Region ID	Source Region Description <sup>1</sup>
1	Arizona (AZ)	10	South Dakota (SD)
2	California (CA)	11	Utah (UT)
3	Colorado (CO)	12	Washington (WA)
4	Idaho (ID)	13	Wyoming (WY)
5	Montana (MT)	14	Pacific off-shore & Sea of Cortez (OF)
6	Nevada (NV)	15	CENRAP states (CE)

Source Region ID	Source Region Description <sup>1</sup>	Source Region ID	Source Region Description <sup>1</sup>
7	New Mexico (NM)	16	Eastern U.S., Gulf of Mexico, & Atlantic Ocean (EA)
8	North Dakota (ND)	17	Mexico (MX)
9	Oregon (OR)	18	Canada (CN)

<sup>1</sup>The abbreviations in parentheses are used to identify source regions in PSAT receptor bar plots.

**Figure H-1: WRAP CAMx/PSAT source region map**

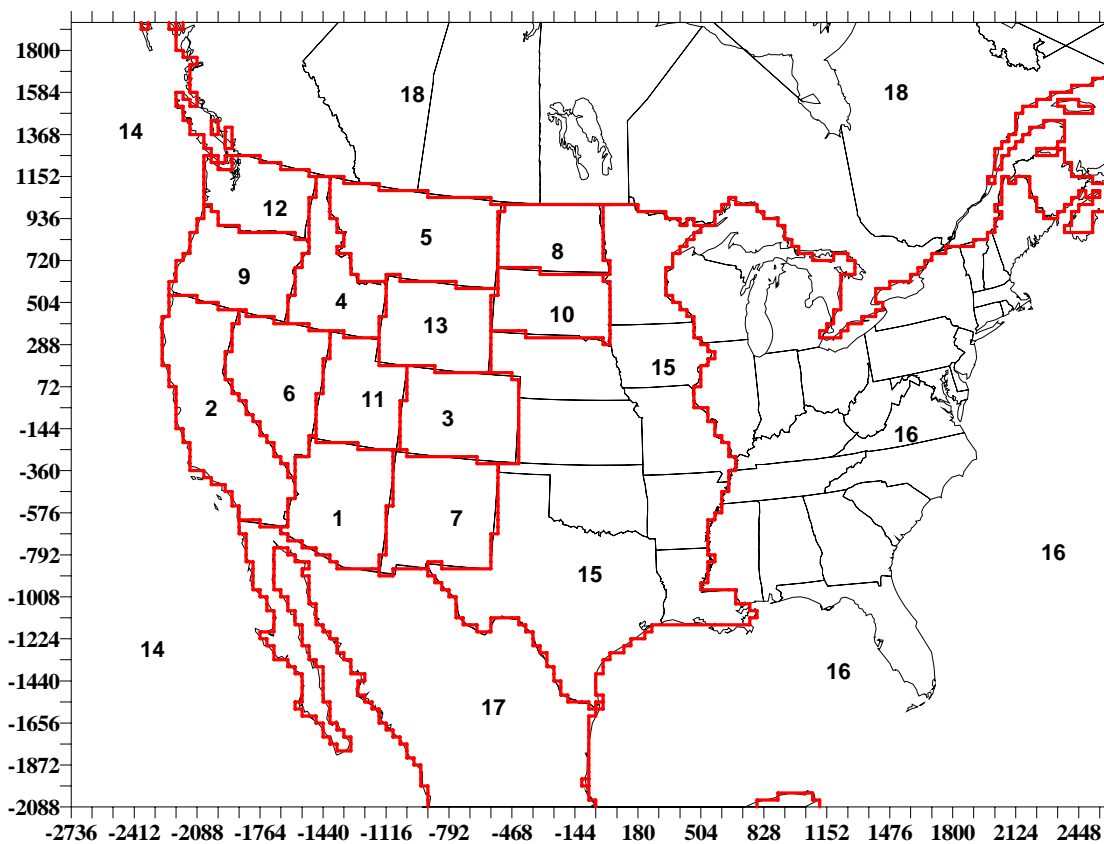


**Table H-5: WRAP CAMx/PSAT emissions source groups**

Emissions Source Groups	Low-level Sources	Elevated Sources
1	Low-level point sources (including stationary off-shore)	Elevated point sources (including stationary off-shore)
2	Anthropogenic wildfires (WRAP only)	Anthropogenic wild fires (WRAP only)
3	Total mobile (on-road, off-road, including planes, trains, ships in/near port, off-shore shipping)	

Emissions Source Groups	Low-level Sources	Elevated Sources
4	Natural emissions (natural fire, WRAP only, biogenics)	Natural emissions (natural fire, WRAP only, biogenics)
5	Non-WRAP wildfires (elevated fire sources in other RPOs)	Non-WRAP wild fires (elevated fire sources in other RPOs)
6	Everything else (area sources, all dust, fugitive ammonia, non-elevated fire sources in other RPOs)	

### **Preparation of Emissions Data**

Emissions datasets for the CAMx/PSAT simulations were prepared directly from the SMOKE-processed emissions developed for CMAQ. A simple format conversion was used to convert the original SMOKE output files from the I/O API format to the CAMx format. For certain source categories, SMOKE was configured to output CAMx-formatted files directly. In addition, CMAQ species names were changed for several of the emissions species to make them consistent with the CAMx species. Additional processing was also required for the PSAT algorithm. For each of the emissions categories that were tracked in PSAT, the intermediate SMOKE output files for those categories were converted to the CAMx/PSAT formats, and read by the CAMx program to distinguish among the emissions source categories. The elevated-point-source CAMx emissions files were also processed files to specify the PSAT source region individually for each point source. This was necessary in order to assign elevated-point-source emissions to the correct PSAT source region (particularly near state boundaries and along coastal regions), due to the relatively coarse (36-km) grid cell resolution.

No additional post-processing QA was performed on the CAMx emissions files, since they were prepared directly from the previously quality-assured CMAQ emissions files. However, the CAMx/PSAT simulations by comparing the CAMx- and CMAQ-predicted species concentrations as part of the overall QA of the model simulations.